Development of Sustainable Composite Construction Materials from Platinum Group Metals Furnace Slag

By

Miriam P. Magavhe

C22148303K

Submitted in fullfilment of the requirements for the degree of

MASTER OF PHILOSOPHY (MPHIL) IN MATERIALS SCIENCE AND ENGINEERING

Supervisor: Dr. C. Sumanya

Co-supervisor: Prof. W. Mtangi

Institute of Materials Science, Processing, and Engineering Technology

Chinhoyi University of Technology

Chinhoyi

2024

DECLARATION

I, Magavhe Miriam Patience, hereby declare that this dissertation is my work with the assistance of my supervisors, technicians, and fellow students. The report has not previously been submitted to any tertiary institution for any related degree.

The undersigned, hereby certify that they have read and agree to submit this final version of the dissertation as the official submission.

Miriam P. Magavhe		24/07/2024
…..…………………	…………………………….	………………………….
Student	Signature	Date

Dr. C. Sumanya		24/07/2024
…..…………………	…………………………….	…………..………………
Main Supervisor	Signature	Date

DEDICATION

I would like to dedicate this work to my family. Thank you for allowing me to pursue what fulfils my passion and I hope this work will make you proud one day. May it serve as a reminder that striving for success and making a positive impact on the world takes a lot of hard work, determination, and commitment.

ACKNOWLEDGEMENTS

Firstly, I would like to express my deepest gratitude to my supervisors: Dr. C. Sumanya and Prof. W. Mtangi for all the guidance, encouragement, and support throughout the project. My appreciation is extended to Zimplats Holdings for sponsoring this project and allowing us to collaborate with them. My appreciation also goes to the Ministry of Transport, Chinhoyi, the University of Zimbabwe Civil Engineering Department, and the Chinhoyi University of Technology Arts Department for their technical assistance and for allowing me to use their facilities. I would like to thank the Materials Science and Engineering department at the Chinhoyi University of Technology for organizing part-time work in the department to enable me to supplement my finances. I would like to express my appreciation to my fellow students: Pride Mutekwa, Denzel Makepa, Miriam Guni, Geoff Mangwiro, and Misheck Mujuru for their encouragement. I would like to extend my gratitude to my parents and family for their patience, and unwavering support during the years of my study.

Last but not least, I would want to thank the Almighty God who has sailed me through to this point, granting me wisdom, vision, and strength during my studies. Even when it seemed like the journey would never finish, I always had faith that the one who started good work in me would see it through to completion.

TABLE OF CONTENTS

DECLARATION....i

DEDICATION....i

ACKNOWLEDGEMENTS....ii

TABLE OF CONTENTS....ii

LIST OF FIGURES.... viii

LIST OF TABLES....x

LIST OF ABBREVIATIONS....x

ABSTRACT....xi

CHAPTER 1: INTRODUCTION.... 1

1.1 Chapter Overview 1
1.2 Background 2
1.3 Problem Statement 3
1.4 Justification 4
1.5 Objectives 5
1.5.1 Main Objective.. 5
1.5.2 Specific Objectives 5
1.6 Scope of the Study.. 5
1.7 Chapter Summary 6

CHAPTER 2: LITERATURE REVIEW 7
2.1 Introduction 7
2.2 Composite Materials 8
2.3 Bricks 9
2.3.1 Classification of Bricks 9
2.3.1.1 Clay Bricks 9
2.3.1.2 Cement Bricks 10
2.3.1.3 Fly Ash Bricks 10
2.3.1.4 Calcium Silicate/ Sand-lime Bricks 10
2.3.1.5 Magnesia Bricks 10
2.4 Mining waste 11
2.4.1 Classification of Mining Waste 11
2.4.1.1 Overburden 12
2.4.1.2 Waste Rock 12
2.4.1.3 Tailings 13
2.4.1.4 Sewage Sludge 14
2.4.1.5 Slags... 15
2.4.2 Disposal Methods of Mining Waste 19
2.4.2.1 Tailing Dams and Slag Dumps 19
2.4.2.2 Underground Filling 19
2.4.2.3 Deepwater Disposal 20
2.4.3 Characterization of Mining Waste 20
2.4.3.1 X-ray Fluorescence 20
2.4.3.2 X-ray Diffraction 21
2.4.3.3 Specific Gravity 21

2.4.3.4 Sieve Analysis 21
2.4.4 Application of Mining Waste in Brick Manufacturing 22
2.4.4.1 Iron Mining Waste 22
2.4.4.2 Copper Mining Waste 24
2.4.4.3 Gold Mining Waste 26
2.4.4.4 Coal Gangue 27
2.4.4.5 Bauxite Residue 28
2.4.5 PGM Mining Waste 30
2.5 Brick Clay 31
2.5.1 Characterization of Brick Clay 31
2.5.2 Chemical Composition for Brick Clay 34
2.6 Brick Manufacturing Process 35
2.6.1 Raw Materials Preparation 35
2.6.2 Brick Forming 35
2.6.2.1 Brick Forming Pressure 36
2.6.3 Brick Drying 37
2.6.3.1 Natural drying 37
2.6.3.2 Artificial Drying 37
2.6.4 Brick Firing 38
2.6.4.1 Clamp Burning 38
2.6.4.2 Kiln Burning 39
2.6.4.3 Desorption of Water 40
2.6.4.4 Dehydroxylation of the Silicate 40
2.6.4.5 Combustion of Carbonaceous Materials 41
2.6.4.6 Quartz Inversion 41
2.6.4.7 Vitrification 41
2.6.4.8 Effects of Firing Temperatures on Brick Properties 43
2.7 Properties of Bricks 44
2.7.1 Compressive Strength 44

2.7.2 Water Absorption 44

2.7.3 Soundness 45

2.7.4 Hardness 45

2.7.5 Efflorescence.. 46

2.8 Cost Evaluation 47

2.9 Chapter Summary 48

CHAPTER 3: RESEARCH METHODOLOGY 49

3.1 Chapter Overview 49

3.2 Study Area 49

3.3 Materials 51

3.3.1 PGM Slag 51

3.3..2 Clay 51

3.3.3 Water 52

3.4 Research Design 53

3.4.1 Characterization of Raw Materials 54

3.4.1.1 X-Ray Florescence 54

3.4.1.2 Specific Gravity 54

3.4.1.3 Sieve Analysis (Particle Size Distribution) 54

3.4.1.4 Atterberg Limits 55

3.4.2 Brick Manufacturing Process 56

3.4.2.1 Preparation of Raw Materials 56

3.4.2.2 Brick Forming.. 58

3.4.2.3 Brick Drying 58
3.4.2.4 Brick Firing.. 59
3.4.3 Physical and Mechanical Tests of the Fabricated Composite Material. 60
3.4.3.1 Compressive Strength Test 61
3.4.3.2 Water Absorption Test 61
3.4.3.3 Soundness Test 62
3.4.3.4 Hardness Test 62
3.4.3.5 Efflorescence Test 62
3.5 Chapter Summary 63

CHAPTER 4: RESULTS AND DISCUSSION 64
4.1 Chapter Overview 64
4.2 Characterization of Raw Materials 64
4.2.1 X-Ray Fluorescence Analysis 64
4.2.2 Specific Gravity Analysis 67
4.2.3 Particle Size Analysis 68
4.2.4 Atterberg Limits Analysis 71
4.3 Brick Manufacturing Process 73
4.3.1 Raw Materials Preparation 73
4.3.2 Brick Drying Analysis 75
4.3.3 Brick Firing Analysis 76
4.4 Physical and Mechanical Properties on the Fabricated Composite Material 78

4.4.1 Compressive Strength Analysis 78
4.4.2 Water Absorption Analysis 82
4.4.3 Compressive Strength and Water Absorption Correlation 85
4.4.4 Soundness Analysis 86
4.4.5 Hardness Analysis 86
4.4.6 Efflorescence Analysis... 86
4.5 Chapter Summary 88

CHAPTER 5: CONCLUSIONS AND RECOMMENDATIONS 89
5.1 Conclusions 89
5.2 Recommendations 91

REFERENCES 92

APPENDICES 1055
7.1 Characterization of Raw Materials 1055
7.1.1 X-Ray Florescence 1055
7.1.2 Specific Gravity 1066
7.1.3 Sieve Analysis 1066
7.1.4 Atterberg Limits 1088
7.2 Brick Manufacturing Process 110
7.2.2 Drying Shrinkage 1122
7.2.3 Firing Shrinkage.. 1122
7.3 Physical and Mechanical Properties of the Fabricated Composite Materials 1133
7.3.1 Compressive Strength 1133

7.3.2 Water Absorption 1133

LIST OF FIGURES

Figure 2.1: Overburden Waste at a Mine Site.. 12
Figure 2.2: Waste Rock Management at a Mine Site 13
Figure 2.3: Tailings Discharged into Tailing Dams.. 14
Figure 2.4: Sewage Sludge 15
Figure 2.5: Slag Accumulated at a Mine Site 15
Figure 2.6: Clamp Burning 39
Figure 2.7: Kiln Burning 40
Figure 2.8: Vitrification Process of Clay 42
Figure 3.1: Locations and Operations of the Zimplats Mine 50
Figure 3.2: PGM Slag 51
Figure 3.3: Chinhoyi Clay.. 52
Figure 3.4: Zvishavane Clay 52
Figure 3.5: Flowchart illustrating Research Methods Implemented in this Study 53
Figure 3.6: Brick Manufacturing Flowchart 56
Figure 3.7: Clay Seiving 57
Figure 3.8: Brick Forming 58
Figure 3.9: Brick Drying 59
Figure 3.10: Brick Firing 60
Figure 3.11: Compressive Strength Test 61
Figure 3.12: Water Absorption Test 62
Figure 3.13: Efflorescence Test 63
Figure 4.1: Particle Size Distribution Curves 68
Figure 4.2: Soil Classification Textural Chart 69
Figure 4.3: The Casagrande Plasticity Chart 72
Figure 4.4: Extrusion Prognostic Chart 73
Figure 4.5: Compaction Curves for Optimum Moisture Content Determination 74
Figure 4.6: Drying Shrinkage of Bricks 75
Figure 4.7: Sample Bricks Before Firing 76
Figure 4.8: Sample Bricks Fired at 950 ℃ 77
Figure 4.9: Sample Bricks Fired at 1100 ℃ 77

Figure 4.10: Firing Shrinkage of Bricks 78
Figure 4.11: Variation of Compressive Strength with PGM Slag wt.% and Temperature for Zvishavane Clay Binder Bricks 79
Figure 4.12: Variation of Compressive Strength with PGM Slag wt.% and Temperature for Chinhoyi Clay Binder Bricks 79
Figure 4.13: Variation of Water Absorption with PGM Slag wt.% and Temperature for Zvishavane Clay Binder Bricks 82
Figure 4.14: Variation of Water Absorption with PGM Slag wt.% and Temperature for Chinhoyi Clay Binder Bricks 83
Figure 4.15: Compressive Strength and Water Absorption Variation with Temperature 85
Figure 4.16: Brick Efflorescence at 50 wt.% Combination 87

LIST OF TABLES

Table 2.1: Properties of Blast Furnace Slag 17
Table 2.2: Properties of Non-ferrous Slags 18
Table 2.3: Properties of Brick Clays 32
Table 2.4: Soil Classification Systems............ 33
Table 2.5: Particle Sizes for Different Soil Classification Systems............ 33
Table 2.6: Acceptable Range for Key Chemical Elements in Brickmaking Materials 34
Table 2.7: Efflorescence Test Observations 46
Table 3.1: PGM Slag-Clay Mixing Combinations 56
Table 4.1: Elemental Composition of the Raw Materials 65
Table 4.2: Elemental Composition of the Key Elements for Brick Manufacture 65
Table 4.3: Specific Gravity of the Raw Materials 67
Table 4.4: Particle Size Distribution Results 69
Table 4.5: Atterberg Limits Results 71
Table 4.6: Efflorescence Test Results 87

LIST OF ABBREVIATIONS

AASHTO	American Association of State Highway and Transportation Officials
ASTM	American Society for Testing and Materials
GB	Chinese National Brick Standards
Inc’s	Incorporated
IS	Indian Standard
JC/T	Chinese Standards for Non-fired Rubbish Gangue Bricks
LL	Liquid Limit
LOI	Loss on Ignition
PGM	Platinum Group Metals
PI	Plasticity Index

PL	Plastic Limit
SDG	Sustainable Development Goals
SEM	Scanning Electron Microscope
USCS	Unified Soil Classification System
USDA	United States Department of Agriculture
XRD	X-ray diffraction
XRF	X-ray fluorescence
ZIMPLATS	Zimbabwe Platinum Mines

ABSTRACT

Waste from mining activities is considered to contribute mostly to the total global waste streams with an annual estimate of over one hundred billion tonnes. Platinum Group Metals mining companies in Zimbabwe generate a significant amount of waste annually, and a continuous increase in waste generation is anticipated due to the expansion of mining activities. This work focuses on mining waste management, targeting PGM furnace slag to make sustainable composite construction materials, particularly bricks. Earth-based clays namely Zvishavane clay (ZC) and Chinhoyi clay (CC) were employed as binders for the slag. Several characterization techniques including, x-ray fluorescence, sieve analysis, specific gravity, and atterberg limits were conducted on the raw materials. The elemental analysis of PGM slag revealed no traces of harmful heavy metals making it safe for use in brick manufacturing. The following PGM slag weight percent combinations were prepared: 0wt.%, 20wt.%, 40wt.%, 50wt.%, and 60wt.%. A manual method was adopted to produce laboratory-scale bricks from a mold of dimensions 230 mm × 115 mm × 75 mm. The bricks were naturally dried and fired at 950 ℃, 1000 ℃, 1050 ℃, and 1100 ℃ in an electric kiln for each defined combination. The physical and mechanical properties of the fired bricks were assessed for their appropriateness in construction through the following tests: compressive strength, water absorption, soundness, hardness, and efflorescence. The compressive strength test results for the defined combinations and firing temperatures ranged from 5.6 MPa to 11.2 MPa for ZC as the binder and 5.4 MPa to 10.1 MPa for CC as the binder. The water absorption test results for the specified combinations and firing temperatures ranged from 7.1% to 11.5% for ZC as the binder and 10.1% to 11.8% for CC as the binder. The optimum brick properties were achieved with 50wt.% slag combination, 10.7% forming water, and 950 ℃ firing temperature with ZC employed as the binder. The optimum compressive strength and water absorption percentage reported from this study were 11.2 MPa and 7.1%, respectively. The bricks revealed positive efflorescence results owing to the existence of Fe and CaO in the raw materials. The compressive strengths and water absorption test results complied with the standard guidelines by ASTM and IS, suggesting that PGM slag can be recycled to make bricks acceptable in the construction industry. Recycling PGM slag in developing sustainable composite construction materials can be the most feasible solution to the disposal challenges.

Keywords: PGM Slag, Clay, Bricks, Compressive Strength, Water Absorption

CHAPTER 1

INTRODUCTION

1.1 Chapter Overview

Waste from mining activities is considered to contribute to the total global waste streams (Sezgin, 2020). Mining waste is undesirable and unprofitable solid or liquid materials that build up at or close to a mine site (Lottermoser, 2010). The mining sector is expanding at the same quick rate as the population, providing raw materials for various industrial, medical, electronic, and other uses. As the mining industry grows, mining and mineral processing activities generate tonnes of waste daily, accumulating in spaces that could have been utilized for other economic activities. The annual global mining waste generation from the primary production of mineral and metal commodities is estimated to be over 100 billion tonnes and is expected to expand with growth in the mining industry (Araujo et al., 2022; Tayebi-Khorami et al., 2019).

The accumulation of mining waste in tailing dams, waste rock piles, and slag dumps without effective management can pose serious risks to the environment and human health, as well as resource wastage (Simao et al., 2021). The mining industry is being challenged by environmental regulations and public awareness to employ eco-friendly and cost-effective waste reduction and recycling methods (Politis et al., 2017). As a result, numerous studies are looking into sustainable ways of managing these waste materials by identifying various application areas to lessen the disposal problems. The concept of utilizing mining waste holds the fundamentals of enhanced reuse, recycling, reprocessing, and creating value-added products from waste as an alternative waste management method, thereby enhancing the circular economy (Kinnunen et al., 2022). Afum et al. (2019) highlighted that based on the rate at which resources are being used up, the world will need more resources than are available today. On that account, using mining waste will not only reduce solid waste and environmental contamination but also enhance the conservation of natural resources by providing a new source of resources.

The development of new materials has led to technological advancement, particularly in the construction sector (Forcael et al., 2020). The use of composite materials has made a significant contribution to these developments. Composite materials are defined as solid materials that result when two or more different substances, each with its characteristics, are combined to create a new substance (Mehta & Monteiro, 2014; Unal, 2012). The properties of the composite material are usually governed by the properties of individual constituents.

In this research, Platinum Group Metals (PGM) furnace slag, mining waste from Zimplats, is combined with a suitable binder to develop sustainable composite construction materials. This is in support of the vision of the Ministry of Water, Environment and Climate Change under the Environmental Management Agency (EMA) of Zimbabwe which is aimed to ensure the sustainable management of natural resources, protection of the environment, and prevention of pollution and environmental degradation as well (*Environmental Management Act [Chapter 20:27]*, *2002*). This vision can be achieved through waste recycling and reuse. The use of mining waste in infrastructure development promotes the sustainability of the mining industry, at the same time enhancing a green and sustainable construction industry.

1.2 Background

Mining companies generate lots of waste from the extraction, processing, and refining of minerals (Liu et al., 2021), and in most cases, the waste is poorly managed. The accumulation of this type of waste with no end use can pose significant environmental and health hazards to society (Simao et al., 2021). Mine dumps occupy space that could be utilized for agricultural, industrial, and residential purposes. Of particular interest, is Zimplats which is the largest PGMs producer in Zimbabwe with approximately 2.8 billion tonnes of PGM ore reserves along the great dyke belt alone (Samanga & Abe, 2019). Zimplats is a subsidiary of Implats, the world's leading South African-based producer of PGMs. In the year 2000, Zimplats took over Minerals International Exploration Inc.'s share of Hartley Mine and is now 87% owned by Implats and 13% by independent shareholders (Zimplats, 2022). At present, Zimplats owns and operates five underground mines that supply ore to four concentrator plants for processing and smelter for further refinery. The ore production for 2022 was approximately 7.1 million tonnes (Zimplats, 2022), and an increase in ore production is anticipated with the expansion of mining activities. Zimbabwe is ranked third globally in PGMs production with a total estimation of

6.83% of the world's reserves, South Africa is the leading producer with a total estimation of 68.32% of the world's reserves and Russia sits in the second position with a total estimation of 15.52% of the world's reserves (Hughes et al., 2021; Connor & Alexandrova, 2021).

At PGM mines, waste from concentrators and smelters is usually disposed of in tailings dams and slag dumps (Glaister & Mudd, 2010). A greater proportion of PGM ores become solid waste due to the relatively low grade of the precious minerals, which is a few grams per tonne (Mudd, 2012). This highlights the importance of controlling waste on the surface environment. Most PGM ore is sourced by underground mining and the ratio of metal-ore is low for opencast mining (Glaister & Mudd, 2010). Zimplats has two major waste disposal facilities namely Ngezi and Selous Metallurgical Complex tailings storage facilities with a storage capacity of 423 ha and 110 ha, respectively (Zimplats, 2022). Studies by Anglo American Platinum suggest that, though tailings have low acid and metalliferous drainage potential, active environmental management is required to prevent impacts on water sources, especially in areas where local communities depend on water sources adjacent to mining projects (Mudd, 2012). Zimplats has recognized that the scale of its operational activities has inevitable impacts on the environment through land disturbances, resource consumption, and pollution (Gwimbi & Nhamo, 2016). Therefore, research on the utilization of waste is being explored to mitigate, minimize, and remediate these environmental impacts. This project explores the feasibility of utilizing PGM slag in developing sustainable composite materials for the construction industry. The development of sustainable composite construction materials is geared to address environmental degradation as a result of the increased demand for construction raw materials due to the rapid increase in population, urbanization, and development.

1.3 Problem Statement

PGM mining companies in Zimbabwe generate lots of waste annually, and a continuous increase in waste generation is anticipated due to the expansion of mining activities. The relatively low grade of the valuable mineral in PGM ores, that is a few grams per tonne, means that a greater percentage of the ore becomes solid waste (Mudd, 2012). According to Zimplats (2022), a total generation of 6.739 million tonnes of tailings, 154 kilo-tonnes of slag, and 70 kilo-tonnes of waste rock were recorded for the year 2022. These large volumes of tailings, slags, and waste rock are accumulated in tailing dams, slag dumps, and or waste rock piles with little or no beneficial use, taking up a lot of space that could be utilized for forestry, agricultural, industrial, and residential purposes. PGM slag poses significant environmental and health hazards to the nearby community as it causes air, land, and water pollution. Drainage water from tailings also finds its way to water bodies resulting in groundwater contamination thereby affecting aquatic life.

1.4 Justification

The utilization of PGM slag to produce sustainable composite construction materials promotes the sustainability of the mining and construction industries. It lessens the disposal challenges and enhances the conservation of natural resources. In addition, the slag is readily available from the local mining industry. Given the high demand for building materials supplies, slag provides an alternative, new low-cost source of raw materials for the construction industry. Waste generation is inevitable in the mining industry, however, the evaluation of the potential uses of these wastes in the construction industry is considered to be the most feasible solution to disposal challenges.

Moreover, at present, clay brick is the predominantly used type in the construction industry, and clay excavation is costly. The quarrying of earth-based clay as a raw material in brick earth can lead to land degradation. Thus, the utilization of PGM slag in brick manufacturing helps conserve clay as a natural resource, reduces clay mining costs, and minimizes environmental impacts. This reduces the overall cost of the brick since there is a very low cost in terms of raw materials abstraction.

1.5 Objectives

1.5.1 Main Objective

To develop a sustainable composite construction material from PGM furnace slag (Zimplats slag).

1.5.2 Specific Objectives

1. To determine the physical and chemical characteristics of Zimplats PGM furnace slag and clay binders (Chinhoyi and Zvishavane clay).
2. To fabricate sustainable composite building materials utilizing Zimplats PGM furnace slag combined with Chinhoyi and Zvishavane clays.
3. To assess the physical and mechanical properties of the fabricated composite building material.

1.6 Scope of the Study

This project investigates the feasibility of utilizing PGM furnace slag from Zimplats combined with earth-based clay to produce a composite material that can be used in the construction industry. The areas to be covered during this project are:

- Characterization of PGM slag (XRF analysis, Sieve Analysis, Specific Gravity).
- Characterization of clay (XRF analysis, Sieve Analysis, Specific Gravity, Atterberg Limits).
- Preparation of several weight percent combinations of PGM slag and clay.
- Brick manufacturing from PGM slag combined with clay as the binder to the slag.
- Assessment of the physical and mechanical properties of the manufactured bricks (Hardness Test, Soundness Test, Water Absorption Test, Compressive Strength Test, Efflorescence Test).

All the laboratory tests were carried out following the American Society for Testing and Materials (ASTM) and Indian Standards (IS) international guidelines. Several tests are performed on the manufactured bricks as part of quality control to meet the requirements of the end user, and to investigate their strength for intended use to avoid consequences during their lifetime use.

1.7 Chapter Summary

Chapter 1 discusses the estimated annual mining waste generation, particularly at Zimplats, the leading PGM producer in Zimbabwe. The waste disposal challenges faced by mining organizations and the risks that they pose to the environment and human health are also discussed. A statement of the problem has been concisely provided. This chapter addresses how the current research contributes to the fundamentals of enhanced reuse, recycling, reprocessing, and creating value-added products from waste as an alternative waste management method. The main objective of the study together with the specific objectives are outlined in this section. This chapter concludes by describing the variables being investigated and outlining the methodologies that will be used to conduct the research.

CHAPTER 2

LITERATURE REVIEW

2.1 Introduction

The mining industry is expanding at a very large scale due to rising living standards and technological innovations. One of the ultimate challenges facing the mining industry is the disposal of waste, predominantly slags and tailings. Mining activities generate a significant amount of waste which finds itself lying idle in spaces that could have been used for other beneficial purposes. Researchers are moving towards sustainable ways of managing these waste materials in various areas of application to lessen the disposal problems. At the same time, the construction industry in modern times has grown into a multibillion-dollar industry. Following the growth of the construction industry, the rate at which building materials are being consumed is escalating resulting in increased demand. Of particular interest within the construction industry are bricks, as they are the common masonry units of almost every structure (Babu & Krishnaiah, 2018). Due to the rapid increase in population, urbanization, and global development, the demand for bricks is accelerating (Bhairappanavar et al., 2021). Bricks are a good example of composite materials and their manufacturing must be done in a sustainable way. Since waste generation is inevitable in the mining industry, evaluating the potential uses of waste in brick manufacturing is considered the most feasible solution to disposal problems. The utilization of earth-based clay material in the manufacturing of construction materials has resulted in resource depletion and environmental degradation. Therefore, various types of mining waste which include slags, tailings, bauxite residues, waste rocks, fly ash, sludge, and coal gangue have been explored as raw materials in the manufacturing of construction materials (Ahmari & Zhang, 2012; Fang et al., 2011; Klauber et al., 2009; Luo et al., 2016, 2020; Oluwasola et al., 2014; Wei et al., 2021; Xiaolong et al., 2021; Xu et al., 2017; Yellishetty et al., 2008; Yonggang et al., 2011). The application of mining waste in the construction industry has been targeted to reduce the number of natural resources extracted as raw materials in new products.

2.2 Composite Materials

Composite materials are solid materials consisting of two or more different substances, combined to create a new substance (Mehta & Monteiro, 2014; Unal, 2012). Each component displays diverse physical or chemical characteristics and the composite material exhibits synergistic properties, not observed from the individual constituents. The individual constituents can be natural or synthetic and are often fused at the interface. The matrix and the reinforcement are the two primary categories of constituent materials needed to create composites (Dawoud & Saleh, 2019). The matrix embraces and supports the reinforcements by maintaining their relative positions. The reinforcement imparts its distinctive chemical and physical features, thus enhancing the mechanical properties of the matrix. The limitless number of binders and reinforcements alongside technological advancement can enable researchers to create tailor-made composites (Dawoud & Saleh, 2019; Park & Seo, 2011). Composite materials often demonstrate several advantageous characteristics; which include, high strength, low density, and cost-effectiveness as they can use locally accessible components in their making.

Bricks can be classified as composite materials since they are made from two or more materials with significantly different properties. They usually consist of clay, sand, water, and sometimes additives. Each raw material contributes to the overall properties and behavior of the final product, determining its strength and suitability for various construction applications. In recent research by Dawood et al. (2021), composite bricks were made from combined mud, sand, and straw. With this combination, straw provided tensile strength, the compressive strength was provided by mud, and sand was a stabilizer to reduce the volumetric changes. The finished brick possessed excellent properties with improved resistance to tearing and wearing. Composite bricks offer several benefits that make them versatile for many construction projects (Dominguez-Santos et al., 2019). Composite bricks can increase the load-carrying capacity of walls, and enhance the seismic performance of structures. The bricks can be lighter and hence reduce the self-weight of structures. The work focuses on developing sustainable composite construction materials, particularly bricks, from mining waste combined with earthbased clay.

2.3 Bricks

Brick is considered one of the most used masonry unit globally (Babu & Krishnaiah, 2018; Bhairappanavar et al., 2021; Rahman et al., 2014). Bricks are a versatile and sustainable building material, which when combined with good building design, are highly durable, require low maintenance, exhibit high thermal mass, and provide a healthy and comfortable environment (Ibrahim et al., 2015). The continuous development of various types of bricks is being explored worldwide, along with skillful methods being adapted during the manufacturing process. Kadir & Mohajerani (2011) highlighted that bricks are considered superior building units due to the following properties: high strength, fire resistance, durability, and satisfactory bonding with mortar. Investigations have been conducted on bricks, and it has been observed that brick structures are the most preferred since bricks have a cooling effect during hot weather and insulate the house against heat loss during the winter season (Binici et al., 2007; Vijayan et al., 2021).

2.3.1 Classification of Bricks

Bricks can be categorized according to their material composition, based on quality, and the manufacturing process, each with distinct properties and applications. This section dwells on brick types based on constituent raw materials.

2.3.1.1 Clay Bricks

Clay brick is the most common type of brick, which is manufactured from clay soil and water. The manufacturing process involves molding the bricks into the desired shape, drying them, and firing them in a kiln at high temperatures to attain strength (Fernandes et al., 2010). For thousands of years, clay bricks have been successfully employed as construction products, and have proven to be fundamental materials for modern architecture due to their outstanding engineering properties (Kadir & Mohajerani, 2011). Clay bricks are known for their hardness and durability and hence can withstand wear and tear. They provide good insulation which allows buildings to remain warm during winter and cool during summer. These properties make clay bricks a reliable material for constructing load-bearing exterior walls, columns, chimneys, facades, and pavements.

2.3.1.2 Cement Bricks

Cement bricks are prepared from cement, sand, coarse aggregates, and water (Samad et al., 2021). They are cast in designated molds, dried, and then cured with water to achieve their strength. Cement bricks are durable, resistant to moisture damage, and fire resistant. They can be preferable for constructing structural walls, facades, and pavements.

2.3.1.3 Fly Ash Bricks

Fly ash bricks are made by mixing fly ash, gypsum, lime, sand, and water. Fly ash is a fine powder that remains from incomplete combustion of coal (Sultana et al., 2021). Hydrated lime and gypsum are employed as the binder materials. Fly ash bricks are molded, dried, and then cured for approximately 28 days giving strength to the bricks. They are environmentally friendly as they incorporate waste from coal combustion. Fly ash bricks are lightweight and thus reduce the self-weight of structures (Sahu & Singh, 2017). They provide good thermal insulation, absorbing less heat which helps keep cool in summer. Fly ash brick has an average weight of 2.6 kg and a compressive strength of 7.5 MPa. Fly ash bricks are often used to construct load-bearing exterior walls, paving, and interior walls.

2.3.1.4 Calcium Silicate/ Sand-lime Bricks

Sand lime bricks are made of sand, lime, and water. The bricks are molded using a rotary table press and then placed in an autoclave where saturated steam pressure is released (Kamal, 2023). Chemical reactions are allowed to take place whereby silica reacts with calcium to form calcium hypo silicate crystals which gives strength to the brick. Pigments can be added to sand and lime during mixing to give color to the bricks. Calcium silicate bricks provide good aesthetics, have good insulation properties, and are durable with a compressive strength of about 10 MPa. Sand lime bricks have found applications in the construction of fireplaces, facades, and ornamental works in buildings.

2.3.1.5 Magnesia Bricks

Magnesia brick is a refractory brick made of periclase as the primary crystal structure (Kujur et al., 2018). Periclase is a magnesium mineral that is found often in metamorphic rocks. Magnesia bricks can be classified into two types based on the manufacturing process: burnt magnesia bricks and chemically bonded magnesite bricks. Burnt magnesia bricks are made by firing magnesite clinker at temperatures over 1600 °C whereas chemical-bonded magnesite bricks are made by combining magnesia with a chemical binder, forming, and drying (Landy, 2004). Magnesia bricks are renowned for their high refractoriness and good resistance against corrosion and thermal shock. These attributes have facilitated their application in hightemperature applications, including incinerators, cement kiln lining, and furnace lining.

All types of bricks exhibit excellent properties, however, there has been a noticeable spike in land degradation over the past years, due to the increased demand for natural resources by an ever-increasing population. This has incentivized researchers to explore the applicability of waste in various construction activities, particularly in the production of building materials.

2.4 Mining waste

The waste from mining and quarrying activities is considered to contribute mostly to the total global waste streams (Sezgin, 2020). The mining and mineral processing activities generate a significant amount of waste annually with an estimation of over 100 billion tonnes worldwide and a continuous increase is anticipated due to the expansion of the mining activities (Araujo et al., 2022; Tayebi-Khorami et al., 2019). Mining waste is undesirable and unprofitable solid or liquid materials that build up at or close to a mine site (Hudson-Edwards et al., 2011). The accumulation of mining waste in tailing dams, slag dumps, or waste rock piles without effective management poses serious risks to the environment and human health (Simao et al., 2021).

2.4.1 Classification of Mining Waste

The mineral resource being mined, the processing techniques used, and the geology of the mining site all have an impact on the type, volume, and characteristics of waste generated (Manyuchi et al., 2019). Waste material from mining activities is obtained at different stages during processing and can be classified into five major groups which are overburden, waste rock, tailings, sewage sludge, and slags (Politis et al., 2017). Generally, slags, tailings, and waste rock are produced in large volumes, thus, to avoid significant negative effects on the environment, society, or the economy, they require active assessment, planning, and management (Yilmaz, 2011).

2.4.1.1 Overburden

Comprises soil and rock removed to enable access to the ore mineral reserves at an open pit mine (Gayana & Chandar, 2018; Politis et al., 2017). It is estimated that the overburden-ore ratio for surface mining of metal ores generally ranges from 2:1 to 5:1 depending on the local conditions (Yellishetty et al., 2008). It is usually stacked on the surface at mine sites where it does not hinder future mining operation expansions since it costs to move large volumes of material. Overburden can be used for land restoration during mine closure, with little to no negative influence on the environment. Figure 2.1 demonstrates overburden waste that has been removed to gain access to the mineral deposits at a mine site.

Figure 2.1: Overburden Waste at a Mine Site (Seo, 2024)

2.4.1.2 Waste Rock

Is the excavated material, primarily rocks with mineral concentrations that are considered to be too low for commercially profitable extraction (Gayana & Chandar, 2018; Politis et al., 2017). They are piled up at the mine site where they do not interfere with mining activities. The reprocessing of waste rock to recover minerals that could have been overlooked during the initial processing can be sustainable in the event mineral values spike. Waste rock dumps can be used for land recovery upon post-mining closure. Figure 2.2 shows waste rock management at a mine site.

Figure 2.2: Waste Rock Management at a Mine Site (Earth Systems, 2018)

2.4.1.3 Tailings

These are waste materials made of finely crushed rock and minerals that remain after extracting precious minerals (Politis et al., 2017). They are typically discharged through slurry pumps into tailing dams as water-based slurry and contain the remnants of processing chemicals as shown in Figure 2.3. Tailing dams are waste-holding ponds surrounded by barriers and liners to collect and confine the slurry. Usually, the source material has a significant impact on the quality and composition of the tailings generated (Ndlovu et al., 2017). This can make mining tailings a potential environmental hazard, thus careful handling during transit and disposal is essential. Tailings can be vaporized and recycled into valuable products which include low carbon geopolymer concrete, mineral fertilizers, and construction materials. Figure 2.3 illustrates tailings discharged through slurry pumps into tailing dams.

Figure 2.3: Tailings Discharged into Tailing Dams (Schmidt, 2021)

2.4.1.4 Sewage Sludge

Mining sewage sludge is the viscous residue produced during the wastewater treatment processes at a mine site (Gayana & Chandar 2018). It entails the compounds that have been added to increase the effectiveness of the process and trace elements of the processed minerals. Sewage sludge has very low economic value and hence can be handled as waste. Sewage sludge can be dewatered and utilized for agriculture or landscaping purposes as it may contain valuable organic substances that promote plant growth (Ding et al., 2021). In extreme cases, sludge can be classified as hazardous waste as it may contain harmful or radioactive material hence special handling and disposal methods are required (Xiong et al., 2019). Figure 2.4 shows sewage sludge during wastewater treatment.

Figure 2.4: Sewage Sludge (MacDonald, 2017)

2.4.1.5 Slags

Slag is produced as a by-product in metallurgical processes, during smelting, converting, and refining (Fisher & Barron, 2019; Pribulova & Futas, 2016). Slags are frequently associated with ashes produced from the cleaning of furnaces or smokestacks. Figure 2.5 shows slag accumulated at a mine site.

Figure 2.5: Slag Accumulated at a Mine Site (Jernigan, 2017)

The chemistry and mineralogy of slags are dependent on the metallurgical processes that generate the material and will influence its fate as waste or as a reusable product (Piatak et al., 2015; Potysz et al., 2015). Substantial amounts of slag are generated during metal smelting. Thus, there is a need to understand the potential environmental impacts of slag and its role as a valuable resource. Slags can be classified into three categories according to their origins and characteristics, namely: ferrous slag, non-ferrous slag, and incineration slag (Fisher & Barron, 2019). Nowadays, slags have found extensive applications in civil engineering works such as the building industry, road construction, cement production, landfill daily cover, and soil reclamation. Due to technological advancement and the use of waste materials in the construction industry being on the rise, the application of both ferrous and non-ferrous metallurgical slags in the manufacturing of building materials has received great attention with environmental and economic benefits. Several global slag institutions which include the Harsco National Slag Association, the European Slag Association, the Nippon Slag Association, the Australasian Slag Association, the Slag Cement Association, and the Brazil Steel Institute focus on promoting the use of slag, predominantly ferrous slag which is generally considered for use in construction and environmental applications.

Ferrous Slag

Ferrous slag is generated during the production and casting of iron and steel from natural ores or recycled materials (Biswal et al., 2020; Piatak et al., 2015). It consists mainly of impurities of iron ores (predominantly silicon and aluminium) fused with calcium and magnesium oxides. Depending on the production process and furnace used, there are generally two types of ferrous slag, known as blast furnace slag and steel slag. Blast furnace slag is generated during the melting and reduction of iron ore in a blast furnace, while steel slag is produced during the conversion of molten iron into steel (Horii et al., 2013; Oluwasola et al., 2014; Piatak et al., 2015). Blast furnace slag is further classified into different types based on the cooling method employed. Unlike blast furnace slag, steel slag is cooled naturally under ambient conditions, but is further classified according to the furnace used during steel production. The three types of steel slag are basic oxygen furnace slag, electric arc furnace slag, and ladle furnace slag (Biswal et al., 2020; Horii et al., 2013). The rate and method of cooling affect the properties of the slag, influencing its commercial use as a useful resource. The hard and dense nature of the air-cooled ferrous slag makes it suitable as a construction aggregate. Table 2.1 describes the cooling methods of molten blast furnace slag and their respective properties.

Table 2.1: Properties of Blast Furnace Slag (Horii et al., 2013; Piatak et al., 2015)

Method of cooling	Description	Properties of the slag
Air-cooled	slow cooling under atmospheric conditions	crystalline and vesicular
Expanded or foamed	moderate cooling with the use of controlled amounts of water	porous crystalline and glassy material
Pelletized	quick cooling in the air	glassy and crystalline pellets
Granulated	quenching with high-volume, high-pressure sprays of water	vitrified granules

Non-ferrous Slag

Non-ferrous metallurgical slags are generated during the recovery and processing of nonferrous metal from natural ores or recycled metal-containing wastes (Nakamura, 2015; Piatak et al., 2015; Piatak & Ettler, 2021). The non-ferrous slags are molten by-products of hightemperature processes that are used to separate the non-ferrous metal from other constituents. As a result of the melting of non-ferrous metals, iron, and silicon are separated to form a silicon-based slag. Upon cooling, the molten slag converts into a granular material. The most common non-ferrous slags are those originating from the processing of copper, gold, nickel, phosphorus, lead, and zinc (Piatak & Ettler, 2021). The chemical properties of these slags depend on several factors, including the quality of ores, extraction technologies, flux additions, smelting conditions, and cooling processes whilst the physical properties are determined by the rate and method of the cooling (Marsh et al., 2021; Piatak, 2018; Potysz et al., 2015; Tian et al., 2021). Non-ferrous slags are normally cooled either under atmospheric conditions or quenched in water (Tripathy et al., 2020). Air-cooled slags are hard and dense, have a porous structure (due to gas escaping), and contain crystalline phases (Shi et al., 2022). Regarding water-quenched slags, the molten slag is rapidly cooled with high-volume and high-pressure sprays of water in a spinning container, resulting in slag particles having a smooth surface texture and rounded shape (Marsh et al., 2021). The rate of cooling has a significant effect on the physical and cementitious properties of the non-ferrous slags. Granulated slags, produced by rapid quenching of the molten slag, are more vitreous and reactive than similar air-cooled slags (Sadek, 2014; Tripathy et al., 2020). Granulated slags solidify to small and uniform particles whereas air-cooled slags harden to a bulky mass. When added to concrete, the cementitious qualities of granulated slag aid in enhancing the strength of concrete. Table 2.2 lists some of the most common non-ferrous slags, the cooling methods, and their corresponding properties.

Table 2.2: Properties of Non-ferrous Slags (Ciocan, 2012; Kumar et al., 2022; Marsh et al., 2021; Sadek, 2014; Tripathy et al., 2020)

Name of Slag	Method of cooling	Description
Copper Slag	Air-cooled	• Black with a glassy appearance • The specific gravity varies with iron content, from as low as 2.8 to as high as 3.8
	Granulated	• Regularly shaped, angular particles • More porous and consequently has lower specific gravity than air-cooled copper slag
Nickel Slag	Air-cooled	• Angular particles that have a smooth, glassy texture and are brownish-black in color • The specific gravity may be as high as 3.5
	Granulated	• Angular, glassy slag which is black • More porous, with lower specific gravity than that of air-cooled
Phosphorus Slag	Air-cooled	• Black to dark grey, glassy, and of irregular shape • Distinct particles are commonly flat and elongated, with sharp fracture faces similar to broken glass
	Granulated	• Regularly shaped, angular particles • More porous than air-cooled slag and therefore has a lower specific gravity
Lead, Zinc, Slag	Air-cooled	• Black to red with a glassy appearance. Consists of sharp, angular particles that are cubical
	Granulated	• Regularly shaped, angular particles • Porous with a specific gravity of less than 2.5

2.4.2 Disposal Methods of Mining Waste

Disposal refers to the accumulation of large amounts of waste in a concentrated area, and it is usually the least preferred option for waste management at mining operations (Adiansyah et al., 2015; Araujo et al., 2022). The disposal of mining waste represents the operating cost of a mining operation. For this reason, mining waste has been disposed of at the lowest cost, often resulting in considerable environmental impacts. In some cases, waste material is directly discharged onto the land without any containment or directly into rivers that are as close as possible to the mine sites without consideration of environmental effects, hence the need for proper disposal methods (Hudson-Edwards et al., 2011). The common methods of mining waste disposal are tailing dams, slag dumps, underground filling, and deepwater disposal.

2.4.2.1 Tailing Dams and Slag Dumps

Tailings dams and slag dumps are the predominant deposition methods of fine tailings and slags from ore grinding (Araujo et al., 2022). The principle behind tailing dams and slag dumps is to dispose of waste material in an optimized, accessible, and environmentally friendly manner, allowing its future reprocessing with the advancement of new technologies (Lebre et al., 2017; Morrison, 2022). There are potential risks associated with the stability of tailing dams following the recent spectacular incidents of Aznalcollar (Spain) in 1998 and Aurul (Romania) in 2000 (Sima & Morosanu, 2022). The Aznalcollar tailings dam failure was a result of high pore pressures caused by the incomplete consolidation of the dam foundation, releasing 5.5 million m^3 of pyrite and pyroclastic tailings (Marti et al., 2021). Aurul tailings dam failure was caused by the overflow following the heavy rain and snowmelt, spilling 100,000 m^3 of cyanide-contaminated liquid (Vaszita, 2014). Therefore, careful evaluation should be developed and applied during the design, construction, and operations progressions.

2.4.2.2 Underground Filling

An underground filling is a method of storing tailings, slags, and sludge which may contain hazardous substances below the ground to reduce surface environmental impacts (Wu et al., 2011). It is the most expensive method of mining waste disposal, and it can only be implemented where there are no nearby aquifers. This method is usually applied when geological stability and safety in operations are required.

2.4.2.3 Deepwater Disposal

Deepwater disposal consists of the deposition of tailings and solid waste directly into underwater marine bodies (Franks et al., 2011). This method has been used in past operations and is now receiving restrictions due to the significant pollution of the receiving waters and the possible adverse impacts on the livelihoods of the local communities (Stauber et al., 2022). In contrast, Araujo et al. (2022) and Dold (2008) highlighted that underwater conditions favor the geochemical stabilization of sulphide mineral residue, therefore an appropriately designed underwater disposal of sulphidic tailings is an ideal solution with water levels controlled.

2.4.3 Characterization of Mining Waste

Mining waste is increasingly utilized in making construction materials (Nakamura, 2015; Oge et al., 2019; Piatak et al., 2015). The characteristics of the mining waste are used to assess its potential to release pollutants into the environment and its feasibility as a resource. The mineralogical composition and phase grains within mining waste are quite different, dependent on several factors such as the type of ores processed, the type of furnaces used, and the cooling methods (Jiang et al., 2018; Liao et al., 2011; Potysz et al., 2015). For furnace slags, a lower cooling rate results in the formation of larger crystallized mineral phases. Rapid cooling produces a glassy, non-crystalline slag which is more homogeneous in metal distribution. These properties of furnace slag have a great influence on its use as a beneficial resource.

To evaluate the capability of mining waste for recycling in the building industry, a comprehensive characterization can be made through the usual physicochemical methods which include; X-ray fluorescence for chemical analysis, X-ray diffraction for mineralogical analysis, sieve analysis for material gradation, and specific gravity for determination of the quality of aggregates. An overview of the physicochemical techniques for characterizing mining waste is given in the following sections.

2.4.3.1 X-ray Fluorescence

X-ray fluorescence (XRF) is a non-destructive method for the elemental analysis of solids and liquids and determines the relative concentration of the elements within the sample under investigation (Hou et al., 2004; Krishna et al., 2008; Rawat et al., 2022; Takahashi, 2015). XRF can be successfully employed to establish quantitative chemical analysis for environmental research studies. During the characterization of mining waste, XRF can be employed to assess the presence of heavy or radioactive metals as they can be life-threatening to humans and the environment. Instruments with high sensitivity and stability are crucial for the accurate determination of the elemental composition of a material.

2.4.3.2 X-ray Diffraction

X-ray diffraction (XRD) is a technique used to establish the crystallographic structure of a material (Bunaciu et al., 2015; Epp, 2016). When characterizing mining waste, XRD analysis provides comprehensive information on its crystal structure and mineralogical makeup, which subsequently provides insight into its behavior in construction-related applications. The XRD technique produces a distinctive pattern known as a diffractogram, which is used to detect crystal deformation, quantify crystallite size, identify minerals, and determine atomic layer thickness.

2.4.3.3 Specific Gravity

Mining waste consists of solid particles and voids that can be filled with air or water. The specific gravity (SG) of a sample refers to the ratio of the unit weight of solid particles at a specified temperature to the unit weight of distilled water at the same temperature (Craig, 2004; Ranjan & Rao, 2011). Specific gravity is correlated to the density of mineral composition, and the formation of a material.

2.4.3.4 Sieve Analysis

Sieve analysis also known as the gradation test is a procedure used to evaluate the particle size distribution of aggregated material (Liu et al., 2019). The particle size of the waste can affect the compressibility, permeability, and workability of the material and the properties of the finished product. The texture of a material is defined by its appearance, which depends on the relative sizes and shapes of the particles. The suitability of a material for a particular use in the construction industry is often dependent on the distribution of the grain size in the material masses (Oyelami & Rooy, 2016).

2.4.4 Application of Mining Waste in Brick Manufacturing

Due to the rapid increase in population, urbanization, and development, there is an increased demand for construction materials. Utilizing earth-based resources in making construction materials has resulted in resource depletion and environmental degradation. Therefore, different types of waste have been investigated for recycling or incorporation as raw materials in brick manufacturing. Each year, the mining industry generates large amounts of waste, representing a plentiful new source of raw materials for the building and construction sector (Ndlovu et al., 2017). The channeling of mining waste towards the production of building materials provides the most feasible solution to disposal problems. The manufacturing of building materials stands out as an application that has the potential to consume a significant volume of mining waste (Klauber et al., 2011). Several nations, like China, have begun to restrict the utilization of clay-based bricks to safeguard the environment and promote sustainable development. Instead, they are promoting the development of eco-friendly building materials and techniques (Ahmari & Zhang, 2013). The following parameters should be considered when making building materials from mining waste: raw material composition, curing conditions, production processes, product quality, and environmental effects. Mining waste is generally non-plastic and cannot be used alone to make bricks. Various additives have been introduced to the waste as binding agents. An overview of the use of mining waste brick manufacturing is given in the succeeding sections.

2.4.4.1 Iron Mining Waste

The demand for steel and iron in the construction industry has led to an increase in iron ore mining activities (Zhang et al., 2021), which in turn generates a lot of iron tailings. According to estimates from iron mining companies, for every tonne of iron ore mined, two tonnes of iron tailings are removed, implying a larger quantity of waste that could be converted into a resource (Kuranchie et al., 2016). The effective utilization of iron ore tailings in brick manufacturing has gained interest on a global scale (Luo et al., 2020). Iron ore tailings primarily contain silica, iron oxides, and alumina and this composition qualifies them as raw materials in the civil construction industry (Yellishetty et al., 2008).

Kuranchie et al. (2016) presented an economical and sustainable technique for utilizing iron ore tailings to make bricks through geopolymerization. Geopolymerization is the process whereby aluminosilicates react in a highly concentrated silicate solution or alkali hydroxide to generate a stable geopolymer, which has amorphous polymeric structures (Ahmari & Zhang, 2012). Kuranchie et al. (2016) introduced sodium silicate to the iron tailings which serve as an activator in the manufacturing process. The reaction between the alumino-silicate minerals from tailings and the sodium silicate activator enhances the strength of the geopolymer bricks

(Diop & Grutzeck, 2008). The following parameters were considered to achieve high-strength bricks: sodium silicate concentration, curing temperature, and curing time. Kuranchie et al. (2016) revealed that 19.18 MPa compressive strength can be achieved with 31% sodium silicate by weight at 80 ℃ curing temperatures for one day. In their report, they highlighted that the geopolymerization method conserves energy as it eliminates high-temperature kiln firing. The researchers also reported that the strength of their prepared bricks satisfied the ASTM and the Australian Standards requirements.

Zhao et al. (2012) investigated the possibility of utilizing hematite tailings combined with lime and sand to prepare hematite tailings autoclaved bricks. Brick specimens were prepared with 15% moisture and 20 MPa forming pressure. The strength of the bricks was enhanced by steam autoclaving at a pressure of 1.2 MPa for six hours. The experimental outcomes from this study revealed that a mixing combination of 70% hematite tailings, 15% lime, and 15% sand could yield a compressive strength of 21.2 MPa and 4.21 MPa flexural strength. According to Zhao et al. (2012), the hematite tailings autoclaved bricks prepared with this combination complied with the GB 11945-1999 Chinese standards for autoclaved lime-sand brick. During brickmaking, the hydration reaction between lime and the siliceous material as shown in Equation 2.1 enhances the compressive strength of hematite tailing autoclave bricks. From their chemical composition analysis, it was observed that hematite tailings have low silica content hence, introducing sand increases the silica content, thus facilitating the hydration reaction.

$$Ca(OH)_2 + SiO_2 + H_2O \rightarrow CaO.SiO_2 \cdot 2H_2O \qquad 2.1$$

Research conducted by Chen et al. (2011) utilized hematite tailings to manufacture non-fired bricks. The tailings were mixed with cementing materials, coarse aggregates, and water and then fed in a hydraulic press to produce molded green bricks. The molded green bricks were cured in determined conditions to enhance their mechanical strength. According to Singh & Kapur (2008), steam curing may accelerate the rate of cement hydration and catalyze the reaction between silica and aluminium in raw materials. For optimal mechanical strength of the bricks, the following factors were accounted for: the hematite tailings composition, the forming moisture content, forming pressure, and the curing environment. The findings from this research indicated that a compressive strength of 15.9 MPa can be attained with 78% hematite tailings prepared with 15% water content and 20 MPa forming pressure, and cured for 28 days at room temperature. Chen et al. (2011) reported that the properties of the nonfired hematite tailing bricks conformed to the Chinese standards for non-fired rubbish gangue bricks (JC/T422-2007).

2.4.4.2 Copper Mining Waste

The demand for copper in the construction industry, medicals, electrical grids, and energy storage applications has increased copper mining operations globally (Bragagni & Xhaferraj, 2021). These copper mining activities generate a significant volume of tailings and slag of which disposal is the major challenge. According to Gabasiane et al. (2021), the annual global production of copper generates approximately 24.6 million tonnes of copper tailings and 4.5 million tonnes of copper slag. There has been extensive research on making building materials from copper mining waste. The waste is rich in silica, alumina, and iron and with this chemical composition, it has been successfully used in the construction industry.

Nikvar-Hassani et al. (2022) researched the feasibility of utilizing copper tailings and slag to produce green bricks with geopolymerization technology. To attain optimum geopolymer brick properties, the following attributes were investigated: alkaline concentration (NaOH), water content, forming pressure, and curing temperature. The reactivity of copper tailings for the geopolymer synthesis was determined by the solubility of silica and aluminium in the alkali solution. In their experiments, Nikvar-Hassani et al., (2022) discovered that copper tailings alone could not produce strong geopolymer bricks due to the low silica and aluminium content. Copper slag was introduced as an additional cementitious material because of its high silica and iron content, to enhance the geopolymerization of the tailings. The results from this study revealed that a compressive strength of 24.3 MPa can be achieved with 10wt.% slag, 10 M NaOH concentration, 14% water content, 20 MPa forming pressure, and seven days of curing at 90 °C. According to Nikvar-Hassani et al. (2022), the geopolymer brick properties satisfied the ASTM standards. The researchers highlighted that, when using the geopolymerization method of brickmaking, the relationship between the forming pressure and water content is critical. Higher forming pressure for a specific moisture content can result in more compact, denser, stronger geopolymer bricks. However, applying high pressure on excessive water content can squeeze out the alkaline solution, reducing the strength of the bricks.

Ahmari & Zhang (2012) explored the possibility of using copper mine tailings in brick manufacturing employing the geopolymerization technique. The copper tailings geopolymer bricks were made by mixing the tailings with a sodium hydroxide solution, compressing the mixture in a mold, and curing the final product. This brick-making technique neither uses clay nor requires high-temperature kiln firing, thus conserving natural resources and energy. To achieve the optimum strength, the following parameters were accounted for: NaOH concentration, forming moisture content, forming pressure, and curing temperature. In their experiments, Ahmari & Zhang (2012) achieved an optimal compressive strength of 33.7 MPa with 15 M NaOH concentration, 18% water content, 0.2 MPa forming pressure, and 90 ℃ curing temperatures. The researchers highlighted that this water content was adequate to develop a geopolymeric binder that bound the partially reacted particles and served as a medium for the geopolymeric reaction. However, excess moisture leads to the formation of big pores, which weakens the entire brick. The curing temperature was maintained at 90 ℃ maxima because too high temperatures could lead to rapid water evaporation and perhaps incomplete geopolymerization. Ahmari & Zhang (2012) concluded that copper tailings can be used to make eco-friendly geopolymer bricks that conform to the ASTM requirements.

Fang et al. (2011) investigated the use of copper tailings to partially substitute river sand in making autoclaved sand-lime bricks. During the preparation of the autoclaved bricks, grounded lime served as the cementing agent that binds copper tailings and sand together. The proportion of lime had a decisive effect on the properties of the brick since it was the main reactant to form hydrated calcium silicates. The copper tailings autoclaved brick specimens were prepared with a lime-sand ratio of 2.0 and autoclaved at 190 ℃ for eight hours. In their work, Fang et al. (2011) found that 23.8 MPa compressive strength can be attained with 40% copper tailings combined with appropriate lime and sand proportions. The compressive strength results of the prepared copper tailings bricks satisfied the Chinese standards for sand–lime brick (GB119451999). Moreover, Fang et al. (2011) found that the density and particle size of the copper tailings limit the amount of copper tailings that can be incorporated during the preparation of autoclaved bricks. The bulk density of the copper tailings is high which accounts for hefty bricks that may not be ideal for construction applications. Subsequently, it was suggested that appropriate proportions of sand and lime powder could reduce the weight of the finished brick.

2.4.4.3 Gold Mining Waste

Gold is considered one of the most valuable minerals in the world and has been a steady commodity in the global financial market (Li et al., 2022). This has led to increased gold extraction and the mineral processing activities generate a significant amount of tailings that is transported to tailing ponds for disposal. An inferior gold processing may generate 0.95 tonnes of gold tailings from one tonne of raw ore (Zheng, 2013). Gold tailings may contain toxic elements such as heavy metals and sulfides, posing environmental risks if poorly managed (Sibanda, 2019). Using the tailings could be an advantage to humanity and minimize environmental risks. In efforts to minimize waste accumulation in tailing dams, alternative uses of gold tailings have been explored.

Li et al. (2022) investigated the feasibility of using gold mine tailings and cementitious binders with low alkalinity to fabricate baking-free bricks. The cementitious binder was synthesized from slag powder, fly ash, 42.5 ordinary Portland cement, Na_2SO_4, CaO, and $CaSO_4$ according to a designed proportion. The following parameters were considered to achieve the optimal brick properties: forming water content, binder/tailing ratio, and curing time. According to Li et al. (2022), calcium aluminate silicate hydrate (C-A-S-H gels were the main products of the hydration process responsible for the mechanical properties of the baking-free bricks. Their experimental results revealed that 15.15 MPa compressive strength and 11.8% absorption percentage can be achieved with 10% water content, 1:6 binder/tailing ratio, and 28 days of curing. The researchers reported that the properties of their prepared bricks complied with the GB/T 4111-2013 Chinese standards.

In research conducted by Wei et al. (2021), sintered bricks were prepared from gold tailings and clay was introduced as an additive. In this study, the brick properties were optimized based on the clay content, forming moisture, firing temperature, and holding time. Due to its plasticity properties, clay was added to bind the gold tailings. Additionally, the gold tailings had a lower SiO_2 and Al_2O_3 hence clay was introduced to the gold tailings to improve the composition of SiO_2 and Al_2O_3 in the raw materials for the sintered bricks. During the sintering process, the SiO_2 and Al_2O_3 melt and form new structural phases which enhance the strength of the bricks. The optimum design parameters for the sintered bricks were 35% clay content, 25% forming moisture, 1030 ℃ firing temperature, and a 105-minute holding period, yielding a compressive strength of 22.48 MPa. Wei et al. (2021) reported that the compressive strength of the sintered bricks complied with the GB/T5101-2003 Chinese requirements.

Roy et al. (2007) prepared bricks from gold mill tailings to solve the waste disposal challenges at the Kolar Gold Fields mine. Cement and soil additives, the binding materials, were mixed with the mill tailings. In their research, Roy et al. (2007) used four different types of soil additives. To achieve optimal properties for gold tailings bricks, the following parameters were considered: the proportions of the additives, curing days, and firing temperature. The results for the gold tailings bricks with cement additives revealed that a compressive strength of 5.5 MPa can be achieved with 25% cement cured for 14 days. For the gold tailings bricks with soil additives, a strength of 23 MPa was attained with 50% gold tailings fired at 950 °C. Roy et al. (2007) reported that the prepared bricks satisfied the IS brick requirements.

2.4.4.4 Coal Gangue

The increasing demand for energy due to the ever-growing population has increased coal consumption as a significant energy source (Zhengfu et al., 2010). The coal mining industry generates massive volumes of waste, which occupies a lot of space and poses environmental hazards. China generates about 315 million tonnes of coal gangue annually, and the Chinese government advocates the incorporation of coal gangue in brick-making to reduce the stockpiled waste (Xu et al., 2017). Lottermoser (2011) carried out a detailed mineralogical characterization of coal refuse. The findings revealed that coal waste can be an alternate source of raw materials for the construction and ceramic industries with no harmful effects.

Mukhtar et al. (2022) explored the feasibility of using coal ash (CA) as the chief ingredient to produce green bricks. Lime and cement were introduced as the additives to bind the coal ash. Sand and quarry dust were also added to enhance the strength of the finished product. In this experiment, CA reacted with lime in the presence of moisture to form a calcium hydrate binder. For optimum CA brick properties, the following parameters were considered: the mix proportions of the raw materials, the forming pressure, and the curing time. In their experiment, Mukhtar et al. (2022) achieved an optimum compressive strength of 19 MPa and 2.1 MPa flexural strength with 60% CA, 10% lime, 10% cement, 10% sand, and 10% quarry dust subjected to 29 MPa forming pressure for three seconds and moisture cured for 28 days. The researchers reported that the compressive strength of the CA bricks from this study satisfied the Pakistan Building Code 2021 which requires a minimum compressive strength of 8.5 MPa.

Xu et al. (2017) examined the use of coal gangue as the only raw material in brickmaking through a conventional sintering process. This study considered the forming pressure and the sintering temperature as the major parameters for optimal brick properties. They achieved an optimum compressive strength of 45.61 MPa and 3.65% water absorption with 80 MPa forming pressure held for three minutes and 1200 ℃ sintering temperatures held for two hours. In their experiments, they discovered that the coal gangue used had low alkaline oxides and Fe_2O_3 content which are crucial for the sintering process of bricks. This could have raised the sintering temperatures of coal gangue brick compared to conventional clay. Xu et al. (2017) reported that the properties of their bricks satisfied the MU30 GB 5101-2003, Chinese National Standard for fired common bricks.

2.4.4.5 Bauxite Residue

The wide range of applications for aluminium owing to its lightweight and corrosion-resistant properties has increased bauxite processing into alumina. Aluminium has found applications in the aerospace industry, construction industry, electrical power grids, electronics, and food packaging (Garg et al., 2019; Nturanabo et al., 2019). The industrial processing activities generate large volumes of bauxite residue, also known as red mud, which can be challenging to manage. An estimated 1.5 tonnes of bauxite residue are generated for every tonne of alumina produced; this equates to an annual global output of 191 million tonnes (Raghubanshi et al., 2022). Incorporating bauxite residue in brick manufacturing presents a value opportunity and solves the disposal challenges. The primary constituent of red mud is Fe_2O_3, which can benefit the strength properties of bricks and provide its red color. According to Klauber et al. (2009, 2011), there are two approaches to brick manufacturing from fine bauxite residue depending on whether they are to be kiln-fired or not. Conventional bricks are fired to achieve the required strength while unfired bricks are made by incorporating cement or other binding agents (organic or inorganic) to achieve the required strength. Common binding agents in the manufacturing of non-fired brick are calcium compounds, which include limestone, gypsum, or quicklime (Klauber et al., 2009; Oti et al., 2014).

Annan et al. (2012) researched the feasibility of using bauxite residue (BR) in brickmaking and incorporating highly plastic clay as the binder. The following parameters were considered for optimum brick properties: the mix proportions of the raw materials and the curing temperature. In their research, Annan et al. (2012) achieved an optimum compressive strength of 12.5 MPa and 16% water absorption with 50% BR and 50% clay sintered at 1100 ℃ at 5 ℃/min heating rate for 5 hours. The optimum brick properties were observed with the 50% BR combination because of a uniform composite mixture and effective adhesion between the BR and the clay particles. The researchers reported that the properties of their bricks complied with the ASTM C99 requirements and hold potential in bauxite residue applications in brickmaking.

Yang & Xiao (2008) investigated the feasibility of using red mud (RM) as the chief ingredient combined with fly ash (FA) and sand to develop unsintered bricks. Lime, gypsum, and Portland cement (PC) were added to boost the activities of RM, FA, and sand. This study considered the proportion of raw materials, forming moisture, forming pressure, and curing time as the primary variables for optimum brick properties. In their experiment, Yang & Xiao (2008) achieved an optimum compressive strength of 19.43 MPa and 5.05 MPa flexural strength with 33% RM, 25% FA, 30% sand, 8% lime, 3% gypsum, and 1% PC formed with 15% moisture content, subjected to 20MPa pressure and moisture cured for 28 days. They concluded that the calcium silicate hydrates (C-S-H) gels formed from the hydration reaction of RM and PC could have contributed to the strength of the brick. These C-S-H gels could have possibly been generated from FA reaction with lime. Moreover, ettringites, the hydrated products of RM and FA reaction with gypsum could have enhanced the strength of the final product. The researchers reported that the properties of their bricks satisfied the Chinese criterion of firstclass brick which requires a minimum compressive strength of 15 MPa and 3.3 MPa flexural strength.

Management of mining waste has attracted attention in recent years. Numerous studies have been conducted on the use of iron ore tailings, copper tailings, gold tailings, coal gangue, and bauxite residues in the construction industry and the results have been exciting as they reveal huge potential for mining waste usage. Researchers have discovered the benefits of incorporating recycled mining wastes in brick manufacturing, including high strength and costeffectiveness, and environmental sustainability. Based on the assessment of various studies on utilizing mining waste in the development of construction materials, research on PGM mining waste has not been done, hence further research and developments targeting this kind of waste are required to enhance the circular economy concept and contribute as a solution to achieve a greener environment. This work focuses on the valuation and optimization of PGM slag to develop composite construction materials to meet the challenge of sustainable development.

2.4.5 PGM Mining Waste

The wide range of applications for PGMs owing to technological innovations has increased PGMs extraction and mineral processing operations. The PGMs elements consist of six noble metals with a white-silver color: platinum (Pt), palladium (Pd), rhodium (Rh), ruthenium (Ru), iridium (Ir), and osmium (Os). These metals have high melting points, high thermal stability, high corrosion resistance, and unique catalytic properties (Liu et al., 2021). Owing to these properties PGMs are highly valued for their wide range of industrial processes and commercial applications including medicals, electronics, catalysts, jewellery, and automotive (Hughes et al., 2021).

With a continuously growing demand and research, the use of PGMs is set to expand. The PGM mining activities generate a significant volume of tailings and slag of which disposal is the major challenge. The PGM mining waste are by-products of comminution, flotation, smelting, converting, and metal refining processes (Thethwayo, 2018). Of particular interest is slag, produced in a very high-temperature smelting furnace with an average of 1600 °C. The molten slag is tapped out of the smelter through slag tapholes and immediately granulated using a high-flow water stream and disposed of in slag dumps. According to Mabiza (2006), PGM slag concentrate is basically regarded as $2FeO.SiO_2$ and other oxides in the concentrate including MgO, Al_2O_3, and CaO also report to the slag. The specific gravity of PGM slag ranges from 2.8 to 3.8 (Thethwayo, 2018). PGM slag has a glassy texture and is often dark grey to black due to the high concentration of metal oxides. The exact color can vary depending on the specific composition of the slag and the smelting process used.

The relatively low percentage of the valuable mineral in PGM ores ranging from two to ten grams per tonne means that a greater percentage of the ore becomes waste (Mudd, 2012). According to Zimplats (2021), an estimated 93% of waste is generated at Zimplats annually from PGM mining operations. Much research has been conducted on PGM mining waste to recover valuable minerals employing pyrometallurgical, hydrometallurgical, biological, and physical separation methods, enabling mineral beneficiation (Jones, 2005.; C. Liu et al., 2021b). PGM mining waste can be recyclable, ensuring not only waste reduction but also supply sustainability. Limited research has been reported on the use of PGM mining waste to make construction materials. PGM slag is rich in silica, iron, magnesium oxide, alumina, and calcium oxide and with this chemical composition, it can be a good candidate for use in the construction industry.

2.5 Brick Clay

Clay is the most used natural resource in brickmaking and it is most valued due to its ceramic characteristics (Kadir & Mohajerani, 2011). The composition of the clays used to make bricks varies greatly and is influenced by the region where the soil has originated (Hapazari et al., 2015; Kadir, 2012; Vyas et al., 2014). Clays are generally formed from the breakdown of rocks like pegmatite and granite, but brick-making clays often come from alluvial or watery deposits. Clay soils are composed mainly of silica and alumina with varying amounts of metallic oxides (particularly those of iron, magnesium, and calcium). Metallic oxides act as fluxes promoting the fusion of the particles at lower temperatures (Kadir & Mohajerani, 2011; Kumari & Mohan, 2021). The important properties of clay that make it highly desirable as brick material are the development of plasticity which permits it to be shaped or molded when mixed with water, and the hardening under the influence of heat allowing the clay particles to fuse (Agbo et al., 2022; Murray, 2006; Valaskova, 2015). Clays must have sufficient wet and air-dried strength to maintain their shape after forming, and when subjected to appropriate temperatures the water content is driven out.

Generally, there are two types of clay, based on how the substance responds when mixed with water: expandable clays and non-expandable clays. Expandable clays swell when water is added to them. They can absorb so much water and change phase to liquid. On the other hand, non-expandable clays become soft but not liquid when mixed with water. Non-expandable clays are used in the ceramics industry to make bricks, tiles, pottery, and porcelain (Olokode et al., 2012). The important properties of clay that must be taken into consideration during the manufacture of ceramic products include plasticity, shrinkage under firing and under air drying, fineness of grain, color after firing, hardness, cohesion, and capacity of the surface to take decoration (Oyelaran, 2014).

2.5.1 Characterization of Brick Clay

Not every type of earth clay is suitable for brickmaking. During clay brick manufacturing, the physical properties of the raw material play an important role. The essential properties considered for suitable brick clay are its plasticity and chemical composition. Clay suitable for brick manufacturing consists of three types of soil particles: clay, silt, and sand. The recommended percentages of physical properties of brick clay are shown in Table 2.3.

Table 2.3: Properties of Brick Clays (Mueller et al., 2008)

Physical Property	Recommended Percentage (%)
Clay	20-35
Silt	24-45
Sand	20-45
Liquid Limit	25-38
Plasticity Index	7-16

Too much sand particles may result in the breaking of the bricks while too much clay results in the cracking of the bricks, hence the need for a careful selection of the raw material (Mueller et al., 2008).

Atterberg Limits

The atterberg limits are a fundamental measure of the water content that defines the physical states of soil-water mixtures: the semisolid, plastic, and liquid states (Sharma & Bora, 2003; Zhou & Lu, 2021). They enable soil classification and are typically correlated with engineering parameters such as permeability and compressibility. Atterberg limits comprise liquid limit, plastic limit, and linear shrinkage tests. The casagrande method can be used to determine the atterberg limits test following ASTM specifications. The casagrande plasticity chart can then be used to determine the plasticity extent of soil samples by extrapolating the intersection of liquid limit (LL) and plasticity index (PI) (Casagrande, 1948).

The liquid limit (LL) of soil is described as the upper limit of the moisture content range beyond which the soil exhibits plastic behavior (Dash & Hussain, 2015; Soltani et al., 2023). Soils having a high liquid limit can absorb a significant amount of water before becoming liquid. Such characteristics are typically observed in clay soils.

The plastic limit (PL) denotes the moisture content at which the soil starts crumbling when kneaded (McBride, 2002; McBride et al., 2008). The plasticity index (PI) denotes the range of moisture content in which the soil exhibits plastic properties. The plasticity index is computed

as the difference between the liquid limit and the plastic limit. Soils with a high plasticity index tend to be clay-dominated, whereas those with a low plasticity index tend to be silt-dominated (Barnes, 2009).
The shrinkage limit (SL) is the water content at which the volume of the soil achieves its lowest value when it dries (Groenevelt & Grant, 2004). At this limit, the transition between the solid and semi-solid states occurs.

The percentages of clay, silt, sand, and gravel particle sizes in soils are determined from the particle size distribution curves obtained from the sieve analysis test. The particle size distribution curves employ soil classification systems in determining fractions of particle sizes in a soil sample. Most of the soil samples contain particle sizes ranging from coarse to fine, however, there is little possibility that a soil sample is composed of same-sized particles (Craig, 2013). The percentages of particle sizes in a soil sample can also be used to determine the soil texture from the soil classification textural chart. The commonly used soil classification systems are described in Table 2.4 and the particle sizes for the mentioned soil classification systems are given in Table 2.5.

Table 2.4: Soil Classification Systems (Gambill et al., 2016)

Soil Classification System	**Application of the Soil Classification System**
Unified Soil Classification System (USCS)	classification is used where soil texture and grain size are significant for engineering structural applications (Casagrande, 1948).
United States Department of Agriculture (USDA)	provides a classification of soil types for agricultural applications (Soil Survey Division Staff, 1993)
American Association of State Highway and Transportation Officials (AASHTO)	employed as a guide to classify soils and soil-aggregate mixtures for highway construction (Hogentogler & Terzaghi, 1929)

Table 2.5: Particle Sizes for Different Soil Classification Systems

	USCS	**USDA**	**AASHTO**
Gravel-sized (mm)	> 4.75	> 2	> 2
Sand-sized (mm)	0.075 - 4.75	0.05 - 2	0.05 - 2
Silt-sized (mm)	0.005 - 0.075	0.002 - 0.05	0.005 - 0.05
Clay-sized (mm)	< 0.005	< 0.002	< 0.005

Clay particles much lower than 0.002 mm are not desirable for brick-making. They make the soil highly porous thus lowering the compressive strength and increasing the water absorption of the brick (Eliche-Quesada et al., 2011; Lertwattanaruk & Choksiriwanna, 2011). The plasticity of brick clay soils is significantly influenced by the silt proportion supplementary to the clay content (Diko-Makia & Ligege, 2020).

2.5.2 Chemical Composition for Brick Clay

The primary chemical elements present in clay significantly impact its suitability for brickmaking. The key chemical makeup components of earth soil are silicon dioxide or silica (SiO_2), aluminium oxide or alumina (Al_2O_3), iron (Fe), and magnesium oxide (MgO) (Elavarasan et al., 2021; Punmia et al., 2003; Velasco et al., 2014). These elements influence the mechanical and physical properties of the final brick product. Table 2.6 presents the acceptable chemical composition for brickmaking raw materials.

Table 2.6: Acceptable Range for Key Chemical Elements in Brickmaking Materials (Elavarasan et al., 2021; Punmia et al., 2003; Velasco et al., 2014).

Chemical Element	Acceptable Composition (%)
SiO_2	50-60
Al_2O_3	20-30
Fe	5-8
MgO	<1

Silica improves the strength and minimizes the shrinkage and cracking of bricks, giving a firm and uniform brick. (Elavarasan et al., 2021; Punmia et al., 2003). Excess SiO_2 destroys the cohesiveness between the clay particles in brick, making it brittle and weak, reducing strength (Iswarya, 2020).

The presence of alumina gives clays their plastic behavior which enables them to be molded in any shape. Alumina also functions as a cementing agent holding brick particles together thus strengthening the brick (Punmia et al., 2003; Velasco et al., 2014). However, it has been reported that bricks made of clay containing a high Al_2O_3 content may crack or shrink, during drying and firing due to the high plasticity imparted by Al_2O_3, resulting in strength reduction

(Punmia et al., 2003). If Al_2O_3 is present in smaller proportions the molding process becomes difficult.

The presence of Fe in raw materials hardens and strengthens bricks, thus making them durable. Fe and MgO are essential during the brick firing process because they serve as fluxes, contributing to the fusing of SiO_2 at low temperatures around 900 ℃ (Elavarasan et al., 2021; Punmia et al., 2003). This is the temperature at which the vitreous bond that holds the entire brick structure together forms, giving strength to the bricks. Iron is also responsible for the color of the finished product and if present in excess it yields bricks with a dark shade. Excessive MgO content is undesirable as it may cause brick expansion during firing, leading to swelling and cracking (Harrisson, 2019).

2.6 Brick Manufacturing Process

The foundations of brick production have remained constant over time. Nonetheless, technical improvements have significantly increased the efficiency of modern brick manufacturers and raised the overall quality of the produced goods. The development of the brick industry has been facilitated by a greater understanding of raw materials and their qualities, improved kiln designs, enhanced firing control, and more advanced machinery.

2.6.1 Raw Materials Preparation

Generally, the physical nature of the raw materials controls the manufacturing methods. To achieve the correct consistency for the brick-forming process, appropriate preparation of the raw materials is essential (Revuelta, 2021). The overall process consists of screening and pulverizing the raw materials into manageable sizes less than 0.075 mm. The presence of impurities in the raw materials can influence the properties of the final brick. Impurities such as organic matter distort the particle bonding within the brick structure, creating cracks and voids that weaken the brick. The amount of water added during brick manufacturing must also be considered. Moisture significantly affects the brick properties thus water input must be optimized. Optimum moisture content determination tests can be conducted to establish the amount of water required for the brick formation. The raw materials are then taken to the next stage which is brick forming.

2.6.2 Brick Forming

Although the fundamentals of manufacturing are largely universal, individual manufacturing facilities adapt their operations to meet their specific raw materials. Brick molding was done manually in the past. However, with the development of brick-making machinery, most bricks produced globally have been manufactured mechanically. Manual molding involves thoroughly hand-mixing dry raw materials with appropriate quantities of water that depend on the soil type. The mixture is then transferred into a brick mold of a desired shape, where it is compacted to eliminate voids followed by demolding, and finally proceed to the drying process. Manual molding is preferred where only a small quantity of bricks is needed. However, during mechanical molding, the dry raw materials are then fed into a mixer in which appropriate quantities of water are added followed by thorough mixing until a homogenous mixture is attained. The mixture is fed from the mixer into a vacuum chamber through which air is removed. Afterward, it is pushed through a mouthpiece and an extrusion die. The column is then cut into bricks using a series of wires. Once cut, the bricks are loaded onto steel rails or pallets and then transported to the drier.

The properties of the brick are significantly influenced by the amount of water added to the dry ingredients during the brick-forming process. As the brick dries, water evaporates from the hardened brick leaving pores within the brick. Therefore, adding too much water during brick formation implies more pores will appear. This weakens the brick, reducing its strength and increasing its absorption capacity. In addition, during the drying process, bricks undergo shrinkage which may lead to crack formation (Fernandes, 2019). A brick with a high amount of forming water may shrink excessively, resulting in numerous cracks which reduces strength. However, when insufficient water is added, bonding between particles becomes difficult, making the bricks weaker and thus reducing their strength. Therefore, to achieve optimal brick properties, appropriate water quantities must be added during the manufacturing process.

2.6.2.1 Brick Forming Pressure

Sufficient forming pressure is essential during brick manufacturing as it determines the quality of the finished product (Indra et al., 2018). It eliminates voids by packing the particles closer together within a brick structure enhancing overall strength. Forming pressure can vary according to the raw materials used, additives introduced, the manufacturing method employed, and the desired properties of the finished bricks. When making bricks using mechanical molding, adhering to the pressure guidelines provided by the brick equipment is crucial. Sufficient compaction pressure ensures regular shape, uniform density, and structural integrity on bricks. Bricks formed by mechanical methods are much stronger bricks than those formed by manual methods because of the improved uniformity and adequate compacting that comes with using a machine. In addition, an increase in compaction effort reduces the number of pores in a brick, thus reducing its water absorption capacity (Indra et al., 2018).

2.6.3 Brick Drying

All bricks when formed contain water, this is what allows them to be formed into a desired shape. This water must be removed before the bricks can be fired, as they may get damaged (Fernandes, 2019; Ndukwu et al., 2021). The science behind the drying of bricks before subjecting them to heat is that if the heat rises too quickly, water contained in bricks may turn to steam. The bricks will rupture as a result of the pressure created by the steam inside of them. In light of this, bricks should be as dry as possible before being fired in the kiln. Bricks that are drying will inevitably shrink, hence this process must be carefully controlled to minimize stresses on the product, which could lead to distortion and cracking. The drying shrinkage is caused by moisture loss during drying and is computed in terms of the length reduction of bricks. If drying is done carefully, some clays may tolerate a linear shrinkage of 5%-10% (Geschke, 2004). Shrinkage problems might be alleviated if the clay proportion in the mix is partially substituted by sand. Bricks become lighter in color as they dry, sample bricks can be broken to check whether the inside is dry, or brick weight should be noted regularly until it remains constant, indicating that the brick is dry. Drying of bricks can be done either naturally or artificially (Araujo et al., 2017; Rajput, 2008).

2.6.3.1 Natural drying

It is often referred to as "hack drying," and it entails lining up molded bricks on their edges, preferably beneath a shed where there is enough air circulation (Rajput, 2008). The time required to dry depends on the weather, nonetheless, it is anticipated that the bricks should be entirely dry in three weeks. The fundamental benefit of natural drying is that it uses no energy. The main drawback is the potential amount of additional handling required, which could increase labor expenses and increase the chance of brick breakage.

2.6.3.2 Artificial Drying

With this technique, bricks are heated in furnaces specifically designed for artificial drying (Rajput, 2008). In the operation of the artificial drying process, energy is required to vaporize water, heat the bricks and the air passing through the dryer, and compensate for heat lost to the surroundings. Artificial drying is costly as it requires large amounts of energy, hence is ideal when bricks are needed to dry on a large scale.

2.6.4 Brick Firing

Brick firing is an essential process that involves the transformation of weak dried bricks into hard and strong bricks (Karaman et al., 2006). During the firing process, certain reactions occur within the clay body, some of which transform the unfired body and develop the fired properties (Rajput, 2008). Most notably, the high temperature, greater than 900 ℃ in the clay brick firing process enables hazardous components to volatilize, changes the chemical makeup of the materials, and integrates potentially toxic components through fixation in the vitreous phase of the waste utilized (Kadir, 2012). The effects of firing on a clay body include shrinkage, weight loss, increased strength, impart hardness, and color change (Karaman et al., 2006). The firing shrinkage is caused by moisture and chemical changes that occur during firing. Firing shrinkage can lead to cracking of the bricks, affecting their strength. To produce well-fired bricks, the firing schedule, that is the time of firing and the rate at which temperature rises, must be regulated so that certain reactions will have enough time to take place at the appropriate temperatures (Fernandes, 2019). Bricks must be fired at high temperatures to get excellent strength and water resistance qualities. Brick firing can be done either by clamp burning or by kiln burning (Iswarya, 2020).

2.6.4.1 Clamp Burning

This is a temporary structure in which firewood, cow dung, and litter may be used resulting in low initial and fuel costs. The bricks and fuel are placed in alternate layers leaving some space that allows free circulation of fume gases (Iswarya, 2020; Rajput, 2008). The top and sides of the kiln are then covered with mud to prevent heat escape. During clamp burning, fire regulation cannot be maintained throughout the process, and no skilled labor and supervision are necessary. The drawback of clamp burning is that it only produces 70% of high-quality bricks and can only burn bricks on a small scale (Subramanian, 2019). This method requires about three months for the burning and cooling of bricks. Figure 2.6 demonstrates brick firing by clamp burning.

Figure 2.6: Clamp Burning (Civil Engineers PK, 2016)

2.6.4.2 Kiln Burning

The technique consists of permanent structures which will have a significant initial cost. The energy cost is quite high as electricity, coal and dust are to be used. During kiln burning, controlled firing can be achieved throughout the process and continuous skilled supervision is necessary (Iswarya, 2020; Rajput, 2008). This technique is employed when bricks are required at a large scale, and it yields 90% of good-quality bricks. This process takes around 24 hours for burning and 12 days for cooling (Subramanian, 2019). Kiln burning is further divided into two types: the intermittent kiln (where burning is discontinuous) and the continuous kiln (burning with no break in between) (Kumar & Maithel, 2016). In an intermittent kiln, raw bricks are loaded, fired, cooled, and then unloaded. Then the subsequent batch of bricks is loaded, and the process repeats. Thus, they must be reheated once more, resulting in energy waste. Whereas, in a continuous kiln, the bricks are heated in various chambers at different temperatures. When the bricks in one chamber are fired, the hot flue gases move to the next chamber, preheating the bricks in that chamber. In some chambers, bricks are loaded, while in other chambers, they are cooled. As a result, the kiln is continuously heated, reducing the amount of fuel needed for brick firing (Weyant et al., 2016). Figure 2.7 illustrates brick firing in a kiln.

Figure 2.7: Kiln Burning (Wangda, 2021)

Brick firing is a crucial process as it contributes to the strength and color of the bricks. The clay body undergoes several physical and chemical changes at certain temperature ranges. The changes may include the removal of water, material decomposition, and formation of new phases, contributing to the properties of the final product (Kumar & Maithel, 2016).

2.6.4.3 Desorption of Water

This is the first phase of brick firing whereby mechanically held moisture that is the water added to clay during the molding process is driven out (Fernandes, 2019). Much of the moisture is removed during the drying process, however, due to various environmental factors, 3% – 10% of moisture typically remains within the bricks. This process takes place between the ambient temperature and a temperature of around 150℃ (Geng & Sun, 2018; Kumar & Maithel, 2016). During this process, the clay does not undergo any chemical change, it still retains its original properties.

2.6.4.4 Dehydroxylation of the Silicate

At this stage, there is the decomposition of clay molecules and the release of combined water (Fernandes, 2019). Clay is comprised of several chemical substances that have been chemically bonded with either water molecules or hydroxyl groups (Kumar & Maithel, 2016). One such combination is kaolin, which is the chief constituent of clay. Kaolinite is a hydroxide of aluminium silicate with the chemical formula of $Al_2O_3{\cdot}2SiO_2{\cdot}2H_2O$. When clay is heated, kaolinite de-hydroxylates between 400 ℃ and 600 ℃ (Geng & Sun, 2018), releasing combined water and undergoing structural distortions. This process entails the removal of the hydroxyl group from silicate minerals within the clay hence the phrase "dehydroxylation of the silicate". It then transforms into a non-crystalline phase, meta-kaolinite. These changes can be described by Equation 2.2.

$$Al_2O_3 \cdot 2SiO_2 \cdot 2H_2O \rightarrow Al_2O_3 \cdot 2SiO_2 + 2H_2O \qquad 2.2$$

2.6.4.5 Combustion of Carbonaceous Materials

Clay is known to contain carbonaceous organic plant components such as grass, roots, branches, leaves, and organic matter which varies from region to region. The combustion of organic material begins at a temperature of about 400 ℃ and is complete at a temperature of about 700 ℃ (Geng & Sun, 2018; Kumar & Maithel, 2016). The decomposition of carbonate and sulphides found in clay also occurs between these temperatures, releasing CO_2 and SO_2.

2.6.4.6 Quartz Inversion

The crystal structure of silica, a common element of clays used to manufacture bricks, occurs naturally as α-quartz (alpha quartz). Quartz enhances the strength of a brick if present in sufficient amounts. When clay is heated to a temperature of 573 ℃, there is a transformation of the α-quartz into β-quartz (beta quartz) (Geng & Sun, 2018; Kumar & Maithel, 2016). At this phase, particles within a brick structure re-arrange themselves and this transition is accompanied by a 2% increase in volume. Upon cooling, at 573 ℃, β-quartz reverts to α-quartz once more. To prevent high stresses that can cause crack formation in bricks, the heating and cooling rates near the quartz inversion temperature must be managed to achieve almost consistent temperatures throughout the brick (Weyant et al., 2016).

2.6.4.7 Vitrification

The final phase of clay-brick firing, known as vitrification, typically starts at around 900 ℃ (Akinshipe & Kornelius, 2017). Vitrification is responsible for the changes in the chemical composition of the materials. The process of vitrification involves the partial melting of clay particles at their points of contact to create a glassy link that holds the entire mass together and provides the strength of the brick (Kumar & Maithel, 2016). The amount of clay that melts during firing is influenced by the type and proportion of minerals constituting the clay, the clay mass temperature, and the heat treatment period (Fernandes, 2019). This justifies the significant variations in firing temperatures, which range from 800 ℃ to 1200 ℃ depending on the nature of the clay. Treatments at 1100 ℃ and above can result in the formation of mullite, cristobalite, and hematite phases, with new structural changes (Cardenas-Ramirez et al., 2019; Geng & Sun, 2018; Gonidanga et al., 2019). At about 925 ℃, there is a transformation from meta-kaolinite to aluminium silicon (Al-Si) spinel and amorphous silica. The aluminium silicon spinel is then transformed to mullite and cristobalite upon reaching about 1100 ℃. Amorphous silica transforms to cristobalite at about 1200 ℃ (Cheng et al., 2019; Aza et al., 2014). These changes can be described by Equations 2.3, 2.4, and 2.5, respectively. Any firing temperature above 1300 ℃ causes the earth brick to start losing its shape.

$$\mathbf{2}(\boldsymbol{Al_2O_3} \cdot \mathbf{2}\boldsymbol{SiO_2}) \rightarrow \mathbf{2}\boldsymbol{Al_2O_3} \cdot \mathbf{3}\boldsymbol{SiO_2} + \boldsymbol{SiO_2}\ \textit{(amorphous)} \qquad 2.3$$

$$\mathbf{3}(\mathbf{2}\boldsymbol{Al_2O_3} \cdot \mathbf{3}\boldsymbol{SiO_2}) \rightarrow \mathbf{2}(\mathbf{3}\boldsymbol{Al_2O_3} \cdot \mathbf{2}\boldsymbol{SiO_2}) + \mathbf{5}\boldsymbol{SiO_2}\ \textit{(cristobalite)} \qquad 2.4$$

$$\boldsymbol{SiO_2}\ \textit{(amorphous)} \rightarrow \boldsymbol{SiO_2}\ \textit{(cristobalite)} \qquad 2.5$$

Vitrification is also responsible for the color of the brick. The minerals in the raw materials impart color to the brick. One of the key elements that provide the typical red color of a brick is iron oxide (Fernandes, 2019; Taha et al., 2016). The acceptable range of iron for brickmaking raw materials is shown in Table 2.6. It was observed that a high iron oxide content gives the brick a dark shade, while a low concentration of iron oxide gives the brick a lighter hue. Figure 2.8a illustrates the pores within a brick structure before vitrification, and Figure

2.8b shows the glassy link that forms during vitrification from the partial melt of clay particles, closing the pores within the brick structure.

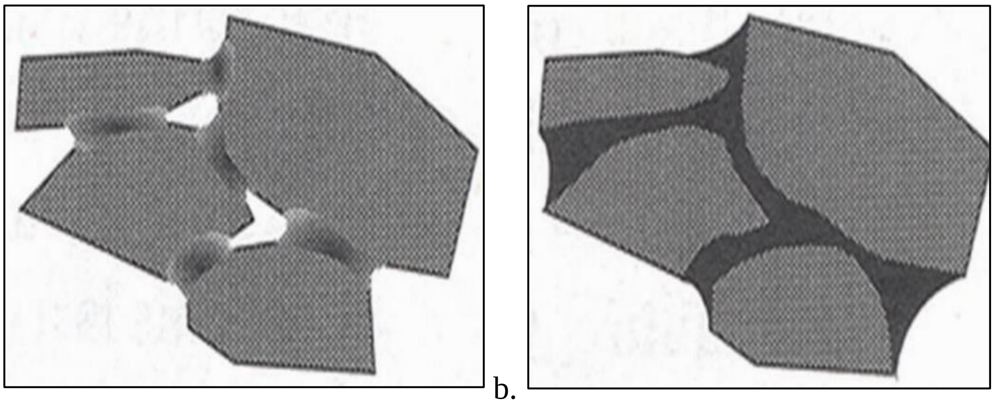

a. b.

Figure 2.8: Vitrification Process of Clay (Kumar & Maithel, 2016)

2.6.4.8 Effects of Firing Temperatures on Brick Properties

The compressive strength of fired bricks generally increases with the firing temperature until the brick fully vitrifies. At vitrification, the brick would have acquired sufficient compressive strength, and the temperatures at which a brick fully vitrifies may vary depending on the nature and the proportion of elements present in the raw materials employed (Fernandes, 2019; Kumar & Maithel, 2016). For instance, the presence of fluxing oxides such as magnesia, ferrous oxide, and lime lowers the vitrification temperature to around 900 ℃, therefore high compressive strength can be achieved at low firing temperatures (Elavarasan et al., 2021; Punmia et al., 2003). The compressive strength of bricks can also be enhanced by structural changes that occur with the formation of mullite, cristobalite, and hematite phases at temperature treatments above 1100 ℃ (Cardenas-Ramirez et al., 2019; Geng & Sun, 2018; Gonidanga et al., 2019). In some cases, beyond vitrification, a further increase in firing temperature may decrease the compressive strength of the brick. The brick will start to soften, and there is the formation of melt which then weakens the entire brick structure. The clay minerals that make up the brick may also expand in response to extremely high temperatures, inducing internal stresses that ultimately cause the brick to crack (Bidoung et al., 2016; Russo & Sciarretta, 2013).

The amount of heat that a brick receives during firing has an impact on its water absorption capacity. The water absorption capacity of fired bricks tends to decrease with a rise in firing temperature. As the firing temperature increases, new structural phases form which enhance the densification of the brick, and as the brick vitrifies, a glassy bond that holds the particle together is formed (Kumar & Maithel, 2016). Densification and vitrification reduce the pores within a brick structure, resulting in a lower water absorption capacity. A further temperature rise beyond vitrification could increase the water absorption of the brick. When exposed to very high temperatures, clay minerals that make up the brick may expand resulting in cracks that then absorb more water (Bidoung et al., 2016; Russo & Sciarretta, 2013).

This section on the effects of firing temperature on brick properties concludes that understanding the vitrification temperature is crucial to ensure that bricks are fired at the appropriate temperature. If the firing temperature is too low, the bricks may not vitrify sufficiently, leading to weak and porous bricks. Conversely, firing at extremely high temperatures can cause over-vitrification, making the bricks brittle and more likely to crack.

2.7 Properties of Bricks

To ensure that the manufactured bricks are fit for purpose, characterization is essential. It involves evaluating the physical, chemical, and mechanical properties to comprehend their performance over time. The appropriateness of bricks for construction use is evaluated using various tests. The tests must be conducted following the recommended methodology for the results to be significant and helpful in the evaluation of brick characteristics. Most tests on bricks are carried out following the American Society for Testing and Material (ASTM) and Indian Standards (IS) guidelines. These tests are carried out either in a laboratory setting or at a construction site. Brick assessment is performed to select the material that provides anticipated lifetime performance for an intended project and quality control.

2.7.1 Compressive Strength

The compressive strength of a masonry unit (brick or block) is a fundamental attribute in the construction industry. Bricks have been extensively used to construct foundations, columns, and walls, which are largely subjected to compression forces. The capacity of a masonry unit to endure crushing stresses can be determined by compressive strength testing (Morel et al., 2007; Rajput, 2008; Singh & Munjal, 2017). Compressive strength tests can be employed by the manufacturer or the end user as a quality control measure. Quality control assures that the brick satisfies the required specifications and is fit for purpose. The strength of a brick is significantly impacted by the raw materials utilized, the forming techniques, and the degree of firing (Fernandes et al., 2010). The minimum compressive strength of a standard brick is 5.5

MPa and 3.5 MPa by the ASTM C67-03 and IS:3495-1-1992 guidelines, respectively. Any value less than this is discarded in the construction industry. The compressive strength of the brick is computed using Equation 2.6:

$$\boldsymbol{Compressive\ Strength = \frac{maximum\ load\ at\ failure}{surface\ area\ of\ brick}} \qquad 2.6$$

2.7.2 Water Absorption

The potential of a brick to absorb water has an impact on its strength and durability. Bricks are porous, which means they can naturally absorb and release moisture from the surroundings (Mahony, 2013). The amount of moisture absorbed is determined by the presence of pores in the brick, hence a high concentration of pores corresponds to a higher water absorption capacity. The water absorption of a brick is largely influenced by the characteristics of the raw materials, the forming methods, and the degree of firing (Fernandes et al., 2010). A water absorption test is conducted on a brick to determine the amount of moisture content absorbed by the brick under adverse conditions (Rajput, 2008; Sathiparan & Rumeshkumar, 2018). The test can be conducted following the standard specifications as per ASTM or IS. According to recommended standard guidelines, a good brick should not absorb more water than 20% of its dry weight. The strength of the brick, as well as the durability of the structure, are negatively impacted if the brick absorbs more moisture than recommended. The percentage of water absorbed by brick is computed using Equation 2.7:

$$\boldsymbol{Water\ Absorption = \frac{wet\ mass - dry\ mass}{dry\ mass} \times 100\%} \qquad 2.7$$

2.7.3 Soundness

The soundness test on bricks shows the nature of bricks against sudden impact (Rajput, 2008; Rao et al., 2019). As part of this test, two bricks are chosen randomly and struck against each other following the standard guidelines as per IS. A good brick should generate a clear bellringing (metallic) sound, and the brick should not break. The soundness of a brick is significantly impacted by the firing temperature and the heat treatment period. The metallic sound arises because of sufficient vitrification and enhanced densification of the bricks during firing (Roudouane et al. 2020).

2.7.4 Hardness

The hardness test typically reflects the resistance of bricks to scratches (Rao et al., 2019). The presence of iron oxide in the raw materials has a positive effect on the hardness of a brick, it helps the fusion of clay particles (Fernandes, 2019; Taha et al., 2016). The compaction pressure applied on bricks during molding significantly impacts the hardness of the finished product (Indra et al., 2018). During compaction, particles are closely packed together enhancing the hardness of the brick (Knappett & Craig, 2012). The hardness of a brick is also affected by the brick composition that is the type of raw materials used, additives introduced, and the firing temperature at which the bricks are treated.

2.7.5 Efflorescence

An efflorescence is a crystalline layer of soluble salts, often white, that develops on the surface of a brick (Brocken & Nijland, 2004; Sutan & Sinin, 2013). The presence of soluble salts in the bricks leads to efflorescence on the brick surfaces thereby decreasing their quality (Rajput, 2008; Rao et al., 2019). The efflorescence mechanism essentially involves the dissolving of internally held salt in water. The salt solution then migrates to the surface of the brick, and surplus water evaporates, depositing a coating of salt on the surface. The brick is then examined for white or grey deposits or patches on its surfaces. The extent to which efflorescence develops in a brick is determined by the concentration of soluble salts in the brick (Brocken & Nijland, 2004; Nhabih et al., 2020). The most prevalent efflorescing salts are sulphate and carbonate compounds of sodium, potassium, calcium, magnesium, and aluminium. Iron oxide and calcium hydroxide are also among the sources of efflorescence in bricks. The efflorescence is only described in four qualitative terms: nil, slight moderate, heavy, and extreme (serious). Heavy salt concentrations can cause powdering of the surface of bricks, which might give rise to the disintegration of bricks. Table 2.7 describes the possible observations that can be derived from the efflorescence test.

Table 2.7: Efflorescence Test Observations (ASTM C67-03; Kumar & Hooda, 2014)

Efflorescence Result	**Observation**
Nil	No efflloresce deposition is visible.

Slight A thin deposit of salt covers less than 10% of the brick surface.

Moderate A thinner deposit of salts covers 10-25% of the surface of the brick, but no surface powdering or flaking is observed.

Heavy A thick layer of salts covers 25-50% of the surface, but no powdering or flaking of the surface.

Extreme (Serious) A heavy deposit of salts covers more than 50% of the brick surface and some powdering and flaking of the surface

2.8 Cost Evaluation

Brick manufacturing is one of the oldest enterprises and has existed for thousands of years (Bhairappanavar et al., 2021; Rahman et al., 2014). The profitability of a brick manufacturing industry is influenced by several operational and overhead expenses that account for the overall production cost. The production cost of brick depends on the raw materials cost, labor costs, energy costs, maintenance and repair expenses, and losses in transportation (Alam et al., 2022). To achieve efficient cost management and control, each of these expenses must be taken into account.

The cost of raw materials makes up a significant percentage of the total operating expenditure (Praseeda et al., 2015). Raw material expenses refer to the cost of obtaining the materials required to manufacture bricks. Clay, sand, cement, and water are among the primary raw materials employed during brick manufacture and their prices may vary contingent on global market conditions. The raw material cost can be influenced by availability, level of demand, and the cost of extraction and processing. In this project, PGM slag, a by-product of the smelting process during mining activity, is employed as a raw material in brickmaking. This lowers the overall operational costs since the slag is readily accessible from the local mining industry, and there are no extraction costs incurred.

Labor expenditures rank among the primary operating expenses for brick mills. Production workers, supervisors, and sales personnel are among the workforce crucial at a brick manufacturing firm. Investing in training and development programs is critical to ensure that personnel acquire the essential skills and knowledge to perform their duties proficiently (Jehanzeb & Bashir, 2013).

Energy is used extensively during the brick-making process to power the machinery and other equipment and supply heat for the firing process (Praseeda et al., 2015). Energy costs may include natural gas, electric power, coal, and fuel oils based on the energy source the firm utilizes.

The manufacturing process requires specialized technology and equipment designed exclusively for the formation of bricks. Maintenance costs are essential for regular maintenance and upkeep of the machinery and equipment to ensure they remain in good working conditions and avoid unforeseen breakdowns (Smith & Mobley, 2011).

Transportation expenses represent an essential operating cost for brick manufacturing plants. Raw materials utilized in the manufacturing must be shipped to the factory site as well as finished bricks must be delivered from the factory to the market accounting for the transport costs (Praseeda et al., 2015).

2.9 Chapter Summary

This chapter discusses composite materials as solid materials that result when two or more different substances are combined to create a new substance. The waste disposal challenges faced by mining firms and the risks that they pose to the environment and human health are discussed in this chapter. Bricks are highlighted as one of the most demanding masonry units globally due to their outstanding engineering properties. The accelerated demand for bricks is resulting in resource depletion, and this has inspired researchers to investigate the potential wastes that can be recycled in brick manufacturing. This chapter has outlined the channeling of mining waste towards the production of building materials as the most feasible solution to disposal challenges and as a new source of raw materials for the building and construction sectors. Based on the assessment of various studies on utilizing mining waste in the development of construction materials, research on PGM mining waste has not been done, hence more research targeting this kind of waste is required. The characterization of the mining waste is essential to assess its potential to release pollutants into the environment and its feasibility as a resource. In addition, the brick manufacturing processes and the processes that take place during brick firing are pointed out. This chapter has also outlined the necessary tests needed to assess the brick quality according to international specifications. Chapter 2 concludes by outlining the general costs incurred during brick manufacturing.

CHAPTER 3

RESEARCH METHODOLOGY

3.1 Chapter Overview

This chapter presents the research methods employed to achieve the specific objectives of this study. The methodology includes laboratory work, research techniques, and instruments used.

The origins of raw materials used in this research are highlighted in this section.

3.2 Study Area

Zimplats is a subsidiary of Implats, the world's leading South African-based producer of PGM. It is located on the Hartley Geological Complex of the Zimbabwean Great Dyke, in the Mashonaland West province and its geometric coordinates are 18°39'56" South and 30°21'23" East. At present, Zimplats owns and operates five underground mines that supply ore to three concentrator modules, two at Ngezi and the third one at Selous. Zimplats has two major waste disposal facilities at Ngezi and Selous Metallurgical Complex (SMC) with a storage capacity of 423 ha and 110 ha, respectively. The bulk of the slag is currently being disposed of at a slag dump at SMC.

The mine began as an open pit in 2001 but has since opened underground mining sections. The mine lies in a resettlement area, between a rural service centre and a recreational park. It is bordered by Mhondoro Ngezi communal lands whose majority population engages in dryland crop production and livestock rearing (Gwimbi & Nhamo, 2016).

The locations and operations of the Zimplats Mine are illustrated in Figure 3.1.

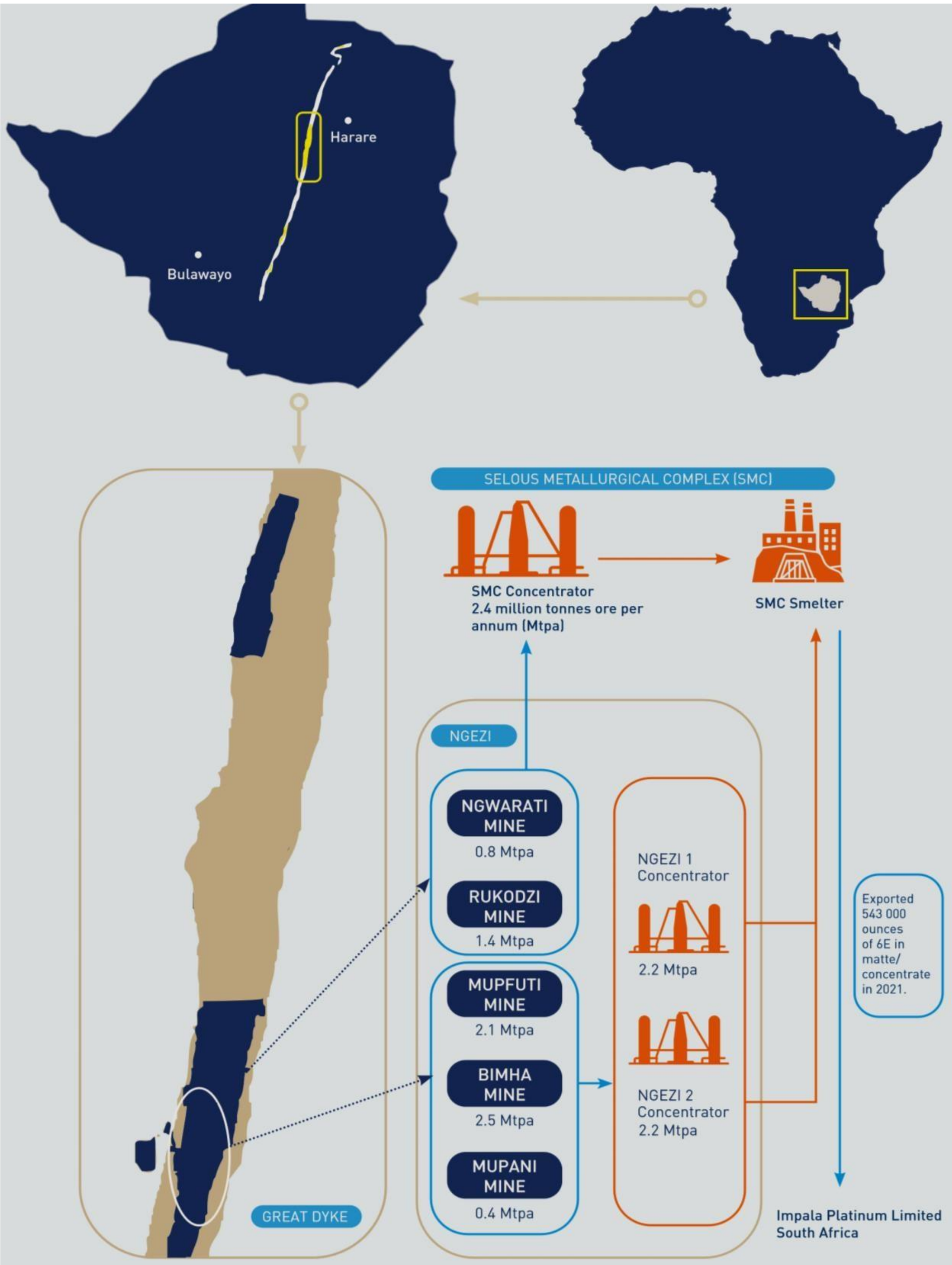

Figure 3.1: Locations and Operations of the Zimplats Mine (Zimplats, 2021)

3.3 Materials

3.3.1 PGM Slag

The PGM slag used in this study is a by-product from smelting, converting, and refining processes at Ngezi and Selous Metallurgical Complexes, Zimplats in Zimbabwe. The slag was collected from the slag dump where it had already been dewatered and dried. A random sampling method was used to collect the slag from the slag dump as it reduces bias and each member has a chance of being selected. It is coarse-grained, non-plastic, and black with a glass appearance. The slag was initially pulverized to generate manageable small and evenly distributed particle sizes. Continuous and dry pulverization methods were adopted. Figure 3.2 shows the PGM slag used in this study.

Figure 3.2: PGM Slag

3.3.2 Clay

The clay samples used in this study were obtained from two different sources in Chinhoyi and Zvishavane by random sampling and were named CC for Chinhoyi clay and ZC for Zvishavane clay. The clay samples were initially air-dried and then pulverized to produce usable homogeneous particle sizes. Continuous and dry pulverization methods were adopted. Figure

3.3 and Figure 3.4 show Chinhoyi clay and Zvishavane clay, respectively.

Figure 3.3: Chinhoyi Clay

Figure 3.4: Zvishavane Clay

3.3.3 Water

The water used in this study was obtained from a clean borehole source free from chemicals that could affect the experimental results. Chemical contaminants in water may react with clay and slag minerals during firing, affecting the final brick properties.

3.4 Research Design

A flowchart that links all the methods and processes employed to fulfil the specific objectives of this research are presented in Figure 3.5.

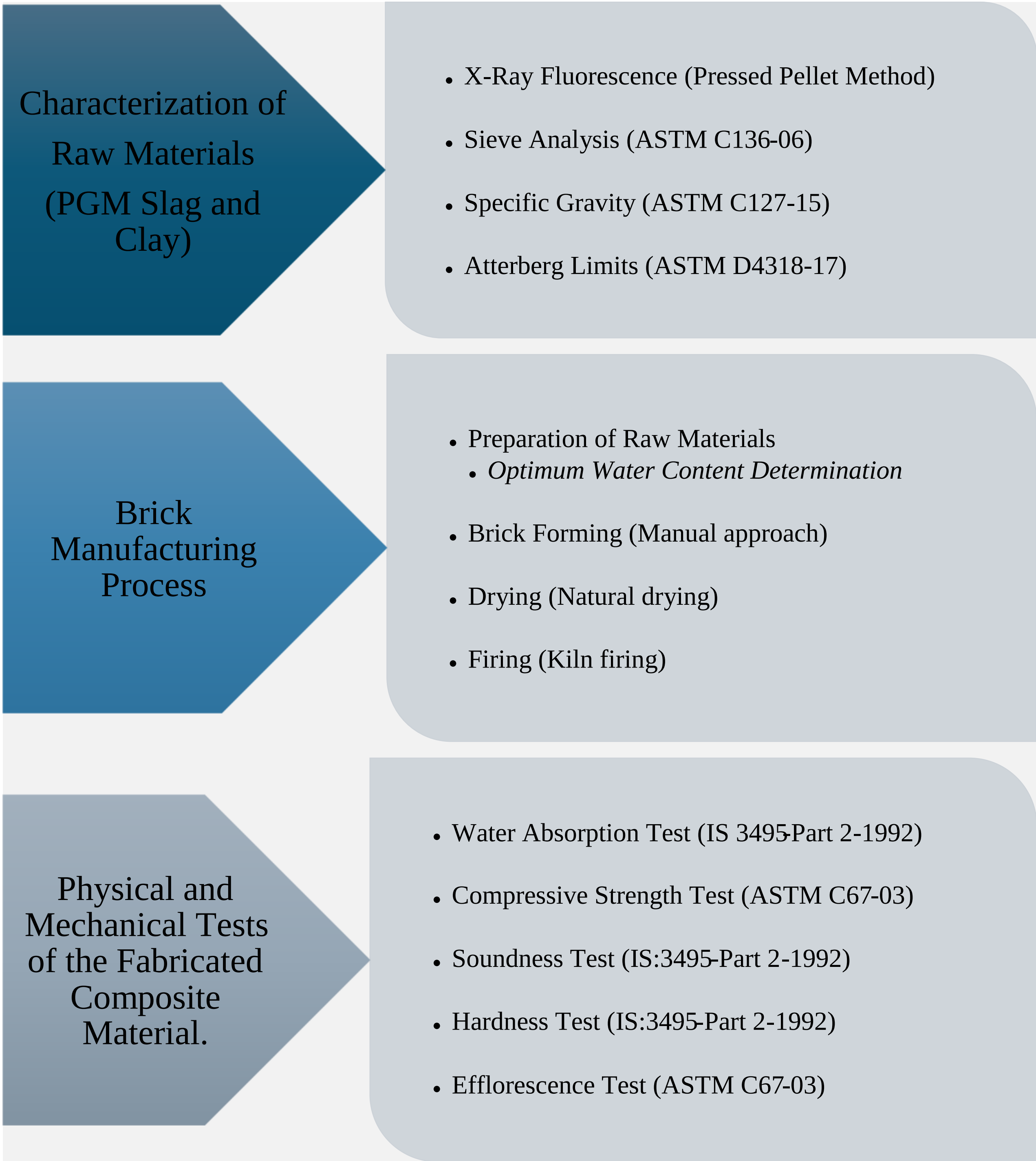

Figure 3.5: Flowchart illustrating Research Methods Implemented in this Study

3.4.1 Characterization of Raw Materials

3.4.1.1 X-Ray Florescence

XRF analysis was conducted to determine the individual elemental composition in the PGM slag and the binding clay samples. The samples were sent to Zimplats, Selous laboratory for analysis. The XRF results are discussed in section 4.2.1 of Chapter 4 and the analysis report is presented in Appendix 7.1.1.

3.4.1.2 Specific Gravity

The specific gravity test was carried out employing the standard specifications as per ASTM C127-15 to determine the relative density of the PGM slag and the clay samples. In this experiment, a clean dry volumetric flask was filled with distilled water up to the mark. The mass of the flask and water was noted. The temperature of the water in the flask was recorded and half of the water was discarded. A measured mass of PGM slag was transferred into the volumetric flask with water ensuring that all the slag samples got into the flask. The slag-water mixture was agitated, and a vacuum pump was inserted to remove the entrapped air. The volumetric flask was then filled with distilled water up to the mark and the final mass of the flask, the water, and the PGM slag was measured. The specific gravity was then calculated from the measured values using the formula in Equation 3.1. The experimental procedure was repeated to determine the specific gravities of the two clay samples. The specific gravity results are presented in section 4.2.2 of Chapter 4 and the raw data is given in Appendix 7.1.2.

$$\boldsymbol{Specific\ Gravity} = \frac{\boldsymbol{M_s}}{\boldsymbol{M_1 + M_s - M_2}} \times \boldsymbol{A} \qquad 3.1$$

Where M_s = mass of a sample

M_1 = mass of flask + water filled to the mark

M_2 = mass of the flask + sample + water filled to the mark

A = temperature correction factor

3.4.1.3 Sieve Analysis (Particle Size Distribution)

Sieve analysis was conducted following the ASTM C136-06 procedures to evaluate the particle size distribution of the aggregates. In this test, 500 g of sample PGM slag was washed under running water, and the wash water was decanted over a 75 µm sieve until it was clean. The washed sample was dried in the oven, and the dried mass was measured using a balance. The mass of the sample washed away by the water during wet sieving was then calculated. The dried sample was allowed to pass through a series of progressively smaller mesh-size BS sieves and the amount of slag that was retained at each sieve was recorded as a fraction of the whole mass. The percentage passing was calculated and a graph of percentage passing against sieve size was plotted on a particle size distribution chart. The particle size analysis procedure was repeated for the two binding clay samples and a graph of percentage passing against sieve size was plotted on a particle size distribution chart. The plotted gradation curves were then analyzed to determine the percentages of various particle sizes and classification textures of the PGM slag and the clay samples. The sieve analysis results are discussed in section 4.2.3 of Chapter 4 and the raw data is presented in Appendix 7.1.3.

3.4.1.4 Atterberg Limits

Atterberg limits test was performed to determine the shrinkage limit, liquid limit, plastic limit, and plasticity index of the binding clay samples according to ASTM D4318-17 specifications. The clay sample was washed under running water. The wash water that passed 425 µm was dried in a bowl at room temperature and the fine soil sample was collected for the experiment.

Liquid Limit: A fine soil sample was mixed with distilled water and the combination was well blended until a smooth homogeneous paste was achieved. The mixture was placed in a casagrande cup with the elimination of air voids and then divided using a grooving tool to form a clean groove. The turning crank was rotated at a rate of two revolutions per second and the number of blows required to close the groove was recorded. The moisture content was immediately taken thereby establishing the liquid limit.

Plastic Limit: A 20 g fine soil sample was mixed with distilled water and kneaded until it was plastic enough to be easily shaped into a ball. The kneaded ball was divided into two and rolled to produce a thread that was 3 mm in diameter and 150 mm long. The thread was then cut into four pieces for moisture content determination which corresponded to the plastic limit.

Shrinkage Limit: Distilled water was added to the fine soil sample and the mixture was thoroughly blended to obtain a smooth, uniform paste. The mixture was transferred into a mold lubricated with hydraulic oil for easy removal. The initial length of the mold was measured, the sample was dried in an oven and the final length of the sample was measured. The shrinkage limit was then computed from the measured values.

The a**tterberg limits** results are presented in section 4.2.4 of Chapter 4 and the raw data is given in Appendix 7.1.4.

3.4.2 Brick Manufacturing Process

Figure 3.6 presents a flowchart diagram describing the brick manufacturing process.

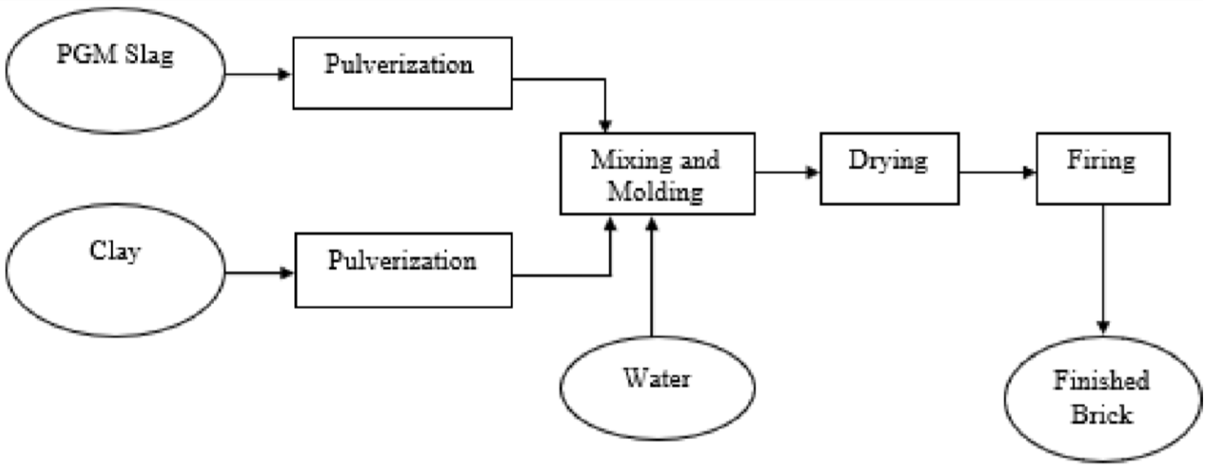

Figure 3.6: Brick Manufacturing Flowchart

3.4.2.1 Preparation of Raw Materials

The overall process consisted of crushing the PGM slag and the clay into manageable sizes, using a crusher followed by sieving through a 600 µm standard BS sieve which further reduces the particle size and helps to achieve consistent particle size of the raw materials. Various mixing combinations of PGM slag to clay by weight percent were prepared to establish an optimum design mix ratio as presented in Table 3.1. *Table 3.1: PGM Slag-Clay Mixing Combinations*

	PGM Slag wt.%				
	0wt.%	20wt.%	40wt.%	50wt.%	60wt.%
PGM Slag (%)	0	20	40	50	60
Clay (%)	100	80	60	50	40

Compaction tests were carried out on the defined mixing combinations to determine the optimum water content for the brick formation. The raw materials were then taken to the next brick-forming stage. Figure 3.7 displays the sieving of clay, the picture on the left shows clay before sieving and the one on the right shows clay after sieving.

Figure 3.7: Clay Seiving

Compaction Test

The test was conducted following the ASTM D698-12 specifications to determine the optimum water content required for the brick formation per combination. A sample of dry PGM slagclay of a predetermined mix ratio was measured. A measured volume of water was added, and the sample was thoroughly mixed until it was uniform. The weight of the compaction mold with its base was measured and the mixture was transferred into the mold and compacted in three layers, applying 25 blows per layer uniformly. The weight of the compacted sample in the mold was measured and the experimental procedure was repeated with variations in the water content until a compaction curve was established. The values of optimum water content were then deduced from the compaction curves and used to determine the volume of water required for brick formation by each predetermined combination. The optimum moisture content determination results are discussed in section 4.3.1 of Chapter 4 and the raw data is presented in Appendix 7.2.1.

3.4.2.2 Brick Forming

In this work, the manual method was adopted for producing laboratory-scale bricks. The prepared PGM slag and clay were mixed in a bowl using a shovel. The amount of water added to each mixing combination was determined by the optimum moisture content from the compaction test results. The measured volume of water was added gradually to the dry mix. Thorough mixing was done to ensure a homogeneous and consistent mixture with a uniform color. A steel mold of dimensions 230 mm × 115 mm × 75 mm was used for brick casting. The interior of the brick mold was lubricated with hydraulic oil for easy removal of the bricks and to give the bricks a smooth surface. The mixture was then transferred into the brick mold and compacted using a compaction hammer to eliminate voids as they create points of weakness. The bricks were de-molded and proceeded to the next process which is drying. Figure 3.8 shows brick forming using the manual method. The picture shows raw materials mixing, a compaction hammer, and brick casting.

Figure 3.8: Brick Forming

3.4.2.3 Brick Drying

The natural drying technique was employed by arranging the molded bricks on their edges under a shed with sufficient air circulation. Sample bricks were broken to check whether the inside was dry and brick weight was noted regularly until it remained constant. The completely dried bricks were then transferred to the firing stage. Figure 3.9 illustrates the drying process of bricks. Figures 3.9a and 3.9b show bricks arranged on their edges to dry and stacked dried bricks, respectively. The brick drying results are presented in section 4.3.2 of Chapter 4 and the raw data is given in Appendix 7.2.2

a. b.

Figure 3.9: Brick Drying

As the bricks were drying, moisture evaporated from the brick structure, and the process was associated with shrinkage. The linear drying shrinkage of the bricks was computed using the formula in Equation 3.2:

$$\textbf{Drying Shrinkage} = \frac{\textbf{initial length} - \textbf{dry length}}{\textbf{initial length}} \times \mathbf{100\%} \qquad 3.2$$

3.4.2.4 Brick Firing

The dried bricks were treated at various temperatures to investigate the effect of temperature on the strength of the final product. They were fired in an electric kiln at 950 °C, 1000 °C, 1050 °C, and 1100 °C for each different PGM slag wt.% combination. The furnace temperatures were increased gradually so that certain reactions had enough time to take place at the appropriate temperatures to prevent the bricks from cracking. The bricks were first heated at 150 °C for 3 hours to drive out the mechanically held moisture that was not removed during the drying process. The temperature in the kiln was then increased at the rate of 10 °C/min until the maximum desired temperature was achieved. Upon reaching the required temperature, the kiln temperature was kept constant for two hours to allow an even distribution of heat before

a.  b. 

Figure 3.10: Brick Firing

switching off the kiln. The fired bricks were allowed to gradually cool in the furnace as abrupt cooling would result in crack formation. The physical properties of the fired brick samples were then assessed. Figures 3.10a and 3.10b show bricks in an electric kiln before and during firing, respectively. The brick firing results are discussed in section 4.3.3 of Chapter 4 and the raw data is presented in Appendix 7.2.3.

During firing, moisture was eliminated from the brick, and chemical changes occurred within the brick. These changes were associated with brick shrinkage. The firing shrinkage of the bricks was computed using the formula in Equation 3.3:

$$\boldsymbol{Firing\ Shrinkage} = \frac{\boldsymbol{initial\ length - fired\ brick\ length}}{\boldsymbol{initial\ length}} \times \mathbf{100\%} \qquad 3.3$$

3.4.3 Physical and Mechanical Tests of the Fabricated Composite Material.

Tests on bricks were performed by employing the ASTM and IS guidelines. These tests were carried out in a laboratory setting. The test results were analyzed for various PGM slag-clay combinations and annealing temperatures. Five replicates were done for each test carried out to reduce the impact of anomalies and also have greater confidence in the results

3.4.3.1 Compressive Strength Test

The compressive strength test was carried out according to the ASTM C67-03 guidelines to determine the strength of the prepared bricks. This experiment was performed on a WDW300E MaxTest universal testing machine. The dimensions of the brick specimen (length, width, and height) were initially measured and loaded into the computer before the test commenced. The brick specimen was placed with flat horizontal and mortar-filled faces facing upwards between plates of the compression testing equipment. An axial stress was applied at a constant rate of 14 N/mm^2 per minute until the brick failed. The maximum load at failure was noted and used to calculate the compressive strength of the brick using the formula in Equation 2.5. Figure 3.11 demonstrates a brick under a compressive strength test on a universal testing machine

Figure 3.11: Compressive Strength Test

3.4.3.2 Water Absorption Test

The test was conducted following the standard specifications as per IS:3495-2-1992 to determine the water absorption capacity of the bricks. Sample dry bricks are weighed and submerged in water for 24 hours at room temperature. To determine the amount of water absorbed by the bricks, the weight of the wet brick specimen was measured and recorded. The percentage of water absorbed by each brick was calculated using the formula in Equation 2.6:

The water absorption test of the bricks is illustrated in Figure 3.12.

Figure 3.12: Water Absorption Test

3.4.3.3 Soundness Test

The soundness test was conducted to investigate the resilience of bricks against abrupt impact. As part of this test, two bricks were chosen randomly and struck against each other following the standard guidelines as per IS:3495-2-1992. The sound produced by the bricks was noted and the bricks were also examined for damages.

3.4.3.4 Hardness Test

The hardness test was performed to evaluate the resistance of bricks against scratches. In this test procedure, a sharp object was used to scratch the surface of the brick according to the

IS:3495-2-1992 specifications. The brick was then examined for any impression on the surface.

3.4.3.5 Efflorescence Test

This test was conducted as per ASTM C67-03 specifications to assess the presence of soluble salts in the prepared bricks. Brick samples were placed vertically in water with one end immersed, the depth of immersion in water was 25 mm. The test was performed in a wellventilated room until all the water had evaporated. The brick was then examined for white or grey deposits or patches on its surfaces. The onset and completion of the efflorescence test are demonstrated in Figures 3.13a and 3.13b, respectively.

3.5 Chapter Summary

a. b.

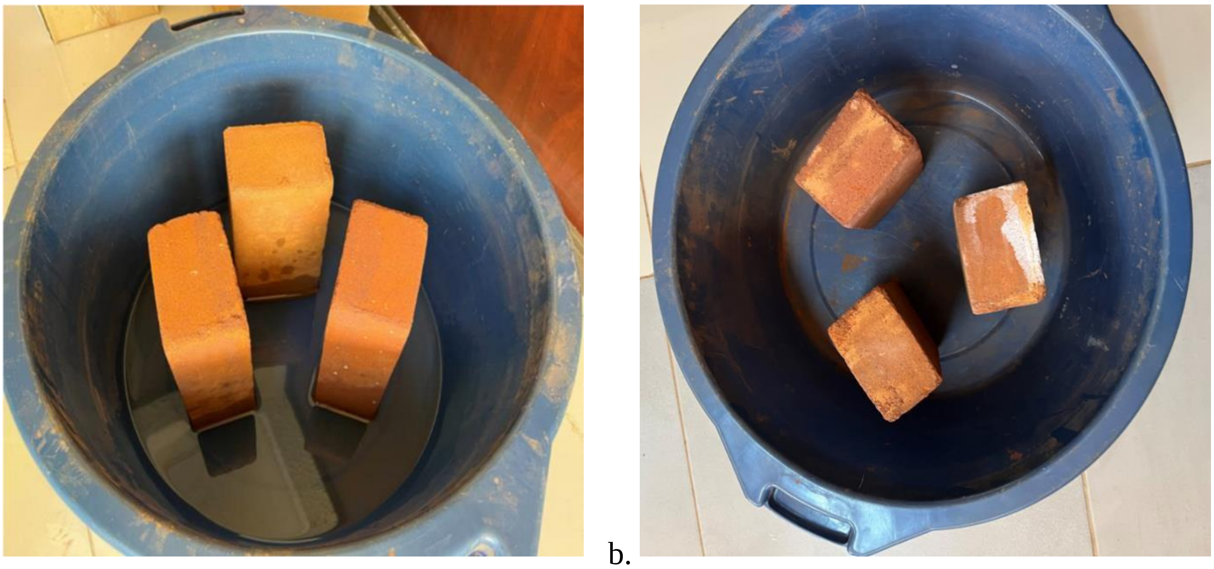

Figure 3.13: Efflorescence Test

This chapter provides the locations and operations of the Zimplats Mine at which the PGM slag was collected. The origins of the binding clay samples used in this research are also discussed. All the experimental procedures undertaken to characterize raw materials and the equipment used have been outlined in this chapter. This chapter also discusses the processes involved in brick manufacturing, the various mixing combinations prepared, and the temperature at which the bricks were treated. Finally, the necessary tests performed to assess the quality of the prepared brick specimens according to the international specifications have been outlined. The analysis of the findings from the experimental procedures described in this chapter is presented in Chapter 4.

CHAPTER 4

RESULTS AND DISCUSSION

4.1 Chapter Overview

The results and discussion of the experimental work are articulated in this chapter. The mix combinations and the firing temperatures at which the optimum mechanical and physical properties of the examined bricks were achieved are discussed. The findings from comparable research are discussed and used to validate the outcomes of this study. The two clay binders are presented as ZC and CC for Zvishavane and Chinhoyi clay, respectively.

4.2 Characterization of Raw Materials

4.2.1 X-Ray Fluorescence Analysis

X-ray fluorescence analysis was conducted on the raw materials for chemical analysis. The quantitative individual elemental compositions of the PGM slag and the clay samples (ZC and CC) from the XRF analysis are displayed in Table 4.1. Table 4.2 displays the elemental composition of the key elements for brick manufacture.

Table 4.1: Elemental Composition of the Raw Materials

Analyte (%)	PGM Slag	ZC	CC
Ni	0.124	0.042	0.098
Cu	0.107	0.032	0.079
Co	0.085	0.003	0.006

Fe	29.743	3.635	2.546
S	0.125	0.062	0.096
MgO	21.379	0.724	0.921
CaO	0.667	2.026	3.776
Al_2O_3	1.347	24.132	22.675
SiO_2	46.090	57.004	55.943
Cr_2O_3	0.337	0.059	0.093
K_2O	0.000	0.786	1.889
Na_2O	0.000	1.003	2.268
TiO_2	0.000	0.185	0.357
LOI		10.307	9.253

Table 4.2: Elemental Composition of the Key Elements for Brick Manufacture

Analyte (%)	**PGM Slag**	**ZC**	**CC**	**Acceptable Composition** (Elavarasan et al., 2021; Punmia et al., 2003; Velasco et al., 2014)
Fe	29.743	3.635	2.546	5 - 8
MgO	21.379	0.724	0.921	<1
Al_2O_3	1.347	24.132	22.675	20 - 30
SiO_2	46.090	57.004	55.943	50 - 60

The elemental composition results in Table 4.1 demonstrate that the three raw material samples contain a high concentration of SiO_2. The percentages of SiO_2 contained in both clay samples fall within the approved range of 50% to 60% for clays used in brick manufacturing (Table 4.2). It has been observed and reported that SiO_2 enhances the stiffness and minimizes the shrinkage and cracking of bricks, giving a symmetrical and uniformly textured brick. The PGM slag also has high SiO_2 content which can also contribute to the strength of the bricks.

The results in Table 4.1 show that Al_2O_3 is the second-highest chemical element present in the clay samples. Both clay samples have Al_2O_3 content within the acceptable range of 20% to 30% for brickmaking clays (Table 4.2). The presence of Al_2O_3 gives clays their plasticity behavior which is critical for brick molding. Additionally, Al_2O_3 is a cementing agent, which can hold the clay particles within a brick structure together. It is worth noting that the silica lowers the plasticity imparted by the Al_2O_3, thus reducing shrinkage, and improving the rigidness of a brick. In combined form, silica and alumina exist as aluminosilicates (Keter, 2016). These aluminosilicates offer advantages, including good corrosion resistance, low heat capacity, low thermal conductivity, and resilience to thermal shock.

Results from Table 4.1 show that the PGM slag contains significant amounts of Fe and MgO. It has been reported that Fe and MgO are beneficial during the firing of bricks as they serve as fluxes, facilitating SiO_2 to fuse at low temperatures (Elavarasan et al., 2021; Punmia et al., 2003). This temperature is required to create a glassy bond that binds the entire brick mass together. The presence of Fe strengthens and hardens the bricks, increasing their durability and impermeability. In addition, Fe is responsible for the reddish color of the bricks. Both clay samples have Fe content less than the acceptable range of 5% to 8% for clays used to make bricks, with 3.6% for ZC and 2.5% for CC. The low Fe content may affect the strength of the bricks. However, during the development of the composite PGM slag bricks, the significant Fe content in slag could compensate for the low Fe content in clay, improving the strength of the bricks.

MgO content in both clay samples is less than 1%, compared to the tolerable range for brick clays (Elavarasan et al., 2021; Punmia et al., 2003). Table 4.1 and 4.2 shows that the slag contains significant amounts of MgO. The combination of slag and clay increases the MgO content in the mix. Excessive free MgO is undesirable, it hydrates slowly in hardened products, leading to localized volume increase which can cause bricks to expand and crack. However, when dissolved in slag, MgO is not harmful and does not cause any adverse impacts on the hardened brick (Harrisson, 2019). This suggests that despite, having a very high MgO content, PGM slag can be used in brick manufacturing without the risk of brick expansion or cracking.

The findings in Table 4.2 show that all raw materials contain CaO which falls within the permissible range of less than 5% for brick-manufacturing raw materials (Punmia et al., 2003). CaO acts as a binding agent, holding the particles within the brick structure together. It reduces brick shrinkage during drying and serves as a flux similar to Fe and MgO, facilitating SiO_2 to fuse at low temperatures (Punmia et al., 2003).
Results in Table 4.1 show that the ZC has a higher loss on ignition (LOI) than CC. This is because it has more organic matter (roots, leaves, grass) compared to CC. Using ZC in

brickmaking implies a higher shrinkage possibility due to the burnt-off of the organic materials during firing than using CC. This variation is attributed to the different origins of the clay soils.

The XRF analysis results reveal no traces of harmful heavy metals such as lead, mercury, and cadmium or radioactive elements, making PGM slag secure for utilization in the construction industry. Heavy metal or radioactive poisoning can be life-threatening and can cause irreversible damage to humans and the environment.

4.2.2 Specific Gravity Analysis

The relative densities of the raw materials were determined from the specific gravity test. The specific gravity values of the PGM slag and clay samples are shown in Table 4.3.

Table 4.3: Specific Gravity of the Raw Materials

	Specific Gravity
Slag	3.25
ZC	2.78
CC	2.74

The range of values for specific gravity in inorganic clays is limited to 2.70 – 2.80 (Roy & Bhalla, 2017). The specific gravity values of both clay samples fall within the recommended range for inorganic clay soils with 2.78 for ZC and 2.74 for CC. Specific gravity is correlated to the density of the mineral composition of a material. The density of the primary chemical constituents (SiO_2, Al_2O_3, Fe, and MgO) of the three raw materials significantly influences the specific gravity of each material. The densities of Fe, Al_2O_3, MgO, and SiO_2 are 7.87 g/cm^3, 3.99 g/cm^3, 3.58 g/cm^3, and 2.65 g/cm^3, respectively. PGM slag has a high specific gravity.

This is expected because it has a high Fe concentration, with the largest density among the primary chemical elements. ZC has a higher specific gravity than CC owing to the higher Fe, Al_2O_3, and SiO_2 content in ZC than in CC. The specific gravity of the raw materials can influence the strength and the water absorption capacity of the finished bricks (Karaman et al., 2006). A high specific gravity can indicate reduced porosity which often contributes to low water absorption capacity and improved strength.

4.2.3 Particle Size Analysis

A sieve analysis test was conducted to evaluate the particle size distribution of the raw materials. The particle size distribution curves of the PGM slag and the clay samples used in this study are presented in Figure 4.1.

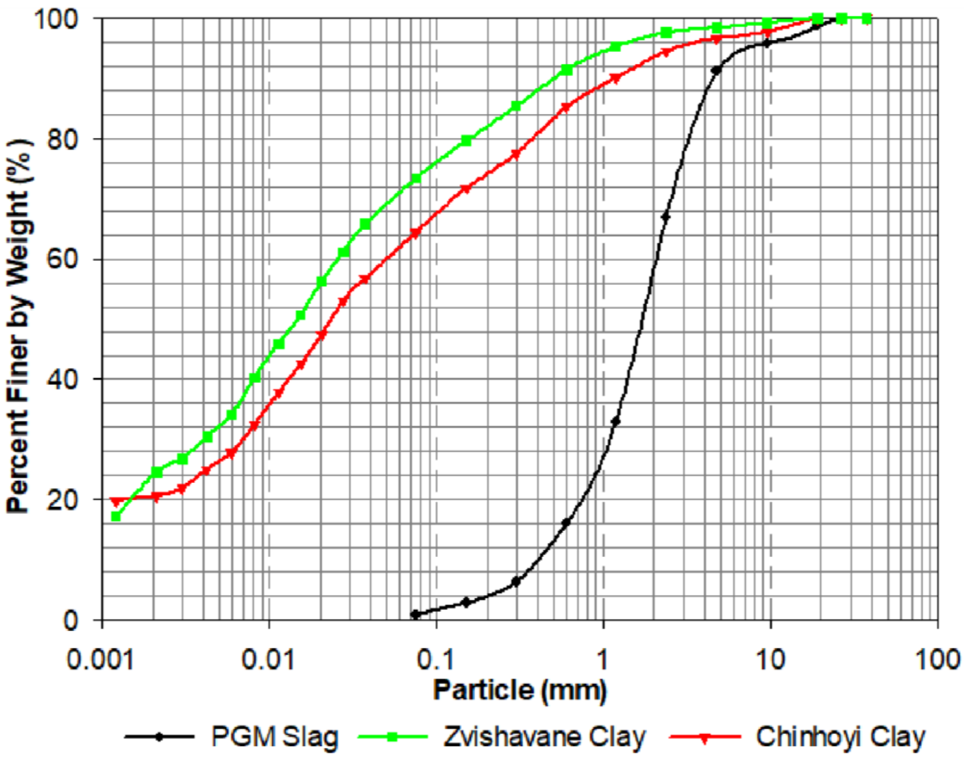

Figure 4.1: Particle Size Distribution Curves

The percentages of different particle sizes in the PGM slag and the clay samples were analyzed using particle distribution curves plotted in Figure 4.1. The particle size fractions were determined employing the Unified Soil Classification System (USCS) which is used to classify soils for engineering structural applications as highlighted in Table 2.4. In addition, the position, shape, and slope of the curves indicate the type of gradation of these raw material samples. The percentages of the particle sizes in all the raw materials are presented in Table 4.4. These percentages were then used to determine the soil texture from the soil classification textural chart shown in Figure 4.2.

Table 4.4: Particle Size Distribution Results

	PGM Slag	ZC	CC	Recommended Percentage (%)
Coarseness Index (+2,36 mm %)	33.2	2.4	5.5	
Fineness Index (-75 µm %)	1	73	65	
Gravel size (%)	8.4	1.4	3.1	
Sand size % (4.75–0.075 mm)	90.7	25.1	32.7	20 - 45
Silt size % (0.075–0.005 mm)	0.9	41.2	37.2	24 - 45
Clay size % (<0.005 mm)		32.3	27.0	20 - 35
Soil Classification Texture (USCS)	Sand	Clay Loam (CL)	Clay Loam (CL)	

*Coarseness Index CI = 100% - Percentage passing the 2.36 mm BS sieve

*Fineness Index FI = Percentage passing the 75 µm BS sieve expressed as a whole number.

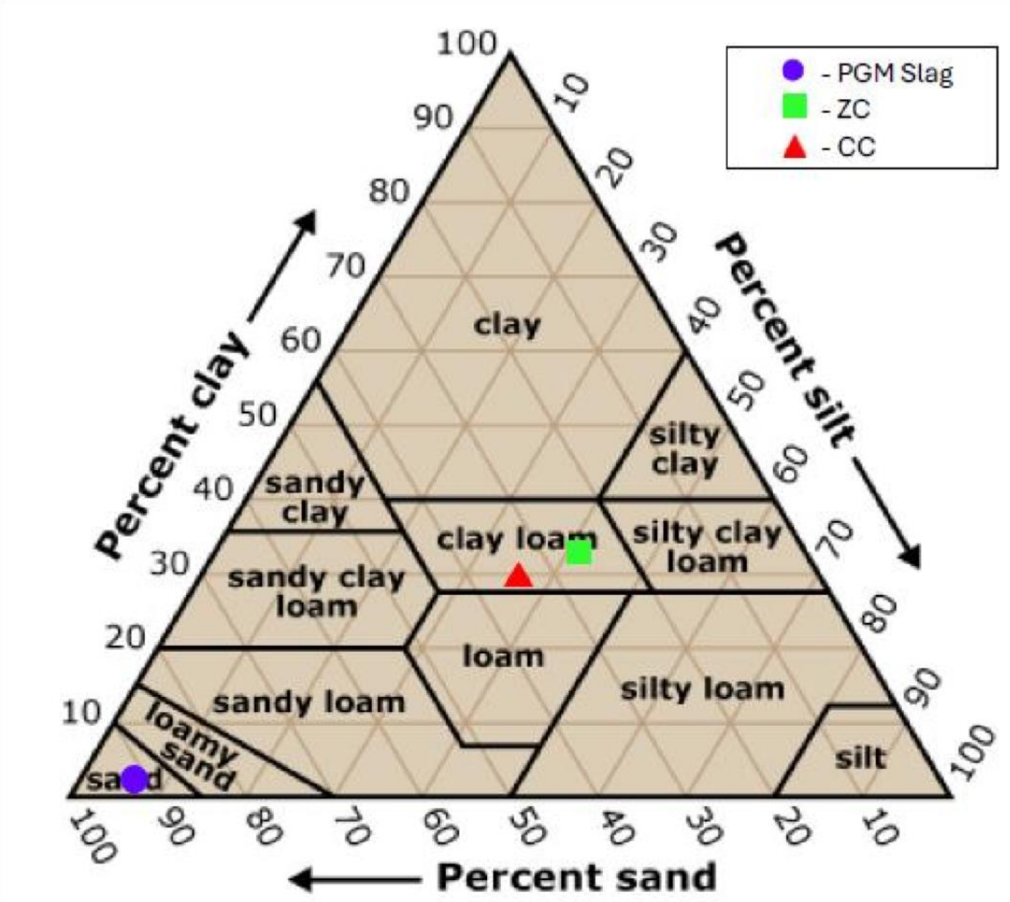

Figure 4.2: Soil Classification Textural Chart (Garcia-Gaines & Frankenstein, 2015)

The position, shape, and slope of the PGM slag particle size distribution curve in Figure 4.1 indicate that the sample is poorly graded. It does not have a good representation of all particle sizes; that is, most of the particles are of the same size. The curve also demonstrates that for

PGM slag, the proportions of gravel-sized, sand-sized, and silt-sized particles are 8.4%, 90.7%, and 0.9%, respectively. The PGM slag has a sand texture from these proportions according to the soil classification textural chart in Figure 4.2. The particle size proportions and the sand texture of the slag are also supported by the high coarseness index and low fineness index provided in Table 4.4 as they are more coarse particles (sand and gravel-sized), and a relatively low fraction of fine particles (silt size) in the sample.

The gradation curve for ZC in Figure 4.1 shows that the percentages of gravel-sized, sandsized, silt-sized, and clay-sized particles in the clay sample are 1.4%, 25.1%, 41.2%, and 32.3%, respectively. The soil classification textural chart (Figure 4.2) reveals that ZC has a Clay Loam texture. The high fineness index and low coarseness index presented in Table 4.4, also validate the particle size fractions in ZC as they contain more fine particles (clay and siltsized) than coarse particles (sand and gravel-sized).

The particle size distribution curve for CC displayed in Figure 4.1 shows that the fractions of gravel-sized, sand-sized, silt-sized, and clay-sized particles in the clay sample are 3.1%, 32.7%, 37.2%, and 27.0%, respectively. From these ratios, it can be deduced that CC has a Clay Loam texture from the soil classification textural chart (Figure 4.2). The particle size proportions in CC are also confirmed by the high fineness index and low coarseness index shown in Table 4.4 since fine particles (clay size and silt size) comprise a greater proportion compared to coarse particles (sand size and gravel size).

The shape, slope, and position of the gradation curves of the clay samples indicate the samples are well-graded. They contain a wide range of particle sizes ranging from gravel to fines, implying all particles of different sizes are represented. Both clay samples have soil texture characteristics of Clay Loam as they have comparable proportions of sand, silt, and clay-sized particles. ZC contains a relatively high fraction of fine particles compared to CC which may differentiate the plasticity properties of the soils. The recommended fractions of clay, silt, and sand-sized particles for brick clay according to Mueller et al. (2008) are 20 – 35%, 24 – 45%, and 20 – 45%, respectively. ZC has 32.3% clay-sized, 41.2% silt-sized, and 25.1% sand-sized particles, which fall within recommended particle size proportions for brick clay. CC also conforms to the specifications for brick clay with 27.0% clay-sized, 37.2% silt-sized, and 32.7% sand-sized particles. From these findings, we can conclude that the two binding clay samples are suitable for use in the brick manufacturing industry.

4.2.4 Atterberg Limits Analysis

The atterberg limits tests also known as the index properties are critical to evaluate the drying behavior and workability of raw materials in their ceramic applications. They include liquid limit (LL), plastic limit (PL), plasticity index (PI), and shrinkage limit (SL). Tests were successfully conducted on the clay samples. For the PGM slag, given that it has a sand texture, implying it is non-plastic, atterberg limits tests could not be performed. The percentages for LL, PL, PI, and SL for the clay samples are tabulated in Table 4.5.

Table 4.5: Atterberg Limits Results

	ZC	**CC**	**Recommended Percentage (%)**
Liquid Limit LL %	44.3	40.2	25 - 38
Plastic Limit PL %	22.3	21.6	
Plasticity Index PI % (LL % - PL %)	22.0	18.6	7 - 16
Shrinkage Limit SL %	6.7%	4.3%	
Soil Classification (Casagrande Plasticity chart)	Low-Plastic Clay	Low-Plastic Clay	

The index properties of clay soils can be influenced by mineral composition, particle size distribution, organic matter, origin of geological formation, and impurities (Kumari & Mohan, 2021). The results in Table 4.5 show that the LL, PL, PI, and SL percentages are higher for ZC than CC. The percentage of fine particles (clay and silt-sized) in a soil sample determines the plastic characteristics of the soil. According to the particle size analysis results, the total fraction of fine particles in ZC is higher compared to those in CC which justifies the higher percentages of index values for ZC over CC. This can be attributed to the high percentage of Al_2O_3 in ZC as observed from the elemental composition results in Table 4.1. This also validates the increased plasticity behavior of ZC over CC.

The casagrande plasticity chart displayed in Figure 4.3 was used to determine the plasticity extent of the clay samples by extrapolating the intersection of LL and PI. Having 44.3% LL and 22% PI, ZC is classified as low-plastic clay (CL) and CC is also identified as low-plastic clay (CL) with 40.2% LL and 18.6% PI.

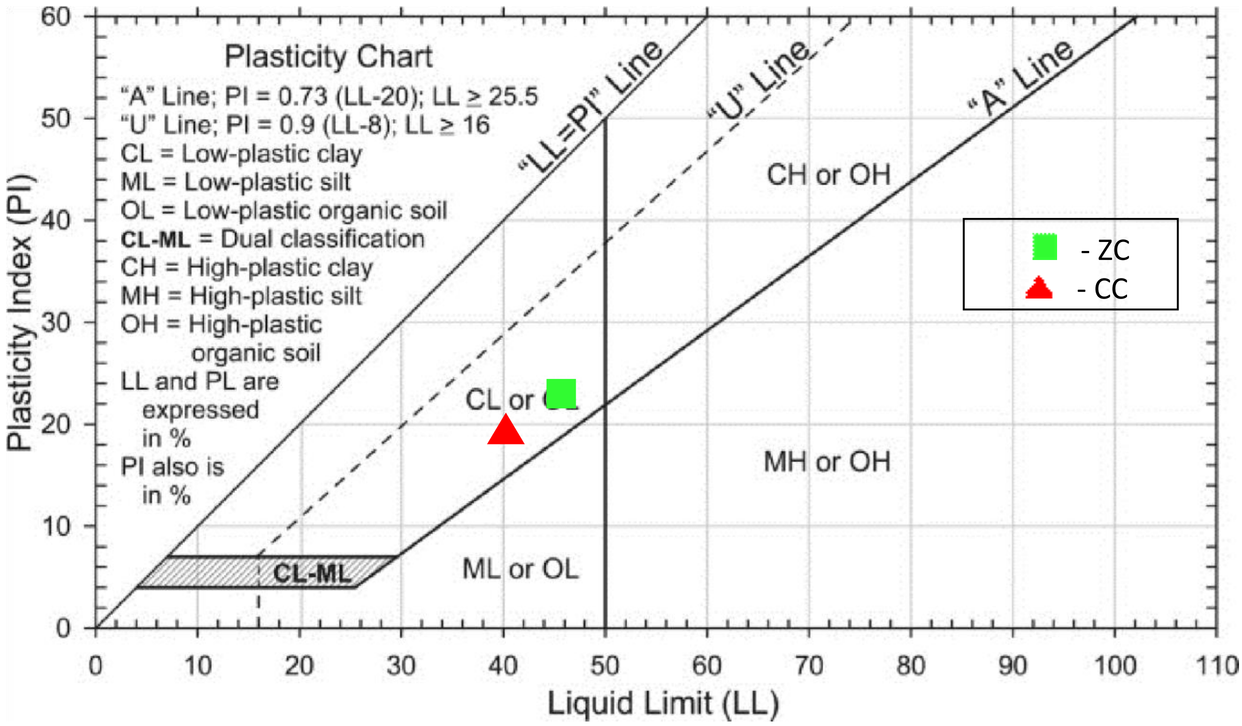

Figure 4.3: The Casagrande Plasticity Chart (Casagrande, 1948)

The recommended percentages of LL and PI for brick clay according to Mueller et al. (2008) are 25 – 38%, and 7 – 16%, respectively as presented in Table 2.3. ZC has 44.3% LL and 22.0% PI, which fails to conform with the range of acceptable index properties for clay used to manufacture bricks. CC sample index values do not comply with the specified index values for brick clays, with 40.2% LL and 18.6% PI. The two explored clay soils have index properties greater than the recommended. Similar research by Diao et al. (2021) on utilizing thick clay deposits for brickmaking reveals PI values ranging between 24% and 30%, failing to satisfy the acceptable index properties range for brick clays by Mueller et al. (2008). However, the researchers recommended that the clay requires treatment before being used in brickmaking. The ZC and CC are good candidates for the development of a composite material suitable for brickmaking when mixed with slag, given slag has a sand texture which will reduce the plasticity of clays. Thus, the clay samples can be used in brick manufacturing without the high risk of shrinkage, and no pretreatment is required.

Another important property of clay for ceramic application is the plastic limit. It determines the minimum moisture content sufficient to achieve plastic conditions that facilitate the extrusion process during brick manufacturing. However, clay soils with high PL are quite difficult to dry and are susceptible to shrinkage (Celik, 2010). The extrusion process or the workability of clays is further explained in the Extrusion Prognostic Chart of Bain and Highley (Bain & Highley, 1979) as shown in Figure 4.4.

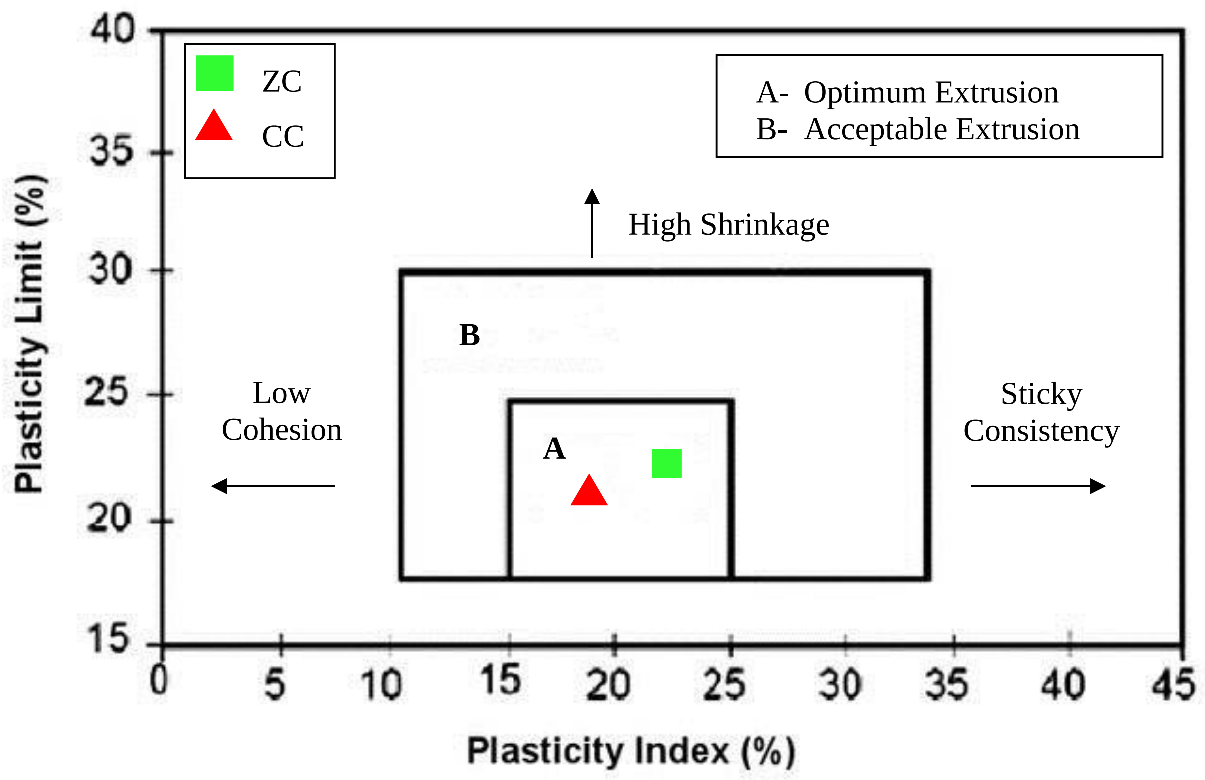

Figure 4.4: Extrusion Prognostic Chart (Bain & Highley, 1979)

Figure 4.4 demonstrates that both clay samples are in the optimum extrusion region which is the ideal range for both effective molding and efficient extrusion during brick production. According to the Extrusion Prognostic Chart, extremely low PI can make the extrusion process difficult while clay with extremely high PI tends to be sticky making it undesirable for utilization in the ceramic industry.

4.3 Brick Manufacturing Process

4.3.1 Raw Materials Preparation

The raw materials were pulverized to produce usable homogeneous particle sizes. Various mixing combinations of PGM slag and clays were prepared. The optimum water content required for the brick formation for each combination was determined by the compaction tests outlined in Section 3.4.2. Figure 4.5 shows the compaction curves from which the optimum moisture contents were deduced for each combination.

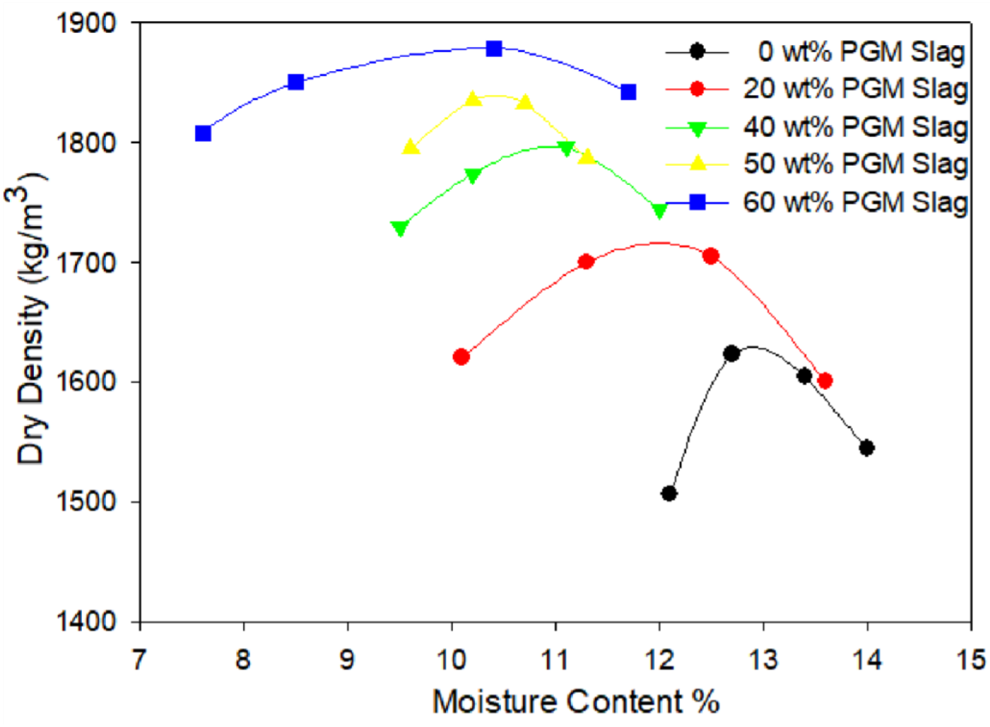

Figure 4.5: Compaction Curves for Optimum Moisture Content Determination

The peak point of the curve for each combination denotes the maximum dry density (MDD) and the moisture content corresponding to the MDD is the optimum moisture content (OMC). According to the compaction curves in Figure 4.5, an increase in moisture content raises the dry density to an optimum value, and a further increase in moisture content results in a decrease in the dry density. The OMC values obtained from the compaction curves for 0wt.%, 20wt.%, 40wt.%, 50wt.%, and 60wt.% PGM slag combinations are 12.8%, 12.1%, 11.2%, 10.7%, and 10.3%, respectively. The OMC results reveal that the amount of water required during brick formation decreases with an increase in PGM slag content (decrease in clay content). Clay soil has a high-water affinity, thus, for example, the water required by 0wt.% PGM slag combination is greater than that required by 60wt.% slag mix. According to Legese et al. (2021), the OMC for sand, silty sand, silt, and clay soils ranges from 6 – 10%, 8 – 12%, 12 – 16%, and 14 – 20%, respectively. These OMC values further support the strong water affinity for clay soils. The OMC of the explored clay samples ranges from 10.3% to 12.8%. The investigated samples are a combination of sand (PGM slag) and clay, thus, the OMC neither falls in the sand nor clay range but the silt range.

4.3.2 Brick Drying Analysis

The prepared brick specimens were naturally dried under a shed. Figure 4.6 graphically presents the drying shrinkage of the bricks for the 0wt.% to 60wt.% PGM slag combinations.

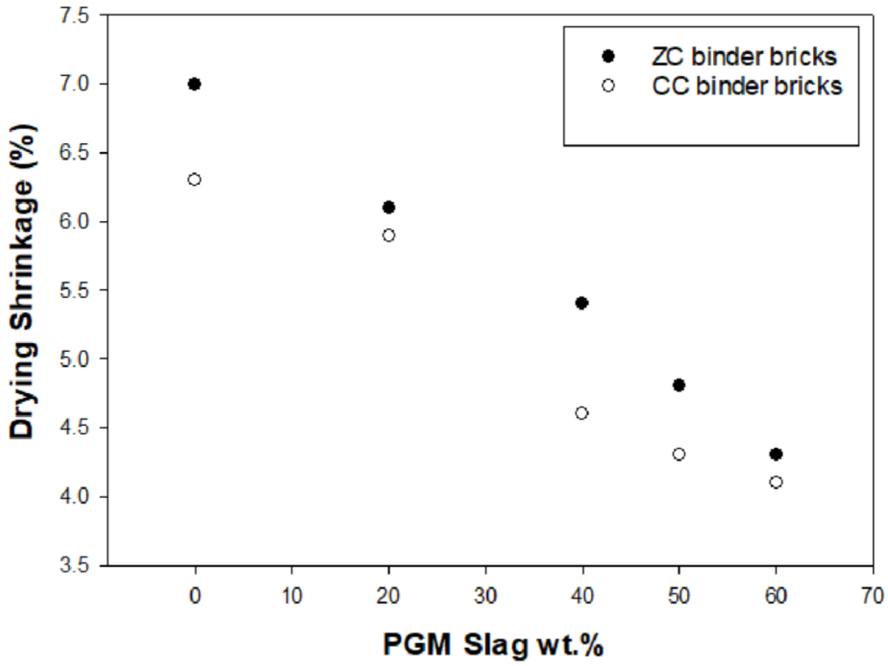

Figure 4.6: Drying Shrinkage of Bricks

As the bricks dry, moisture evaporates from the brick structure, and the process is associated with shrinkage. The drying shrinkage of the bricks is found to decrease with an increase in PGM slag content. The amount of water added to the 0wt.% slag combination during the brick forming is higher than the other combinations. During drying, more water evaporated from the bricks with 0wt.% slag combination resulting in higher shrinkage than other bricks. The 0wt.% slag combination with the entire clay has a higher shrinkage owing to the high plasticity of the clay. As the PGM slag increases, the plasticity of the combined mix decreases due to the sand texture of the slag, reducing the overall shrinkage of the brick. The drying shrinkage of the bricks from this study satisfies the tolerable linear shrinkage of less than 10% by Geschke (2004).

At any given PGM slag weight percent, bricks with ZC binder always have a higher drying shrinkage than those employing CC. The variation in the index properties of the clays could account for the difference in drying shrinkage of the bricks. The outcomes tabulated in Table 4.5 show that ZC has a PI of 22% and CC has a PI of 18.6%. This implies that bricks with ZC binder have a higher shrinkage possibility than bricks with CC binder.

4.3.3 Brick Firing Analysis

Brick samples were formed with various wt.% PGM slag combinations, dried under natural conditions and then fired at different temperatures in an electric kiln. After the firing process, the bricks show good ceramic properties. The bricks reveal no deformities and no visible firing defects are observed. However, the fired bricks have a noticeable color difference for the different firing temperatures. The color of the bricks changes from reddish to dark red when the firing temperature is raised from 950 ℃ to 1100 ℃. At elevated temperatures, ferrous oxides are produced from the oxidation of iron compounds in the raw materials and these ferrous oxides are responsible for the darker shade as illustrated in Equation 4.1.

$$4Fe + 3O_2 \rightarrow 2Fe_2O_3 \qquad 4.1$$

The dark red color reflects a high concentration of Fe_2O_3 continuously generated as the temperature increases. The darker hue at 1100 ℃ compared to 950 ℃ indicates ongoing vitrification since vitrification is also responsible for the color of the brick. The visually distinctive features of the unfired bricks, bricks fired at 950 ℃, and bricks fired at 1100 ℃ for the 50 wt.% PGM slag combinations are demonstrated in Figure 4.7, Figure 4.8, and Figure 4.9, respectively.

Figure 4.7: Sample Bricks Before Firing

Figure 4.8: Sample Bricks Fired at 950 ℃

Figure 4.9: Sample Bricks Fired at 1100 ℃

The firing shrinkage of the bricks with 50wt.% PGM slag at different temperatures is graphically presented in Figure 4.10.

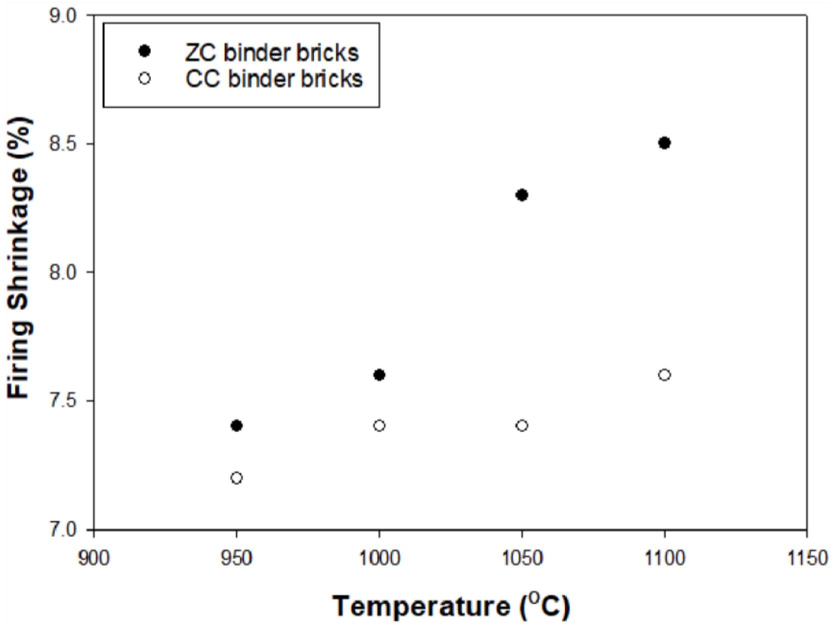

Figure 4.10: Firing Shrinkage of Bricks

The firing shrinkage of the bricks increases with temperature. During brick firing, moisture is eliminated from the brick, resulting in brick shrinkage. The decomposition of carbonate and sulphides in clay releasing CO_2 and SO_2 also contributes to the firing shrinkage of the bricks. At elevated temperatures, the density of the bricks improved, leading to volume reduction and increased shrinkage. Enhanced densification at higher temperatures is facilitated by faster diffusion of atoms, leading to effective particle bonding and hence densification.

4.4 Physical and Mechanical Properties on the Fabricated Composite Material

Tests were performed on the finished brick products to assess the brick quality and confirm its fitness for the construction industry following the ASTM and IS guidelines.

4.4.1 Compressive Strength Analysis

The ability of the bricks to endure crushing stresses was determined by compressive strength testing. Figure 4.11 presents the compressive strength results for ZC as the binder and Figure

4.12 shows the compressive strength results for CC as the binder.

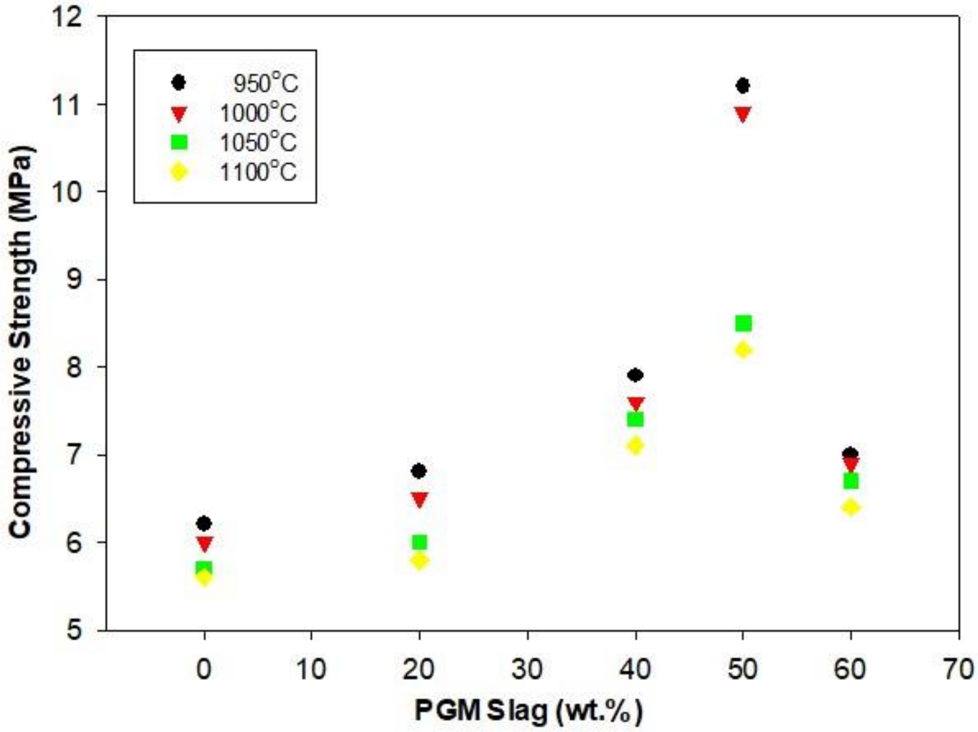

Figure 4.11: Variation of Compressive Strength with PGM Slag wt.% and Temperature for Zvishavane Clay Binder Bricks

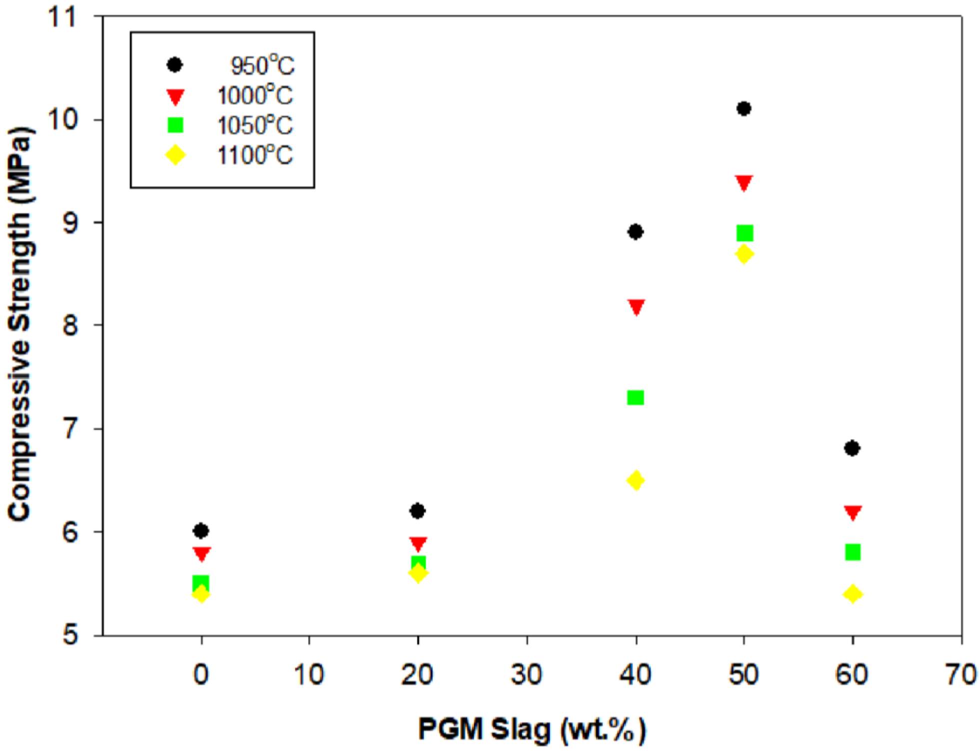

Figure 4.12: Variation of Compressive Strength with PGM Slag wt.% and Temperature for Chinhoyi Clay Binder Bricks

Figures 4.11 and 4.12 graphically present the compressive strength test results obtained on the bricks for 0wt.% slag to 60wt.% slag combinations at 950 ℃ to 1100 ℃ firing temperatures. The test results for the defined combinations and firing temperatures range from 5.6 MPa to 11.2 MPa for ZC as the binder and 5.4 MPa to 10.1 MPa for CC as the binder. The compressive strength test results for all the combinations, except for the 0wt.% slag and 60wt.% slag fired at 1100 ℃ when CC was used as the binder conforms to the recommended standard guidelines by ASTM C67-03 which states that the minimum compressive strength of a standard brick is 5.5 MPa. Higher compressive strength evaluations have always been preferred for high-quality clay bricks. The strength of the brick specimens is found to improve from 0wt.% slag to 50wt.% slag, after which there is a drop at 60wt.% slag. The 50wt.% slag combination records the highest compressive strength for both ZC and CC as the binders with a strength of 11.2 MPa and 10.1 MPa, respectively.

According to the XRF results, SiO_2, Al_2O_3, Fe, and MgO are the main chemical constituents of the raw materials and they affect the strength of a brick. The 0wt.% slag combination is comprised entirely of clay, in which SiO_2 and Al_2O_3 are the major constituents with Fe and MgO present in small amounts. SiO_2, Al_2O_3, and MgO content in the 0wt.% PGM slag is sufficient for the strength development of the bricks, minimizing the shrinkage, and cracking of bricks. However, the Fe content is significantly lower than the 5%-8% acceptable range for brick clays. Bricks comprising of 0wt.% PGM slag exhibits lower strength than other combinations. This can be attributed to the low Fe content since Fe enhances the strength and hardens bricks, increasing their durability and impermeability. Bricks with 50wt.% PGM slag outperforms the other combinations in terms of compressive strength because of the stronger matrix created by the 50wt.% combination. The combination of SiO_2, Al_2O_3, Fe, and MgO in the 50wt.% mix is sufficient to strengthen, harden, and minimize shrinkage, and cracking of bricks. The compressive strength in the 60wt.% combination is expected to be high since there is high Fe and MgO, and sufficient SiO_2. However, from the chemical point of view, the drop can be explained as a result of reduced Al_2O_3 content in the 60wt.% PGM combination.

The PI% and SL% significantly influence the strength of bricks. The recommended PI% for brick clay according to Mueller et al. (2008) is 7% - 16%, however, the binding clays explored have PI% of 22.0% for ZC and 18.6% for CC which is beyond the recommended range. The 0wt.% slag combination with the entire clay has a higher shrinkage possibility compared to the other combinations. A larger extent of shrinkage could lead to crack formation during drying or firing, weakening the bricks and reducing their compressive strength. From 20wt.% to 50wt.% combination there is a reduction in the clay content and an increase in the slag. As a result, the plasticity of the clay in the combined mixture during brick formation is suppressed by the sand texture of the PGM, reducing the degree of shrinkage and improving the strength of the bricks. However, in the 60 wt.% combinations, the slag predominated over the clay. The plasticity effect of the clay is no longer sufficient to cement the slag, weakening particle bonding between the slag and clay, and hence strength reduction. The PI% of the PGM slag and clay combinations could not be provided to substantiate the plasticity effect of clay on the slag. The reason is that LL and PL tests could not be successfully conducted on the slag-clay mixture due to the sand texture of PGM slag, implying it is non-plastic.

The compressive strength of the bricks from this study decreases with increasing firing temperature. The highest compressive strength among the tested bricks is recorded at 950 ℃ and the minimum strength at 1100 ℃. This strength-temperature relationship reflects that when the temperature reaches 950 ℃, the bricks could have already developed enough strength since vitrification commences at around 900 ℃. The presence of Fe and MgO in significant amounts in the slag is advantageous during the firing of bricks. They serve as fluxes, facilitating silica to fuse at low temperatures hence lowering the temperature required to create a glassy bond that binds the entire structure, providing the strength of the brick. The subsequent increase in temperature up to 1100 ℃ could induce internal stresses that ultimately weaken the brick resulting in strength reduction. Bohara et al. (2020) discovered a similar behavior in their prepared bricks. The compressive strength of their bricks increased with temperature from 4.12 MPa at 700 ℃ to 17.06 MPa at 950 ℃ and then decreased to 2.55 MPa at 1100 ℃. The maximum compressive strength observed at 950 ℃ is advantageous because it reduces the energy required during brick firing compared to 1100 ℃.

At any given combination and annealing temperature, bricks with ZC as the binder always have better compressive strength than those employing CC. At 950 ℃, ZC binder bricks demonstrate a maximum compressive strength of 11.2 MPa, and CC binder bricks exhibit a maximum of 10.1 MPa. The reason for the difference in the compressive strength could be the variation in the chemical constituents, particle size, and index properties of the clay samples. The main chemical constituents of the clay samples; SiO_2, Al_2O_3, Fe, and MgO, that enhance the strength of bricks are present in almost similar proportions. However, the lower content of these chemical elements in CC than in ZC as tabulated in Table 4.1 could account for the reduced compressive strength of bricks with the CC binder compared to the bricks with ZC binder. Although both clay samples are classified as Clay Loam according to the USCS textural chart and low-plastic clay by the casagrande plasticity chart, the PI% of CC is lower than that of the ZC as shown in Table 4.5. For this reason, the binding effect of CC is less effective in cementing the PGM slag, weakening the bond between the slag and CC resulting in a lower compressive strength of CC binder bricks compared to ZC binder bricks.

The compressive strength test results conclude that the optimum compressive strength was achieved with 50wt.% PGM slag combination fired at 950 °C with ZC as the binder.

4.4.2 Water Absorption Analysis

The potential of the bricks to absorb water from the surroundings was determined by the water absorption test. Figure 4.13 displays the water absorption results for ZC as the binder and Figure 4.14 presents the water absorption results for CC as the binder.

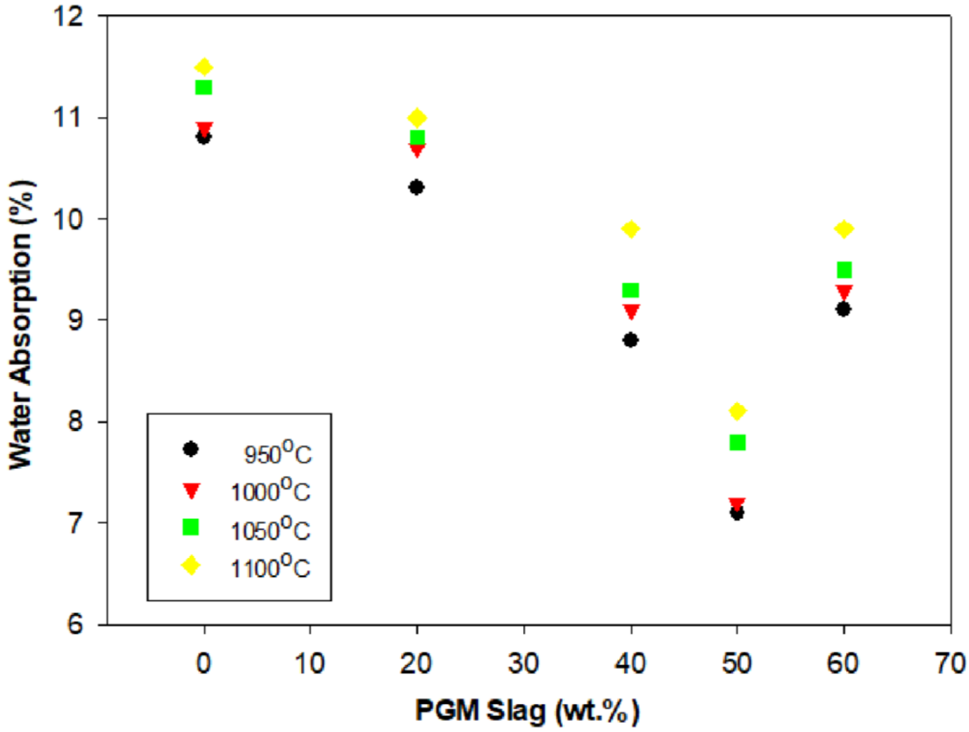

Figure 4.13: Variation of Water Absorption with PGM Slag wt.% and Temperature for Zvishavane Clay Binder Bricks

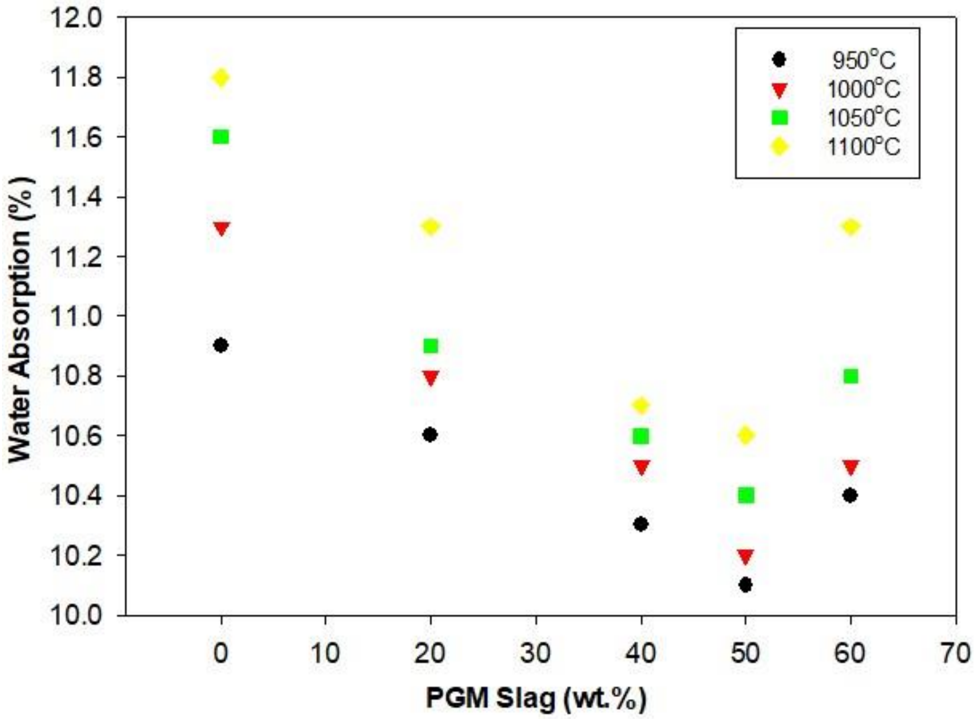

Figure 4.14: Variation of Water Absorption with PGM Slag wt.% and Temperature for Chinhoyi Clay Binder Bricks

The water absorption test results of the bricks for 0wt.% to 60wt.% PGM combinations fired between 950 °C and 1100 °C are graphically shown in Figures 4.13 and 4.14. The test results for the specified combinations and firing temperatures range from 7.1% to 11.5% for ZC as the binder and 10.1% to 11.8% for CC as the binder. The water absorption test results for all the combinations comply with the acceptable standard guidelines by IS:3495-2-1992 which states that a brick should not absorb more water than 20% of its dry weight. Lower water absorption capacity evaluation is always desirable for quality clay bricks. The brick specimens are found to have a decrease in water absorption from 0wt.% to 50wt.% PGM, followed by an increase at 60wt.% combination. The 50wt.% PGM combination records the lowest water absorption for both ZC and CC as the binders with absorption values of 7.1% and 10.1%, respectively.

The amount of water introduced to the dry raw materials during brick formation significantly influences the water absorption capacity of bricks. This water is driven out of the brick during drying and firing, leaving pores within it. During the water absorption test, water is drawn into these pores, therefore the more the pores, the more the water absorbed by the brick. The 0wt.% PGM combination is comprised entirely of clay and clay soil has a strong water affinity. According to the compaction test results, the OMC value for the 0wt.% slag combination is

12.8% and it is found to decrease with the decrease in clay content to an OMC of 10.3% at 60wt.% PGM mix. This implies more water has been added to the 0wt.% combination during brick formation and more pores were left within the bricks after drying and firing. As a result of more pores, the 0wt.% PGM combination absorbs more water during the water absorption test compared to the other combinations. The water absorption capacity of the 60wt.% combination is expected to be low since minimal water was introduced during the brick formation. However, the increase in water absorption value at 60wt.% PGM is accounted for by the binding effect of the clay to the slag. In the 60wt.% combinations, the slag is more prevalent than the binding clay, hence the clay content could no longer bind the slag effectively. As a result of the poor binding effect, more pores are left within the brick structure, which increases its water absorption capacity.

The water absorption of the bricks from this study increases with firing temperature. The minimum water absorption among the tested bricks is recorded at 950 ℃ and the highest at 1100 ℃ firing temperatures. This water absorption-temperature relationship reflects that at 950 ℃, the bricks could have already developed a glassy bond that holds the entire structure together, closing pores and voids within the bricks through the vitrification process. With a further increase in temperature up to 1100 ℃, the brick could have expanded in response to extreme temperatures, inducing internal stresses that eventually caused the brick to crack resulting in high absorption capacity. The findings from this study are comparable with those reported by Tsega et al. (2017) on their studied bricks. Their results reveal a decrease in water absorption with a temperature increase from 17.4% at 700 ℃ to 10.8% at 970 ℃ and then rise to 19.6% at 1200 ℃. The water absorption rise is explained as a result of internal cracks that form at elevated temperatures.

In all combinations and annealing temperatures, bricks that employed ZC as the binding material have consistently lower water absorption values than those that used CC. ZC binder bricks exhibit a minimum water absorption value of 7.1% at 950 ℃, whereas CC binder bricks record a minimum of 10.1% at the same temperature. The variation in the index properties of the clays could have accounted for the difference in the water absorption values. The casagrande plasticity chart classified both clay samples as low-plastic clays; however, the PI% of CC is lower than that of ZC as tabulated in Table 4.5. Consequently, the binding effect of CC is less effective in binding the PGM slag compared to ZC. Inadequate binding implies more pores within the brick structure, which may result in a higher water absorption capacity for bricks with CC binder over ZC binder.

The water absorption findings conclude that the optimal water absorption value is obtained from the 50wt.% PGM slag combination annealed at 950 °C with ZC as the binder.

4.4.3 Compressive Strength and Water Absorption Correlation

The compressive strength and water absorption test results reveal a correlation between the strength of the brick and its water absorption capacity. In all the combinations and annealing temperatures, the highest compressive strength is associated with the lowest water absorption value, and so as for the lowest compressive strength with the highest water absorption. The 50wt.% PGM combination at ZC has been decided upon to demonstrate the relationship between compressive strength and water absorption since it exhibits better properties over the other combinations. Figure 4.15 shows a correlation between the compressive strength and the water absorption.

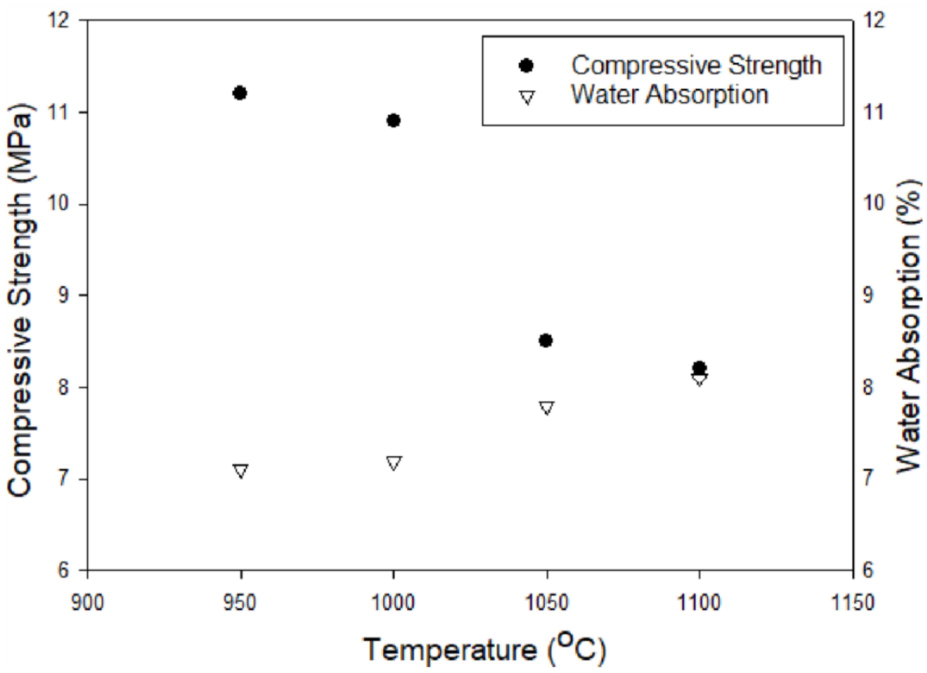

Figure 4.15: Compressive Strength and Water Absorption Variation with Temperature

A decrease in compressive strength corresponds to an increase in water absorption as shown in Figure 4.15. The rationale is that lower strength implies more pores or cracks hence an increased water absorption capacity for the PGM-clay bricks.

4.4.4 Soundness Analysis

A soundness test was conducted on the prepared bricks to assess their performance against a sudden impact. The soundness test results for all combinations and firing temperatures conform to the recommended standard guidelines by IS:3495-2-1992 that bricks should generate a clear metallic sound and should not break when struck against each other. This metallic sound arises owing to sufficient vitrification of the bricks during the firing. There is a noticeable metallic sound difference on the bricks fired at 950 ℃ and 1100 ℃. The bricks annealed at 1100 ℃ are more sonorous than the ones fired at 950 ℃. At elevated temperatures, there is enhanced densification of the product due to the new structural phases, mullite, and gehlenite, that occur within the brick structure. The reason for the more sonorous metallic sound of the product fired at 1100 ℃ is the improvement in the densification of the brick. This observation aligns with the findings by Roudouane et al. (2020), who discovered that the metallic sound of the brick structure improves with a temperature rise from 800 ℃ to 1100 ℃ owing to the enhanced densification of the product.

4.4.5 Hardness Analysis

A hardness test was performed on the prepared bricks to evaluate their resistance against scratches. The hardness test results for all combinations and annealing temperatures fail to satisfy the recommended standard guidelines by IS:3495-2-1992 that brick should leave no impression on the surface when struck by a sharp object. Scratches are observed on the brick surfaces upon this test. The possible reason could be the manufacturing method employed in this study. A manual method was employed during molding, and the pressure applied to the brick may not have been sufficient to make the final brick scratch-resistant. Bricks treated at 1100 ℃ reveal fewer scratches than those treated at 950 ℃. At 1100 ℃, atomic diffusion increases, resulting in effective particle bonding and hence enhanced densification, which subsequently improves the hardness of the bricks.

4.4.6 Efflorescence Analysis

An efflorescence test was carried out to assess the presence of soluble salts in the bricks. The efflorescence test results for all combinations are tabulated in Table 4.6.

Table 4.6: Efflorescence Test Results

	Efflorescence Result				
	Nil No Observation	Slight < 10%	Moderate 10-25%	Heavy 25-50%	Extreme >50%
0wt.% Slag		▯			
20wt.% Slag		▯			
40wt.% Slag			▯		
50wt.% Slag			▯		
60wt.% Slag			▯		

White deposits are observed on the surfaces of the bricks as illustrated in Figure 4.16. These white deposits demonstrate the presence of soluble salts in the bricks that have migrated and collected on the surface.

Figure 4.16: Brick Efflorescence at 50 wt.% Combination

The concentration of soluble salts in the brick determines the extent to which efflorescence emerges. Figure 4.16 shows moderate efflorescence of a brick with 50wt.% PGM slag. The most common efflorescing salts are sulphate and carbonate compounds of sodium, potassium, calcium, magnesium, and aluminium (Brocken & Nijland, 2004; Nhabih et al., 2020). Iron oxide and calcium hydroxide are also among the sources of efflorescence in bricks (Kazmi et al., 2016; Velasco et al., 2014). In this study, the bricks at all the combinations show some presence of efflorescence. The efflorescence in the bricks is due to the existence of Fe and CaO in the raw materials. Iron compounds in raw materials undergo oxidation to form ferrous oxides, which react with carbonates and sulphides from the decomposition reaction (brick firing process). Efflorescence develops if there is moisture in or on a brick. The iron sulphates compounds formed are water-soluble and can migrate on the surface of the brick during the experimental procedure leaving white deposits. In addition, when iron oxides come into contact with water, they can undergo hydration and oxidation reactions, forming iron hydroxides. The resulting compounds can contribute to the efflorescence of the bricks. The efflorescence of the bricks could have been contributed by the calcium oxide in the brick, which reacted with the water during the experimental procedure to generate calcium hydroxide. The 0wt.% and 20wt.% PGM slag combinations reveal slight efflorescence whereas the 40wt.%, 50wt.%, and 60wt.% slag combinations exhibit moderate efflorescence. The Fe concentration at 0wt.% and 20wt.% PGM combinations is lower than that at 40wt.%, 50wt.%, and 60wt.% PGM combinations. As a result of lower Fe content, fewer iron oxides are generated from the oxidation process resulting in slight efflorescence. This could have accounted for the variation in the efflorescence intensity.

4.5 Chapter Summary

This chapter discussed the experimental findings throughout the research. The outcomes obtained from the characterization of the raw materials are well articulated. The elemental analysis of PGM slag reveals no traces of harmful heavy metals making it safe for use in brickmaking as heavy metals can be life-threatening to humans and the environment. The experimental observations of the brick manufacturing process which includes the preparation of raw materials and brick firing have been outlined in this chapter. This chapter contains the experimental findings from the mechanical and physical tests conducted on the bricks. The optimum compressive strength and water absorption values of the examined bricks are achieved with 50wt.% PGM slag combination fired at 950 ℃ on both clay binders. The distinctive features (color and sound) of the bricks fired at 950 ℃ and 1100 ℃ are explained. The bricks reveal positive efflorescence owing to the existence of Fe and CaO in the raw materials. The findings from similar studies are also discussed and compared with the outcomes from this study. The conclusions and recommendations drawn from this study are discussed in the following chapter.

CHAPTER 5

CONCLUSIONS AND RECOMMENDATIONS

5.1 Conclusions

The application of PGM Furnace Slag combined with earth-based clay to produce a sustainable construction material has been successfully demonstrated. Utilizing PGM slag in making building materials lessens the slag disposal challenges and conserves natural resources.

The elemental analysis of PGM slag reveals no traces of harmful heavy metals and could be used safely in brickmaking. The key chemical elements: SiO_2, Al_2O_3, and MgO required for earth-based clay are present in sufficient amounts to enhance the strength of the bricks. The PGM slag contains significant amounts of Fe and MgO. These elements may be beneficial during the firing of bricks as they facilitate silica to fuse at low temperatures, giving strength and hardening the bricks. Both clay samples have low Fe content, however, the significant Fe in slag could compensate for the low Fe content in clay improving the strength of the bricks.

Various PGM slag weight percent mixing combinations were prepared to establish an optimum design mix ratio. The strength of the brick specimens is found to improve from 0wt.% slag to 50wt.% slag, after which there is a drop at 60wt.% slag. Bricks with a low PGM slag content have low strength because of the high plasticity imparted by clay which could lead to crack formation, weakening the bricks and reducing their compressive strength. The increase in PGM slag weight percent reduces the plasticity of the clay and improves the workability of the mixture, enhancing the strength of the finished product. Further addition beyond 60% implies PGM slag has dominated over the clay. Clay is no longer sufficient to bind the slag, weakening the bond between the slag and clay, resulting in strength reduction.

The dried bricks were treated at various temperatures to investigate the effect of temperature on the properties of the finished product. The color of the bricks is observed to change from reddish to dark red when the firing temperature rises from 950 ℃ to 1100 ℃. The darker hue at 1100 ℃ compared to 950 ℃ indicates ongoing vitrification since vitrification is responsible for the color of the brick. The bricks annealed at 1100 ℃ are more sonorous than the ones fired at 950 ℃. The more resonant metallic sound of the product fired at 1100 ℃ is a result of enhanced densification that occurs at elevated temperatures. The compressive strength of the studied bricks decreases with increasing firing temperature. At 950 ℃, the bricks have developed enough strength owing to the presence of Fe and MgO that facilitate silica to fuse at low temperatures giving strength to the bricks. Further temperature rise could induce internal stresses that ultimately weaken the brick resulting in strength reduction. These internal stresses are caused by phase transitions and thermal contractions within the brick matrix.

Mechanical and physical test results of the prepared bricks satisfy the ASTM C67-03 and IS:3495-2-1992. The optimum brick properties are achieved with 50wt.% PGM slag combination, 10.7% forming water, and 950 firing temperature with ZC employed as the binder. The optimum compressive strength and water absorption percentage reported from this study are 11.2 MPa and 7.1%, respectively. The optimum compressive strength and water absorption percentage for CC binder bricks are 10.1 MPa and 10.1%, respectively.

The bricks reveal positive efflorescence results owing to the existence of Fe and CaO in the raw materials. The ferrous oxides from the oxidation of Fe and calcium hydroxide from the hydration reaction of CaO could have contributed to the white deposits on the bricks. Bricks that contain low PGM slag weight percent reveal slight efflorescence whereas those with high PGM slag content exhibit moderate efflorescence. The variation in the efflorescence intensity is attributed to the Fe content in the PGM slag-clay brick mix.

An average brick of dimensions 230 mm × 115 mm × 75 mm weighs 3 kg. The exceptionally heavy weight of the PGM slag-clay brick, approximately 4 kg is attributed to the high specific gravity of PGM Slag.

It is noteworthy to conclude that, PGM Furnace Slag, a by-product from metallurgical processes can be used to produce sustainable composite construction materials acceptable in the construction industry. The overall use of PGM slag promotes the sustainability of the mining industry, at the same time enhancing a green and sustainable construction industry.

5.2 Recommendations

Additional research has to be conducted in the areas that have been highlighted:

- The weight of the brick can be reduced by incorporating perforations in the brick. Perforated holes also provide better strength to structures as they fill with mortar, securing the bricks to one another;

- The weight of the brick can be reduced by incorporating alternative lightweight binders such as fly ash or lime. Fly ash or lime are common binding agents in the construction industry and can enhance the strength of the finished product;

- Employing the geopolymerization technique, which conserves energy by eliminating hightemperature kiln firing;

- XRD needs to be conducted on the raw materials to establish the crystallographic structure and phases of the materials;

- Perform SEM test on the bricks to observe their microstructure.

REFERENCES

Adiansyah, J. S., Rosano, M., Vink, S., & Keir, G. (2015). A framework for a sustainable approach to mine tailings management: disposal strategies. Journal of Cleaner Production, 108(Part A), 1050–1062.

Afum, B. O., Caverson, D., & Ben-Awuah, E. (2019). A conceptual framework for characterizing mineralized waste rocks as future resources. International Journal of Mining Science and Technology, 29(3), 429–435.

Agbo, A. O., Nwogbu, C. C., & Udeh, B. C. (2022). Engineering Characterization of Agbani Clay Deposit as Refractory Material for Furnace Lining. American Journal of Applied Sciences and Engineering, 3(3), 1-9.

Ahmari, S., & Zhang, L. (2012). Production of eco-friendly bricks from copper mine tailings through geopolymerization. Construction and Building Materials, 29, 323–331.

Ahmari, S., & Zhang, L. (2013). Utilization of cement kiln dust (CKD) to enhance mine tailings-based geopolymer bricks. Construction and Building Materials, 40, 1002–1011.

Akinshipe, O., & Kornelius, G. (2017). Chemical and Thermodynamic Processes in Clay Brick Firing Technologies and Associated Atmospheric Emissions Metrics-A Review. Journal of Pollution Effects & Control, 5(2), 190-200.

Alam, P., Singh, D., & Kumar, S. (2022). Incinerated municipal solid waste bottom ash bricks: A sustainable and cost-efficient building material. Materials Today, 49(5), 1566–1572.

Aneke, F. I., & Awuzie, B. (2018). Conversion of industrial wastes into marginal construction materials. Acta Structilia, 25(2), 119–137.

Annan, E., Agyei-Tuffour, B., Konadu, D., Damoah, L. N. W., Konadu, D. S., & Mensah, B. (2012). Physico-mechanical properties of bauxite residue-clay bricks Energy View project Statistical Analysis of Strength and Fracture toughness of Electro-porcelains View project, 7(12), 1587-1594.

Araujo, F. S. M., Taborda-Llano, I., Nunes, E. B., & Santos, R. M. (2022). Recycling and reuse of mine tailings: A review of advancements and their implications. Geosciences, 12(9), 319.

Araújo, M. V., Delgado, J. M. P. Q., & Barbosa de Lima, A. G. (2017). On the use of CFD in thermal analysis of industrial hollow ceramic brick. Diffusion Foundations, 10, 70–82.

ASTM, A. (2015). Standard test method for relative density (specific gravity) and absorption of coarse aggregate. PA.

ASTM, C. (2003). 67-03, Standard test methods for sampling and testing brick and structural clay tile. American Society for Testing and Materials, Philadelphia, PA.

ASTM, C. (2006). Standard Test Method for Sieve Analysis of Fine and Coarse Aggregates. ASTM International: West Conshohocken, PA, USA. ASTM C136-06.

ASTM, D. (2012). Standard test methods for laboratory compaction characteristics of soil using standard effort (12 400 ft-lbs/ft3 (600 kN-m/m3)). D698-12.

ASTM D4318-17 2017, Standard Test Methods for Liquid Limit, Plastic Limit, and Plasticity Index of Soils (Superseded), ASTM International, West Conshohocken, PA,

Babu, S. V. G., & Krishnaiah, S. (2018). Manufacturing of eco-friendly brick: A critical review. International Journal of Computational Engineering Research, 8(2), 24–32.

Bain, J. A., & Highley, D. E. (1979). Regional appraisal of clay resources-a challenge to the clay mineralogist. In Developments in Sedimentology. Elsevier, 27, 437–446.

Barnes, G. E. (2009). An apparatus for the plastic limit and workability of soils. Proceedings of the Institution of Civil Engineers-Geotechnical Engineering, 162(3), 175–185.

Bhairappanavar, S., Liu, R., & Shakoor, A. (2021). Eco-friendly dredged material-cement bricks. Construction and Building Materials, 5(2), 190-200.

Bidoung, J. C., Pliya, P., Meukam, P., Noumowé, A., & Beda, T. (2016). Behaviour of clay bricks from small-scale production units after high temperature exposure. Materials and Structures, 49(12), 4991–5006.

Binici, H., Aksogan, O., Bodur, M. N., Akca, E., & Kapur, S. (2007). Thermal isolation and mechanical properties of fibre-reinforced mud bricks as wall materials. Construction and Building Materials, 21(4), 901–906.

Biswal, S., Pahlevani, F., & Sahajwalla, V. (2020). Wastes as resources in steelmaking industry—current trends. Current Opinion in Green and Sustainable Chemistry, 26, 100377.

Bohara, N., Ghale, D., Chapagain, Y., Duwal, N., & Bhattarai, J. (2020). Effect of firing temperature on physico-mechanical properties of contemporary clay brick productions in Lalitpur, Nepal. Bangladesh Journal of Scientific and Industrial Research, 55(1), 43–52. Bragagni, M., & Xhaferraj, L. (2021). Copper and our sustainable future.

Brocken, H., & Nijland, T. G. (2004a). White efflorescence on brick masonry and concrete masonry blocks, with special emphasis on sulfate efflorescence on concrete blocks. Construction and Building Materials, 18(5), 315–323.

Brocken, H., & Nijland, T. G. (2004b). White efflorescence on brick masonry and concrete masonry blocks, with special emphasis on sulfate efflorescence on concrete blocks. Construction and Building Materials, 18(5), 315–323.

Bunaciu, A. A., UdriŞTioiu, E. G., & Aboul-Enein, H. Y. (2015). X-ray diffraction: instrumentation and applications. Critical Reviews in Analytical Chemistry, 45(4), 289– 299.

Bustillo Revuelta, M., & Bustillo Revuelta, M. (2021). Ceramic Products. Construction Materials: Geology, Production and Applications, 339–374.

Cárdenas-Ramírez, C., Gómez, M., & Jaramillo, F. (2019). Characterization of a porous mineral as a promising support for shape-stabilized phase change materials. Journal of Energy Storage, 26, 101041.

Casagrande, A. (1948). Classification and identification of soils. Transactions of the American Society of Civil Engineers, 113(1), 901–930.

Celik, H. (2010). Technological characterization and industrial application of two Turkish clays for the ceramic industry. Applied Clay Science, 50(2), 245–254.

Chen, Y., Zhang, Y., Chen, T., Liu, T., Zhao, Y., & Jiao, X. (2011). Notice of Retraction: Utilization of hematite tailings in non-fired bricks production. In 5th International Conference on Bioinformatics and Biomedical Engineering, iCBBE 2011. IEEE Computer Society.

Cheng, Y., Xing, J., Bu, C., Zhang, J., Piao, G., Huang, Y., Xie, H., & Wang, X. (2019). Dehydroxylation and structural distortion of kaolinite as a high-temperature sorbent in the furnace. Minerals, 9(10), 587.

Ciocan, A. (2012). An Overview of Assessment of the Blast Furnace Slag Transformation into Value Added by-Products on Basis of its Characteristics Knowledge. The Annals of "Dunarea de Jos" University of Galati. Fascicle IX, Metallurgy and Materials Science, 35(2), 38–48.

Civil Engineers PK. (2016). Burning of Bricks. Civil Engineers PK. Retrieved October 10, 2023, from https://civilengineerspk.com/burning-of-bricks/ Craig, R. F. (2004). Craig's soil mechanics. CRC press.

Craig, R. F. (2013). Soil mechanics. Springer.

D698, A. (2012). Standard test methods for laboratory compaction characteristics of soil. Annual book of ASTM standards.

Danish, A., Totiç, E., Bayram, M., Sütçü, M., Gencel, O., Erdoğmuş, E., & Ozbakkaloglu, T. (2022). Assessment of mineralogical characteristics of clays and the effect of waste materials on their index properties for the production of bricks. Materials, 15(24), 8908.

Das, B. M. (2019). Advanced soil mechanics. CRC press.

Dash, S. K., & Hussain, M. (2015). Influence of lime on shrinkage behavior of soils. Journal of Materials in Civil Engineering, 27(12), 04015041.

Dawood, A. O., Mussa, F. I., Al Khazraji, H., Abd Ulsada, H. A., & Yasser, M. M. (2021). Investigation of compressive strength of straw reinforced unfired clay bricks for sustainable building construction. Civil and Environmental Engineering, 17(1), 150–163.

De Aza, A. H., Turrillas, X., Rodriguez, M. A., Duran, T., & Pena, P. (2014). Time-resolved powder neutron diffraction study of the phase transformation sequence of kaolinite to mullite. Journal of the European Ceramic Society, 34(5), 1409–1421.

Diao, I., Diagne, M., & Dia, I. (2021). Characterization of Fired Clay Bricks for an Economic Contribution of the Exploitation of Thicky Clay Deposit. Materials Sciences and Applications, 12(9), 389–416.

Diko-Makia, L., & Ligege, R. (2020). Composition and technological properties of clays for structural ceramics in Limpopo (South Africa). Minerals, 10(8), 700.

Ding, A., Zhang, R., Ngo, H. H., He, X., Ma, J., Nan, J., & Li, G. (2021). Life cycle assessment of sewage sludge treatment and disposal based on nutrient and energy recovery: A review. Science of the Total Environment, 769, 144451.

Diop, M. B., & Grutzeck, M. W. (2008). Low temperature process to create brick. Construction and Building Materials, 22(6), 1114–1121.

Dold, B. (2008). Sustainability in metal mining: from exploration, over processing to mine waste management. Reviews in Environmental Science and Bio/Technology, 7, 275–285.

Dominguez-Santos, D., Mora-Melia, D., Pincheira-Orellana, G., Ballesteros-Pérez, P., & Retamal-Bravo, C. (2019). Mechanical properties and seismic performance of woodconcrete composite blocks for building construction. Materials, 12(9), 1500.

Earth Systems. (2018). Waste Rock Management. Acid & Metalliferous Drainage. Retrieved July 11, 2023, from https://www.acidmetalliferousdrainage.com/waste-rockmanagement/

Elavarasan, S., Priya, A. K., & Kumar, V. K. (2021). Manufacturing fired clay brick using fly ash and M− Sand. Materials Today: Proceedings, 37, 872–876.

Eliche-Quesada, D., Martínez-García, C., Martínez-Cartas, M. L., Cotes-Palomino, M. T., Pérez-Villarejo, L., Cruz-Pérez, N., & Corpas-Iglesias, F. A. (2011). The use of different forms of waste in the manufacture of ceramic bricks. Applied Clay Science, 52(3), 270–276.

Epp, J. (2016). X-ray diffraction (XRD) techniques for materials characterization. In Materials characterization using non-destructive evaluation (NDE) methods (pp. 81–124). Elsevier.

Espuelas, S., Omer, J., Marcelino, S., Echeverría, A. M., & Seco, A. (2017). Magnesium oxide as alternative binder for unfired clay brick manufacturing. Applied Clay Science, 146, 23–26.

Fang, Y., Gu, Y., Kang, Q., Wen, Q., & Dai, P. (2011). Utilization of copper tailing for autoclaved sand–lime brick. Construction and Building Materials, 25(2), 867–872.

Fernandes, F. M. (2019a). Clay bricks. In Long-Term Performance and Durability of Masonry Structures (pp. 3–19). Elsevier.

Fernandes, F. M., Lourenço, P. B., & Castro, F. (2010). Ancient clay bricks: manufacture and properties. Materials, Technologies and Practice in Historic Heritage Structures, 29–48.

Fisher, L. V, & Barron, A. R. (2019). The recycling and reuse of steelmaking slags—A review. Resources, Conservation and Recycling, 146, 244–255.

Forcael, E., Ferrari, I., Opazo-Vega, A., & Pulido-Arcas, J. A. (2020). Construction 4.0: A literature review. Sustainability, 12(22), 9755.

Franks, D. M., Boger, D. V, Côte, C. M., & Mulligan, D. R. (2011). Sustainable development principles for the disposal of mining and mineral processing wastes. Resources Policy, 36(2), 114–122.

Gabasiane, T. S., Danha, G., Mamvura, T. A., Mashifana, T., & Dzinomwa, G. (2021). Characterization of copper slag for beneficiation of iron and copper. Heliyon, 7(4), e06757.

Gambill, D. R., Wall, W. A., Fulton, A. J., & Howard, H. R. (2016). Predicting USCS soil classification from soil property variables using Random Forest. Journal of Terramechanics, 65, 85–92.

García-Gaines, R. A., & Frankenstein, S. (2015). USCS and the USDA soil classification system: Development of a mapping scheme.

Garg, P., Jamwal, A., Kumar, D., Sadasivuni, K. K., Hussain, C. M., & Gupta, P. (2019). Advance research progresses in aluminium matrix composites: manufacturing & applications. Journal of Materials Research and Technology, 8(5), 4924–4939.

Gayana, B. C., & Ram Chandar, K. (2018). Sustainable use of mine waste and tailings with suitable admixture as aggregates in concrete pavements-A review.

Geng, J., & Sun, Q. (2018). Effects of high temperature treatment on physical-thermal properties of clay. Thermochimica Acta, 666, 148–155.

Geschke, R. (2004). Ceramic gap-fills for ceramic restoration. The Conservator, 28(1), 74–83.

Glaister, B. J., & Mudd, G. M. (2010). The environmental costs of platinum–PGM mining and sustainability: Is the glass half-full or half-empty? Minerals Engineering, 23(5), 438–450.

Gonidanga, B. S., Njoya, D., Lecomte-Nana, G., & Njopwouo, D. (2019). Phase Transformation, Technological Properties and Microstructure of Fired Products Based on Clay-Dolomite Mixtures. Journal of Materials Science and Chemical Engineering, 7(11), 1–14.

Groenevelt, P. H., & Grant, C. D. (2004). Analysis of soil shrinkage data. Soil and Tillage Research, 79(1), 71–77.

Gwimbi, P., & Nhamo, G. (2016). Translating mitigation measures proposed in environmental impact statements into planning conditions: Promises and practices by multinational platinum mining firms along the Great Dyke of Zimbabwe. Environmental Science & Policy, 57, 10–21.

Hapazari, I., Ntuli, V., & Taele, B. M. (2015). Waste generation and Management in Lesotho and waste to clay brick recycling: A review. Br. J. Applied. Science. Technology 8(2), 148–161.

Harrisson, A. M. (2019). Constitution and specification of Portland cement. Lea's Chemistry of Cement and Concrete, 5, 87–155.

Hogentogler, C. A., & Terzaghi, K. (1929). Interrelationship of load, road and subgrade. Public Roads, 10(3), 37–64.

Horii, K., Tsutsumi, N., Kitano, Y., & Kato, T. (2013). Processing and reusing technologies for steelmaking slag. Nippon Steel Technical Report, 104, 123–129.

Hou, X., He, Y., & Jones, B. T. (2004). Recent advances in portable X-ray fluorescence spectrometry. Applied Spectroscopy Reviews, 39(1), 1–25.

Huang, P.-T., Bobet, A., & Santagata, M. (2012). Identification of low-organic-content soils: an engineering approach. Geotechnical Testing Journal, 35(4), 596–606.

Hudson-Edwards, K. A., Jamieson, H. E., & Lottermoser, B. G. (2011). Mine wastes: past, present, future. Elements, 7(6), 375–380.

Hughes, A. E., Haque, N., Northey, S. A., & Giddey, S. (2021). Platinum group metals: A review of resources, production and usage with a focus on catalysts. Resources, 10(9), 93.

Ikhsan, S. N. W., Yusof, N., Aziz, F., Ismail, A. F., Jaafar, J., Salleh, W. N. W., & Misdan, N. (2021). Superwetting materials for hydrophilic-oleophobic membrane in oily wastewater treatment. Journal of Environmental Management, 290, 112565.

Indra, A., Edison, E., & Nofrianto, H. (2018). Optimization of compaction pressure on brick. MATEC Web of Conferences, 215.

Iswarya, E. (2020). Utilization of Granite Saw Powder Waste in Brick.

Jehanzeb, K., & Bashir, N. A. (2013). Training and development program and its benefits to employee and organization: A conceptual study. European Journal of Business and Management, 5(2).

Jernigan, Z. (2017). Company tackles city slag pile. Journalaz.com. Retrieved May 15, 2023, from https://journalaz.com/2017/04/26/company-tackles-city-slag-pile/

Jiang, Y., Ling, T.-C., Shi, C., & Pan, S.-Y. (2018). Characteristics of steel slags and their use in cement and concrete—A review. Resources, Conservation and Recycling, 136, 187–197.

Jones, R. T. (2005.). An overview of Southern African PGM smelting.

Kadir, A. A. (2012). An overview of wastes recycling in fired clay bricks. International Journal of Integrated Engineering, 4(2).

Kadir, A. A., & Mohajerani, A. (2011). Bricks: an excellent building material for recycling wastes-a review. Proceedings of the IASTED International Conference Environmental Management and Engineering (EME 2011), Calgary, AB, Canada, 4–6.

Kamal, M. A. (2023). Exploratory study of calcium silicate bricks as a potential material for building construction. Journal of Construction and Built Environment, 3(1), 1–12.

Karaman, S., Ersahin, S., & Gunal, H. (2006). Firing temperature and firing time influence on mechanical and physical properties of clay bricks. Journal of Scientific and Industrial, 65(2), 153-159

Kazmi, S. M. S., Abbas, S., Munir, M. J., & Khitab, A. (2016). Exploratory study on the effect of waste rice husk and sugarcane bagasse ashes in burnt clay bricks. Journal of Building Engineering, 7, 372–378.

Kimutai Keter, C. (2016). Development and Testing of Composite Refractory Bricks (A case study of selected Kenyan clays). Journal of Cleaner Production.

Kinnunen, P., Karhu, M., Yli-Rantala, E., Kivikytö-Reponen, P., & Mäkinen, J. (2022). A review of circular economy strategies for mine tailings. Cleaner Engineering and Technology, 8, 100499.

Klauber, C., Gräfe, M., & Power, G. (2009). Review of bauxite residue "re-use" options. Waterford, WA: CSIRO Minerals, 1–77.

Klauber, C., Gräfe, M., & Power, G. (2011). Bauxite residue issues: II. options for residue utilization. Hydrometallurgy, 108(1–2), 11–32.

Knappett, J., & Craig, R. F. (2012). Craig's soil mechanics. CRC press.

Krishna, A. K., Mohan, K. R., Murthy, N. N., & Govil, P. K. (2008). Comparative study of Xray fluorescence and inductively coupled plasma optical emission spectrometry of heavy metals in the analysis of soil samples. At Spectrosc, 29(3), 83–89.

Kujur, M. K., Roy, I., Kumar, K., Chintaiah, P., Ghosh, S., & Ghosh, N. K. (2018). Raw materials for manufacturing of Superior quality MgO-C bricks. Materials Today: Proceedings, 5(1), 2359–2366.

Kumar, R., & Hooda, N. (2014). An experimental study on properties of fly ash bricks. International Journal of Research in Aeronautical and Mechanical Engineering, 2(9), 56–67.

Kumar, R., Sen, S., & Ramna, R. V. (2022). Utilization Of Air-Cooled Blast Furnace Slag as A 100% Replacement of River Sand in Mortar and Concrete. Indian Concrete Journal.

Kumar, S., & Maithel, S. (2016). Introduction to brick kilns & specific energy consumption protocol for brick kilns. New Delhi: Greentech Knowledge Solutions Pvt. Ltd, 7–20.

Kumari, N., & Mohan, C. (2021). Basics of clay minerals and their characteristic properties. Clay Clay Miner, 24, 1–29.

Kuranchie, F. A., Shukla, S. K., & Habibi, D. (2016). Utilisation of iron ore mine tailings for the production of geopolymer bricks. International Journal of Mining, Reclamation and Environment, 30(2), 92–114.

Landy, R. A. (2004). Magnesia refractories. Mechanical Engineering-New York and BaselMarcel Dekker Then Crc Press/Taylor and Francis, 178, 109.

Lèbre, É., Corder, G. D., & Golev, A. (2017). Sustainable practices in the management of mining waste: A focus on the mineral resource. Minerals Engineering, 107, 34–42.

Legese, A. M., Kenate, T. G., & Feyessa, F. F. (2021). Termite mound soils for sustainable production of bricks. Studia Geotechnica et Mechanica, 43(2), 142–154.

Lertwattanaruk, P., & Choksiriwanna, J. (2011). The physical and thermal properties of adobe brick containing bagasse for earth construction. International Journal of Building, Urban, Interior and Landscape Technology (BUILT), 1, 57–66.

Li, J., Si, T., Li, L., Fan, C., He, Z., & Qian, Y. (2022). Fabrication of Baking-Free Bricks Using Gold Tailings and Cemented Materials with Low Alkalinity. Journal of Renewable Materials, 10(11), 3041–3058.

Liao, Y. L., Chai, X. J., Li, J. T., Xu, F. C., & Li, D. B. (2011). Study on the reduction of ferrous compounds disseminated in fayalite, vitreous and magnetite in dumped copper slag by means of carbonthermic method. Advanced Materials Research, 233, 684–688.

Liu, C., Sun, S., Zhu, X., & Tu, G. (2021). Metals smelting-collection method for recycling of platinum group metals from waste catalysts: A mini review. Waste Management and Research, 39(1), 43–52.

Liu, X., Qu, S., & Huang, J. (2019). Relationship between physical properties and particle-size distribution of geomaterials. Construction and Building Materials, 222, 312–318.

Lottermoser, B. G. (2011). Recycling, reuse, and rehabilitation of mine wastes. Elements, 7(6), 405–410.

Lottermoser, B., & Lottermoser, B. G. (2010). Tailings. Mine Wastes: Characterization, Treatment and Environmental Impacts, 205–241.

Luo, L., Li, K., Fu, W., Liu, C., & Yang, S. (2020). Preparation, characteristics and mechanisms of the composite sintered bricks produced from shale, sewage sludge, coal gangue powder and iron ore tailings. Construction and Building Materials, 232, 117250.

Luo, L., Zhang, Y., Bao, S., & Chen, T. (2016). Utilization of iron ore tailings as raw material for Portland cement clinker production. Advances in Materials Science and Engineering, 2016.

M. Dawoud, M., & M. Saleh, H. (2019). Introductory Chapter: Background on Composite Materials. In Characterizations of Some Composite Materials. IntechOpen.

Mabiza, L. (2006). An overview of PGM Smelting in Zimbabwe-Zimplats Operations.

MacDonald, M. (2017). Filamentous Foaming Causes and Remedies. SlidePlayer. Retrieved July 10, 2023, from https://slideplayer.com/slide/10332902/ Mahony,

C. (2013). Contains water. Building Surveying Journal, 18.

Manyuchi, M. M., Mbohwa, C., & Muzenda, E. (2019). Mining waste management for sustainable mining practices. Proceedings of the International Conference on Industrial Engineering and Operations Management Bangkok, Thailand, 137–142.

Marsh, A. T. M., Yang, T., Adu-Amankwah, S., & Bernal, S. A. (2021). Utilization of metallurgical wastes as raw materials for manufacturing alkali-activated cements. In Waste and Byproducts in Cement-Based Materials (pp. 335–383). Elsevier.

Martí, J., Riera, F., & Martínez, F. (2021). Interpretation of the failure of the Aznalcóllar (Spain) Tailings Dam. Mine Water and the Environment, 40(1), 189–208.

Marvila, M. T., Azevedo, A. R. G., Delaqua, G. C. G., Mendes, B. C., Pedroti, L. G., & Vieira, C. M. F. (2021). Performance of geopolymer tiles in high temperature and saturation conditions. Construction and Building Materials, 286, 122994.

McBride, R. A. (2002). 2.9 Atterberg Limits. Methods of Soil Analysis: Part 4 Physical Methods, 5, 389–398.

McBride, R. A., Carter, M. R., & Gregorich, E. G. (2008). Soil consistency: upper and lower plastic limits. Soil Sampling and Methods of Analysis. CRC Press, Boca Raton, FL, 761–781.

Mehta, P. K., & Monteiro, P. J. M. (2014). Concrete: microstructure, properties, and materials. McGraw-Hill Education.

Mhetre, M. T., Pathan, H. M., Thakur, A. V, & Lokh, B. J. (2022). Preparation of magnesium oxide (MgO) thin films by spray pyrolysis and its capacitive characterizations. ES Energy & Environment, 18, 41–46.

Morel, J.-C., Pkla, A., & Walker, P. (2007). Compressive strength testing of compressed earth blocks. Construction and Building Materials, 21(2), 303–309.

Morrison, K. F. (2022). Tailings Management Handbook: A LifeCycle Approach. Society for Mining, Metallurgy & Exploration.

Mudd, B. G. M. (2012). Sustainability reporting and the platinum group metals: A global mining industry leader? Platinum Metals Review, 56(1), 2–19.

Mueller, H., Maithy, S., Prajapati, S., Bhatta, D. A., & Shrestha, L. B. (2008). Green Brick Manual. Kathmandu: Hillside Press.

Mukhtar, A., Qazi, A. U., Khan, Q. S., Munir, M. J., Kazmi, S. M. S., & Hameed, A. (2022). Feasibility of Using Coal Ash for the Production of Sustainable Bricks. Sustainability (Switzerland), 14(11).

Murray, H. H. (2006). Applied clay mineralogy: occurrences, processing and applications of kaolins, bentonites, palygorskitesepiolite, and common clays. Elsevier.

Nakamura, T. (2015). Resource Recycling of Non-Ferrous Metals. Topical Themes in Energy and Resources: A Cross-Disciplinary Education and Training Program for Environmental Leaders, 229–243.

Ndlovu, S., Simate, G. S., & Matinde, E. (2017). Waste production and utilization in the metal extraction industry. CRC Press.

Ndukwu, M. C., Bennamoun, L., Simo-Tagne, M., Ibeh, M. I., Abada, U. C., & Ekop, I. E. (2021). Influence of drying applications on wood, brick and concrete used as building materials: A review. Journal of Building Pathology and Rehabilitation, 6, 1–19.

Nhabih, H. T., Arat, K. K., & Haidi, A. S. (2020). Methods of processing efflorescence of clay Brick. International Journal of Scientific Engineering and Science, 3(12), 48–56.

Nielsen, B. N., & Nielsen, S. D. (2019). Casagrande cup method. DCE Lecture Notes No. 60 by the Department of Civil Engineering, Aalborg University.

Noémi, S., István, S., & Balázs, K. (2021). Investigation of mechanical behaviour of bricks with treated red mud residue additives. Multidiszciplináris Tudományok, 11(1), 104–114.

Nikvar-Hassani, A., Vashaghian, H., Hodges, R., & Zhang, L. (2022). Production of green bricks from low-reactive copper mine tailings: Chemical and mechanical aspects. Construction and Building Materials, 324.

NRCS, U. (1993). Soil survey division staff (1993) soil survey manual. Soil conservation service. US Department of Agriculture Handbook, 18, 315.

Nturanabo, F., Masu, L., & Kirabira, J. B. (2019). Novel applications of aluminium metal matrix composites. Aluminium Alloys and Composites, 12(3), 123-132

O'Connor, C., & Alexandrova, T. (2021). The geological occurrence, mineralogy, and processing by flotation of platinum group minerals (PGMs) in South Africa and Russia. Minerals, 11(1), 54.

Oge, M., Ozkan, D., Celik, M. B., Gok, M. S., & Karaoglanli, A. C. (2019). An overview of utilization of blast furnace and steelmaking slag in various applications. Materials Today: Proceedings, 11, 516–525.

Olokode, O. S., Aiyedun, P. O., Oluwadare, G. O., Alamu, O. J., Fakolujo, S. O., & Lee, W. E. (2012). Chacterization of Ajebo Clay in South West Nigeria. Asset: An International Journal (Series B)}, 9(2), 50–59.

Oluwasola, E. A., Hainin, M. R., Aziz, M. M. A., Yaacob, H., & Warid, M. N. M. (2014). Potentials of steel slag and copper mine tailings as construction materials. Materials Research Innovations, 18(sup6), S6-250.

Oti, J. E., Kinuthia, J. M., & Robinson, R. B. (2014). The development of unfired clay building material using Brick Dust Waste and Mercia mudstone clay. Applied Clay Science, 102, 148–154.

Oyelami, C. A., & Van Rooy, J. L. (2016). Geotechnical characterisation of lateritic soils from south-western Nigeria as materials for cost-effective and energy-efficient building bricks. Environmental Earth Sciences, 75, 1–16.

Oyelaran, O. A. (2014). Physic-chemical characterization of "Namu" clay for industrial use. Engineering and Applied Science Research, 41(3), 283–290.

Park, S.-J., & Seo, M.-K. (2011). Element and processing. In Interface science and technology. Elsevier, 18, 431–499.

Piatak, N. M. (2018). Environmental characteristics and utilization potential of metallurgical slag. In Environmental Geochemistry (pp. 487–519). Elsevier.

Piatak, N. M., & Ettler, V. (2021). Introduction: metallurgical slags–environmental liability or valuable resource?

Piatak, N. M., Parsons, M. B., & Seal II, R. R. (2015). Characteristics and environmental aspects of slag: A review. Applied Geochemistry, 57, 236–266.

Politis, A., Paspaliaris, I., & Taxiarchou, M. (2017). Management of Wastes From Primary Resource Processing: Identification and Environmental Evaluations. MSP-REFRAMContract.

Potysz, A., van Hullebusch, E. D., Kierczak, J., Grybos, M., Lens, P. N. L., & Guibaud, G. (2015). Copper metallurgical slags–current knowledge and fate: a review. Critical Reviews in Environmental Science and Technology, 45(22), 2424–2488.

Praseeda, K. I., Reddy, B. V. V., & Mani, M. (2015). Embodied energy assessment of building materials in India using process and input–output analysis. Energy and Buildings, 86, 677–686.

Pribulova, A., & Futas, P. (2016). Treatment Of Slags from Metallurgical Processes. 16th International Multidisciplinary Scientific GeoConference SGEM 2016, 171–178.

Punmia, B. C., Jain, A. K., & Jain, A. K. (2003). Basic civil engineering. Firewall Media.

Raghubanshi, A. S., Mudgal, M., Chouhan, R. K., Kumar, A., & Srivastava, A. K. (2022). Recycling and potential utilization of red mud (Bauxite Residue) for construction industry applications. Indian Journal of Engineering and Materials Sciences (IJEMS), 29(4), 401–410.

Rahman, M. E., Boon, A. L., Muntohar, A. S., Tanim, M. N. H., & Pakrashi, V. (2014). Performance of masonry blocks incorporating palm oil fuel ash. Journal of Cleaner Production, 78, 195–201.

Rajput, R. K. (2008). Engineering materials. S. Chand Publishing.

Ranjan, G., & Rao, A. S. R. (2011). Basic and applied soil mechanics. New Age International.

Rao, B. J., Teja, K. A., & Satyanarayan, K. (2019). Effect of different waste materials addition on the properties of clay bricks. Int. J. Res. Appl. Sci. Eng. Technol, 7, 2552–2557.

Rawat, K., Sharma, N., & Singh, V. K. (2022). X-Ray Fluorescence and Comparison with Other Analytical Methods (AAS, ICP-AES, LA-ICP-MS, IC, LIBS, SEM-EDS, and XRD). X-Ray Fluorescence in Biological Sciences: Principles, Instrumentation, and Applications, 1–20.

Reddi, L. N., Jain, A. K., & Yun, H.-B. (2012). Soil materials for earth construction: Properties, classification and suitability testing. In Modern Earth Buildings (pp. 155–171). Elsevier.

Rock, A. C. D.-18 on S. and. (2010). Standard test methods for liquid limit, plastic limit, and plasticity index of soils. ASTM international.

Ross, K. (2013). 60Co Contamination in Iron and Steel. Sandia National Lab.(SNL-NM), Albuquerque, NM (United States).

Roudouane, H. T., Mbey, J. A., Bayiga, E. C., & Ndjigui, P. D. (2020). Characterization and application tests of kaolinite clays from Aboudeia (southeastern Chad) in fired bricks making. Scientific African, 7, e00294.

Roy, S., Adhikari, G. R., & Gupta, R. N. (2007). Use of gold mill tailings in making bricks: A feasibility study. Waste Management and Research, 25(5), 475–482.

Roy, S., & Bhalla, S. K. (2017). Role of geotechnical properties of soil on civil engineering structures. Resources and Environment, 7(4), 103–109.

Russo, S., & Sciarretta, F. (2013). Masonry exposed to high temperatures: Mechanical behaviour and properties—An overview. Fire Safety Journal, 55, 69–86.

Ruvimbo Samanga, B., & Omogboyega Abe, O. (2019). The Impact of the Zimbabwean Space Agency's Programme for the Mapping of Mineral Reserves on Foreign Direct Investment in Zimbabwe.

Sadek, D. M. (2014). Effect of cooling technique of blast furnace slag on the thermal behavior of solid cement bricks. Journal of Cleaner Production, 79, 134–141.

Sahu, M. K., & Singh, L. (2017). Critical Review on Fly Ash Bricks. International Journal of Advance Engineering and Research Development, 4(03), 16–22.

Sahu, M. K., Singh, L., & Choudhary, S. N. (2016). Critical review on bricks. International Journal of Engineering and Management Research (IJEMR), 6(5), 80–88.

Samad, A., Baidya, S., Akhtar, U. S., Ahmed, K. S., Roy, S. C., & Islam, S. (2021). Manufacture Of Refractory Brick from Locally Available Red Clay Blended with White Portland Cement and Its Performance Evaluation. International Journal of GEOMATE, 20(80), 105–112.

Sathiparan, N., & Rumeshkumar, U. (2018). Effect of moisture condition on mechanical behavior of low strength brick masonry. Journal of Building Engineering, 17, 23–31.

Sezgin, N. (2020). Submarine disposal method of mine tailings (slurry sludge). Nat Hazards Appl Res Cent, 6, 209–217.

Sharma, B., & Bora, P. K. (2003). Plastic limit, liquid limit and undrained shear strength of soil—reappraisal. Journal of Geotechnical and Geoenvironmental Engineering, 129(8), 774–777.

Shi, J., Liu, B., Chu, S. H., Zhang, Y., Zhang, Z., & Han, K. (2022). Recycling air-cooled blast furnace slag in fiber reinforced alkali-activated mortar. Powder Technology, 407, 117686.

Sibanda, L. K. (2019). Repurposing of mine waste: an alternative management approach to gold tailings in South Africa.

Sima, M., & Morosanu, G. A. (2022). Mining Hazard Risk Reduction and Resilience. Disaster Risk Reduction for Resilience: Disaster Risk Management Strategies, 73–99.

Simão, F. V., Chambart, H., Vandemeulebroeke, L., Nielsen, P., & Cappuyns, V. (2021). Turning mine waste into a ceramic resource: Plombières mine tailing case. Copernicus Meetings.

Singh, M., & Kapur, P. C. (2008). Preparation of alinite based cement from incinerator ash. Waste Management, 28(8), 1310–1316.

Singh, S. B., & Munjal, P. (2017). Bond strength and compressive stress-strain characteristics of brick masonry. Journal of Building Engineering, 9, 10–16.

Smith, R., & Mobley, R. K. (2011). Rules of thumb for maintenance and reliability engineers. Butterworth-Heinemann.

Soltani, A., Azimi, M., & O'Kelly, B. C. (2023). Reappraisal of linear shrinkage test for plasticity index determination and classification of fine-grained soils. Applied Clay Science, 238, 106920

Sorout, J., Raj, S., Kaur, D. P., & Lamba, P. (2023). Waste-Based Bricks: Evaluation of Strength Behaviour of Bricks Containing Different Waste Materials as an Additive. Water, Air, & Soil Pollution, 234(7), 424.

Standard, A. (2006). C136 Standard Test Method for Sieve Analysis of Fine and Coarse Aggregates. ASTM International: West Conshohocken, PA, USA.

Standard, I. (1992). 3495 Part 1 & 2: Methods of tests of burnt clay building bricks. Bureau of Indian Standards, New Delhi.

Stauber, J. L., Adams, M. S., Batley, G. E., Golding, L. A., Hargreaves, I., Peeters, L., ReicheltBrushett, A. J., & Simpson, S. L. (2022). A generic environmental risk assessment framework for deep-sea tailings placement. Science of the Total Environment, 845, 157311.

Subramanian, N. (2019). Brick Kilns and their Effect on Environment.

Sultana, S., Ahsan, S., Tanvir, S., Haque, N., Alam, F., & Yellishetty, M. (2021). Coal fly ash utilisation and environmental impact. In Clean Coal Technologies: Beneficiation, Utilization, Transport Phenomena and Prospective (pp. 381–402). Springer.

Sutan, N. M., & Sinin, H. (2013). Efflorescence phenomenon on concrete structures. Advanced Materials Research, 626, 747–750.

Taha, M. A., Youness, R. A., & Ibrahim, M. (2020). Biocompatibility, physico-chemical and mechanical properties of hydroxyapatite-based silicon dioxide nanocomposites for biomedical applications. Ceramics International, 46(15), 23599–23610.

Taha, Y., Benzaazoua, M., Hakkou, R., & Mansori, M. (2016). Natural clay substitution by calamine processing wastes to manufacture fired bricks. Journal of Cleaner Production, 135, 847–858.

Takahashi, G. (2015). Sample preparation for X-ray fluorescence analysis. Rigaku J, 31(1), 26–30.

Tayebi-Khorami, M., Edraki, M., Corder, G., & Golev, A. (2019). Re-thinking mining waste through an integrative approach led by circular economy aspirations. Minerals, 9(5), 286.

Thejas, H. K., & Hossiney, N. (2022). Alkali-activated bricks made with mining waste iron ore tailings. Case Studies in Construction Materials, 16. Thethwayo, B. M. (2018). Extraction of Platinum Group Metals. In Noble and Precious Metals - Properties, Nanoscale Effects and Applications. InTech.

Tian, H., Guo, Z., Pan, J., Zhu, D., Yang, C., Xue, Y., Li, S., & Wang, D. (2021). Comprehensive review on metallurgical recycling and cleaning of copper slag. Resources, Conservation and Recycling, 168, 105366.

Tripathy, S. K., Dasu, J., Murthy, Y. R., Kapure, G., Pal, A. R., & Filippov, L. O. (2020). Utilisation perspective on water quenched and air-cooled blast furnace slags. Journal of Cleaner Production, 262, 121354.

Tsega, E., Mosisa, A., & Fufa, F. (2017). Effects of firing time and temperature on physical properties of fired clay bricks. American Journal of Civil Engineering, 5(1), 21–26.

Unal, P. G. (2012). 3D woven fabrics. In Woven fabrics. IntechOpen.

Valaskova, M. (2015). Clays, clay minerals and cordierite ceramics-A review. CeramicsSilikáty, 59(4), 331-340.

Vaszita, E. (2014). Environmental risk of mining. Engineering Tools for Environmental Risk Management, 1, 113–133.

Velasco, P. M., Ortíz, M. P. M., Giró, M. A. M., & Velasco, L. M. (2014). Fired clay bricks manufactured by adding wastes as sustainable construction material–A review. Construction and Building Materials, 63, 97–107.

Vijayan, D. S., Mohan, A., Revathy, J., Parthiban, D., & Varatharajan, R. (2021). Evaluation of the impact of thermal performance on various building bricks and blocks: A review. Environmental Technology & Innovation, 23, 101577.

Vyas, D., Vyas, C. M., & Pitroda, J. (2014). Utilization of barley husk ash in clay bricks in aspect of indian context: A literature review. International Journal of Civil, Structural, Environmental and Infrastructure Engineering Research and Development (IJCSEIERD), 4(1), 61–68.

Wan Ibrahim, W. M., Kamarudin, H., Al Bakri Abdullah, M. M., Abdul Kadir, A., & Binhussain, M. (2015). A review of fly ash-based geopolymer lightweight bricks. Applied Mechanics and Materials, 754, 452–456.

Wangda. (2021). Brick making factory Tunnel kiln basic Parameter. Retrieved October 10, 2023, from https://www.wd-brickmachine.com/news/brick-making-factory-tunnel-kilnbasic-parameters/

Wei, Z., Zhao, J., Wang, W., Yang, Y., Zhuang, S., Lu, T., & Hou, Z. (2021). Utilizing gold mine tailings to produce sintered bricks. Construction and Building Materials, 282, 122655.

Weyant, C., Kumar, S., Maithel, S., Thompson, R., Baum, E., Floess, E., & Bond, T. (2016). Brick Kiln measurement guidelines: Emissions and energy performance, climate and clean air coalition.

Wu, A., Jiao, H., Wang, H., & Yang, S. (2011). Notice of Retraction: Paste Filling-A Underground Disposal Technique of Mine Solid Waste. 2011 5th International Conference on Bioinformatics and Biomedical Engineering, 1–4.

Xiaolong, Z., Shiyu, Z., Hui, L., & Yingliang, Z. (2021). Disposal of mine tailings via geopolymerization. Journal of Cleaner Production, 284, 124756.

Xiong, X., Liu, X., Iris, K. M., Wang, L., Zhou, J., Sun, X., Rinklebe, J., Shaheen, S. M., Ok, Y. S., & Lin, Z. (2019). Potentially toxic elements in solid waste streams: Fate and management approaches. Environmental Pollution, 253, 680–707.

Xu, H., Song, W., Cao, W., Shao, G., Lu, H., Yang, D., Chen, D., & Zhang, R. (2017). Utilization of coal gangue for the production of brick. Journal of Material Cycles and Waste Management, 19, 1270–1278.

Yang, J., & Xiao, B. (2008). Development of unsintered construction materials from red mud wastes produced in the sintering alumina process. Construction and Building Materials, 22(12), 2299–2307.

Yellishetty, M., Karpe, V., Reddy, E. H., Subhash, K. N., & Ranjith, P. G. (2008). Reuse of iron ore mineral wastes in civil engineering constructions: A case study. Resources, Conservation and Recycling, 52(11), 1283–1289.

Yilmaz, E. (2011). Advances in reducing large volumes of environmentally harmful mine waste rocks and tailings. Gospodarka Surowcami Mineralnymi, 27, 89–112.

Yonggang, Y., Shenhong, Z., Qiuyi, L., Benju, Y., & Yu, C. (2011). Research on making fired bricks with gold tailings. 2011 International Conference on Computer Distributed Control and Intelligent Environmental Monitoring, 1687–1690.

Zhang, N., Tang, B., & Liu, X. (2021). Cementitious activity of iron ore tailing and its utilization in cementitious materials, bricks and concrete. Construction and Building Materials, 288, 123022.

Zhao, Y., Zhang, Y., Chen, T., Chen, Y., & Bao, S. (2012). Preparation of high strength autoclaved bricks from hematite tailings. Construction and Building Materials, 28(1), 450–455.

Zheng, W. (2013). Analysis of the proportion of aerated concrete block materials produced by using gold tailings. Science Technology, 24–25.

Zhengfu, B., Inyang, H. I., Daniels, J. L., Frank, O., & Struthers, S. (2010). Environmental issues from coal mining and their solutions. Mining Science and Technology (China), 20(2), 215–223.

Zhou, B., & Lu, N. (2021). Correlation between Atterberg limits and soil adsorptive water. Journal of Geotechnical and Geoenvironmental Engineering, 147(2), 04020069.

ZIMPLATS. (2021). Creating a better future, Integrated Annual Report 2021.

ZIMPLATS. (2022). Creating a Future Better, 2022 Integrated Annual Report.

APPENDICES

7.1 Characterization of Raw Materials

7.1.1 X-Ray Florescence (XRF)

SMC Laboratory

P O Box 61, Makwiro Road, Selous, Zimbabwe

Tel: +263 (628) 44888-9+263 (628) 772 513 906-9 Fax: +263 (628) 44123/6

Certificate of Analysis

CLIENT NAME & ADDRESS: Chinhoyi University of Technology
Private Bag 7724
Chinhoyi Zimbabwe

Lab Reference Number: N/A	Total Number of Samples: Nine
Date Received:	12/08/2022
Date Analysed:	23/08/2022
Date Reported:	25/08/2022
Samples Analysed at:	SMC Laboratory
Nature of Samples:	Ores, Quartz and Furnace slags

ASSAY REPORT

ANALYTE	Ni	Cu	Co	Fe	S	MgO	CaO	Al2O3	SiO2	Cr2O3	K2O	Na2O	TiO2
UNITS	%	%	%	%	%	%	%	%	%	%	%	%	%
CLAY SOIL	0.098	0.079	0.006	2.546	0.096	0.921	3.776	22.675	55.943	0.093	1.889	2.268	0.357
CUCW1	0.081	0.147	0.003	2.381	0.074	1.698	2.802	10.551	64.318	0.077	2.987	1.027	0.3476
CUDL4	0.041	0.032	0.000	0.337	0.079	16.899	67.068	1.769	10.353	0.027	0.129	0.032	0.010
CUPC5	0.028	0.031	0.001	1.349	1.145	1.957	62.809	3.763	22.784	0.023	0.000	0.000	0.000
EMRD2	0.034	0.033	0.005	4.950	0.043	0.400	0.749	0.686	84.516	0.113	0.677	0.098	0.435
EMDG1	0.160	0.071	0.009	8.637	0.164	12.333	10.048	8.040	47.779	0.227	2.009	0.876	0.785
MAFUWE CLAY	0.042	0.032	0.003	3.635	0.062	0.724	2.026	24.132	57.004	0.059	0.786	1.003	0.185
CUZS2	0.124	0.107	0.065	29.743	0.125	21.379	0.667	1.347	46.090	0.337	0.000	0.000	0.000
CUFA3	0.105	0.085	0.013	10.207	0.203	8.786	3.205	26.772	46.550	0.127	0.002	1.002	0.098

TEST METHOD USED: SMCL/XRF/04

Pressed pellet, XRF finish

COMMENTS:

CUZS2 and CUFA3 Fe result analysed as FeO
Some of the samples did not match our sample matrix

TECHNICAL SIGNATORY
Name & Surname: Fungai Chisango Signature: Date: 25.08.2022
LABORATORY MANAGER
Name & Surname: Richard Ncube Signature: Date: 25.08.2022

The analytical results reported here in refer to the samples as received and are analysed on a dry basis.
Reproduction of this analytical report in full or in part is prohibited.

7.1.2 Specific Gravity

Table 7.1: Temperature Correction Factors

Temperature (T°C)	A	Temperature (T°C)	A
16	1.0007	24	0.9991
17	1.0006	25	0.9988
18	1.0004	26	0.9986
19	1.0002	27	0.9983
20	1.0000	28	0.9980
21	0.9996	29	0.9977
22	0.9998	30	0.9974
23	0.9993		

Table 7.2: Specific Gravity

Sample	**PGM Slag**		**ZC**		**CC**	
Mass of flask + Water (W_1)	119.2	122.5	107.7	122.8	105.6	118.8
Mass of flask + Sample + water (W_2)	174.6	175.9	157.2	167.4	154.1	167.1
Mass of Sample (W_s)	80.0	77.2	77.3	69.7	76.5	76.0
Temperature Recorded (A)	25	26	26	27	26	25
Temperature Factor	0.9988	0.9986	0.9988	0.9983	0.9986	0.9988
SG = $\frac{W_s}{W_1+W_s-W_2} \times A$	3.25	3.24	2.78	2.77	2.73	2.74
Average SG	**3.25**		**2.78**		**2.74**	

7.1.3 Sieve Analysis

Zvishavane Clay (ZC)

Table 7.3: Wet Sieving (ZC)

Mass of dried sample before washing (g)	500.00
Mass of dried sample after washing (g)	134.49
Mass of washed material through 0.075mm sieve (g)	365.51

Table 7.4: Dry Sieving (ZC)

B.S. Sieve	Mass Retained	Percentage Retained	Percentage Passing	Cumulative Percentage retained (%)
19.0	0	0	100	0
9.5	3.51	0.7	99.3	0.7
4.75	4.63	0.9	98.4	1.6
2.36	4.06	0.8	97.6	2.4
1.18	11.58	2.3	95.3	4.7
0.600	19.09	3.8	91.5	8.5
0.300	30.62	6.1	85.4	14.6
0.150	28.44	5.7	79.7	20.3
0.075	31.65	6.3	73.4	26.6
-0.075 dry	1.28			
-0.075 wet	365.51			
-0.075 total	366.79	73.4		
TOTAL	**500.00**	**100.0**		

Chinhoyi Clay (CC)

Table 7.5: Wet Sieving (CC)

Mass of dried sample before washing (g)	500.00
Mass of dried sample after washing (g)	179.46
Mass of washed material through 0.075mm sieve (g)	320.54

Table 7.6: Dry Sieving (CC)

B.S. Sieve	Mass Retained	Percentage Retained	Percentage Passing	Cumulative Percentage retained (%)
19.0	0	0	100	0
9.5	11.56	2.3	97.7	2.3
4.75	5.61	1.1	96.6	3.4
2.36	10.49	2.1	94.5	5.5
1.18	22.13	4.4	90.1	9.9
0.600	24.07	4.8	85.3	14.7
0.300	38.71	7.7	77.6	22.4
0.150	28.97	5.8	71.8	28.2
0.075	36.68	7.3	64.5	35.5
-0.075 dry	2.04			
-0.075 wet	320.54			
-0.075 total	322.58	64.5		

TOTAL	**500.00**	**100.0**		

PGM Slag

Table 7.7: Wet Sieving (PGM Slag)

Mass of dried sample before washing (g)	500.00
Mass of dried sample after washing (g)	496.82
Mass of washed material through 0.075 mm sieve (g)	3.18

Table 7.8: Dry Sieving (PGM Slag)

B.S. Sieve	**Mass Retained**	**Percentage Retained**	**Percentage Passing**	**Cumulative Percentage retained (%)**
26.5	0	0	100	0
19.0	6.93	1.4	98.6	1.4
9.5	13.87	2.8	95.8	4.2
4.75	23.42	4.7	91.1	8.9
2.36	121.44	24.3	66.8	33.2
1.18	170.19	34.0	32.8	67.2
0.600	83.52	16.7	16.1	83.9
0.300	48.91	9.8	6.3	93.7
0.150	17.42	3.5	2.8	97.2
0.075	9.69	1.9	0.9	99.1
-0.075 dry	1.43			
-0.075 wet	3.18			
-0.075 total	4.61	0.9		
TOTAL	**500.00**	**100.0**		

7.1.4 Atterberg Limits

Table 7.9: Correction factors

Number of blows	Factor	Number of blows	Factor	Number of blows	factor
15	0.95	22	0.99	29	1.01
16	0.96	23	0.99	30	1.02
17	0.96	24	0.99	31	1.02

18	0.97	25	1.00	32	1.02
19	0.97	26	1.00	33	1.02
20	0.98	27	1.01	34	1.03
21	0.98	28	1.01	35	1.03

Table 7.10: Liquid Limit (LL)

Sample	**ZC**		**CC**	
Tare number	214	203	154	222
Mass of tare (m_1) g	99	102	105	100
Mass of tare+ wet soil (m_2) g	402	341	329	380
Mass of tare +dry soil (m_3) g	314	264	262	304
Mass of water g	88	77	67	76
Mass of soil g	215	162	157	204
Moisture content, *w*%	40.9	47.5	42.6	37.2
Number of blows	21	30	33	24
Factor	0.98	1.02	1.02	0.99
Liquid limit, **LL** (*w*% × Factor)	40.1	48.5	43.5	36.8
Average **LL%**	**44.3**		**40.2**	

Table 7.11: Plastic Limit (PL)

Sample	**Z C**		**CC**	
Tare number	34	45	68	40
Mass of tare (m_1) g	113	98	106	101
Mass of tare + wet sample (m_2) g	501	510	450	436
Mass of tare + dry sample (m_3) g	431	434	387	376
Mass of water g	70	76	63	60
Mass of dry sample g	318	336	281	275
Moisture content, *w*	22.0	22.6	21.4	21.8
Plastic Limit, **PL %**	**22 .3**		**21.6**	

Table 7.12: Plastic Index (PI)

Sample	ZC	CC
Liquid Limit, LL%	44.3	40.2
Plastic Limit, PL%	22.3	21.6
Plasticity Index, PI% (LL % - PL %)	**22.0**	**18.6**

Table 7.13: Shrinkage Limit (SL)

Sample	Z C		CC	
Tare number	81	95	88	67
Initial length (cm)	15.0	15.0	15.0	15.0
Final length (cm)	13.9	14.1	14.4	14.3
Percentage linear shrinkage %	7.33	6.00	4.00	4.67
	6. 7		**4. 3**	

7.2 Brick Manufacturing Process

7.2.1 Optimum Moisture Content Determination

Table 7.14: OMC (0wt.% PGM Slag combination)

Mould Number	**4**	**5**	**3**	**8**
Mass of empty mold (g)	4438	3762	4499	4423
Mass of mold + wet sample (g)	8236	7877	8592	8383
Mass of wet sample (g)	3798	4115	4093	3960
Wet density (kg/m^3)	1688	1829	1819	1760
Tare Number	20	19	17	26
Mass of empty tare (g)	263	260	254	273
Mass of tare + wet sample (g)	682	690	679	684
Mass of tare + dry sample (g)	637	642	629	633
Mass of water (g)	45	48	50	51
Mass of dry sample (g)	374	380	375	360
Water content (%)	**12.1**	**12.7**	**13.4**	**14.0**
Dry density, $\varrho_{dry} = \frac{\varrho}{1+w}$ (kg/m^3)	**1506**	**1623**	**1604**	**1544**

Table 7.15: OMC (20wt.% PGM Slag combination)

Mould Number	**9**	**7**	**4**	**3**
Mass of empty mold (g)	4445	4129	4438	4499
Mass of mold + wet sample (g)	8459	8386	8753	8590

Mass of wet sample (g)	4014	4257	4315	4091
Wet density (kg/m^3)	1784	1892	1918	1818
Tare Number	28	21	15	12
Mass of empty tare (g)	271	284	257	272
Mass of tare + wet sample (g)	674	683	676	682
Mass of tare + dry sample (g)	637	642	629	633
Mass of water (g)	37	41	47	49
Mass of dry sample (g)	366	358	372	361
Water content (%)	10.1	11.3	12.5	13.6
Dry density, $\varrho_{dry} = \frac{\varrho}{1+w}$ (kg/m^3)	**1620**	**1700**	**1705**	**1600**

Table 7.16: OMC (40wt.% PGM Slag combination)

Mould Number	**1**	**5**	**8**	**7**
Mass of empty mold (g)	3997	3765	4422	4135
Mass of mold + wet sample (g)	8259	8164	8911	8529
Mass of wet sample (g)	4262	4399	4489	4394
Wet density (kg/m^3)	1894	1955	1995	1953
Tare Number	16	04	10	13
Mass of empty tare (g)	291	266	267	284
Mass of tare + wet sample (g)	716	684	697	721
Mass of tare + dry sample (g)	679	645	654	674
Mass of water (g)	37	39	43	47
Mass of dry sample (g)	388	379	387	390
Water content (%)	9.5	10.2	11.1	12.0
Dry density, $\varrho_{dry} = \frac{\varrho}{1+w}$ (kg/m^3)	**1730**	**1774**	**1796**	**1744**

Table 7.17: OMC (50wt.% PGM Slag combination)

Mould Number	**2**	**6**	**4**	**9**
Mass of empty mold (g)	4382	4129	4439	4447
Mass of mold + wet sample (g)	8808	8679	9002	8922
Mass of wet sample (g)	4426	4550	4563	4475
Wet density (kg/m^3)	1967	2022	2028	1989

Tare Number	01	07	11	18
Mass of empty tare (g)	258	242	269	271
Mass of tare + wet sample (g)	687	670	705	706
Mass of tare + dry sample (g)	649	630	663	662
Mass of water (g)	38	40	42	44
Mass of dry sample (g)	391	388	394	391
Water content (%)	9.6	10.2	10.7	11.3
Dry density, $\varrho_{dry} = \frac{\varrho}{1+w}$ (kg/m^3)	**1795**	**1835**	**1832**	**1787**

Table 7.18: OMC (60wt.% PGM Slag combination)

Mould Number	**13**	**10**	**6**	**7**
Mass of empty mold (g)	4402	4378	4138	4139
Mass of mold + wet sample (g)	8778	8894	8805	8767
Mass of wet sample (g)	4376	4516	4667	4628
Wet density (kg/m^3)	1945	2007	2074	2057
Tare Number	22	00	03	14
Mass of empty tare (g)	251	287	275	268
Mass of tare + wet sample (g)	685	719	718	720
Mass of tare + dry sample (g)	654	685	676	673
Mass of water (g)	31	34	42	47
Mass of dry sample (g)	403	398	401	405
Water content (%)	7.6	8.5	10.4	11.7
Dry density, $\varrho_{dry} = \frac{\varrho}{1+w}$ (kg/m^3)	**1808**	**1850**	**1879**	**1842**

7.2.2 Drying Shrinkage

Table 7.19: Drying Shrinkage (%)

	ZC-Binder Bricks (%)	**CC-Binder Bricks (%)**
0wt.%	7.0	6.3

20wt.%	6.1	5.9
40wt.%	5.4	4.5
50wt.%	4.8	4.3
60wt.%	4.3	4.1

7.2.3 Firing Shrinkage

Table 7.20: Firing Shrinkage (%)

	ZC-Binder Bricks (%)	**CC-Binder Bricks (%)**
950 ℃	7.4	7.2
1000 ℃	7.6	7.4
1050 ℃	8.3	7.4
1100 ℃	8.5	7.6

7.3 Physical and Mechanical Properties of the Fabricated Composite Materials

7.3.1 Compressive Strength

Table 7.21: Compressive Strength (MPa)

	950 ℃		**1000 ℃**		**1050 ℃**		**1100 ℃**	
	ZC	**CC**	**ZC**	**CC**	**ZC**	**CC**	**ZC**	**CC**
0wt.%	6.2	6.0	6.0	5.8	5.7	5.5	5.6	5.4
20wt.%	6.8	6.2	6.5	5.9	6.0	5.7	5.8	5.6
40wt.%	7.9	8.9	7.6	8.2	7.4	7.3	7.1	6.5
50wt.%	11.2	10.1	10.9	9.4	8.5	8.9	8.2	8.7
60wt.%	7.0	6.8	6.9	6.2	6.7	5.8	6.4	5.4

7.3.2 Water Absorption

Table 7.22: Water Absorption (%)

	950 ℃		**1000 ℃**		**1050 ℃**		**1100 ℃**	
	ZC	**CC**	**ZC**	**CC**	**ZC**	**CC**	**ZC**	**CC**
0wt.%	10.8	10.9	10.9	11.3	11.3	11.6	11.5	11.8
20wt.%	10.3	10.6	10.7	10.8	10.8	10.9	11.0	11.3

40wt.%	8.8	10.3	9.1	10.5	9.3	10.6	9.6	10.7
50wt.%	7.1	10.1	7.2	10.2	7.8	10.4	8.1	10.6
60wt.%	9.1	10.4	9.3	10.5	9.5	10.8	9.9	11.3

PAPER NAME

MAGAVHE MIRIAM_DISSERTATION.pdf

WORD COUNT

35607 Words

CHARACTER COUNT

199346 Characters

PAGE COUNT

130 Pages

FILE SIZE

4.1MB

SUBMISSION DATE

Jul 29, 2024 3:04 PM GMT+2

REPORT DATE

Jul 29, 2024 3:09 PM GMT+2

14% Overall Similarity

The combined total of all matches, including overlapping sources, for each database.

- 9% Internet database
- 6% Publications database
- Crossref database
- Crossref Posted Content database
- 9% Submitted Works database

Excluded from Similarity Report

- Bibliographic material
- Small Matches (Less then 10 words)